



Title	SYNAPTIC PLASTICITY OF RED NUCLEUS NEURONS
Author(s)	藤戸, 裕
Citation	大阪大学, 1982, 博士論文
Version Type	VoR
URL	https://hdl.handle.net/11094/2787
rights	
Note	

The University of Osaka Institutional Knowledge Archive : OUKA

<https://ir.library.osaka-u.ac.jp/>

The University of Osaka

SYNAPTIC PLASTICITY OF RED NUCLEUS NEURONS

BY

YUTAKA FUJITO

from the Department of Biophysical Engineering

Faculty of Engineering Science

Osaka University

This thesis is based on the following articles.

- I. Formation of functional synapses in the adult cat red nucleus from the cerebrum following cross-innervation of flexor and extensor nerves. I. Appearance of new synaptic potentials. Exp. Brain Res. (1982) in press.
Tsukahara, N., Fujito, Y., Oda, Y., and Maeda, J.
- II. Formation of functional synapses in the adult cat red nucleus from the cerebrum following cross-innervation of forelimb flexor and extensor nerves. II. Analysis of newly appeared synaptic potentials. Exp. Brain Res. (1982) in press.
Fujito, Y., Tsukahara, N., Oda, Y., and Yoshida, M.
- III. Synaptic inputs of rubrospinal neurons from association cortex, pretectum, medial lemniscus in the cat and their plasticity. (in preparation)
Fujito, Yutaka, Maeda, Jun, Murakami, Fujio, and Tsukahara, Nakaakira.
- IV. Lesion-induced sprouting in the kitten red nucleus.
Fujito, Yutaka, Kubota, Michinori, and Tsukahara, Nakaakira (in preparation)

CONTENTS

		page
Chapter	I General introduction -----	4
Chapter	II Formation of functional synapses in adult --- cat red nucleus from the cerebrum following cross-innervation of flexor and extensor nerves. I. Appearance of new synaptic potentials.	10
Chapter	III Formation of functional synapses in adult --- cat red nucleus from the cerbrum following cross-innervation of forelimb flexor and extensor nerves. II. Analysis of newly- appeared synaptic potential.	49
Chapter	IV Synaptic inputs of rubrospinal neurons ----- from association cortex, pretectum, medial lemniscus in the cat and their plasticity.	70
Chapter	V Lesion-induced sprouting in the kitten ----- red nucleus.	108
Chapter	VI List of publications -----	140
	Acknowledgements -----	142

CHAPTER I

GENERAL INTRODUCTION

GENERAL INTRODUCTION

"Plasticity" of the central nervous system is one of the most characteristic function of it. Mechanisms of the plasticity in higher animals, such as learning, memory and neural compensation, have not been understood yet. However, some modifications of neural system have been found and extensively investigated in the neonatal visual system (Wiesel and Hubel, 1965; Blakemore and Van Sluyters, 1974; Hirsch and Spinelli, 1971) and for vestibuloocular reflex (Ito, 1980). It is difficult to analyze the neural mechanisms concerning the behavioural plasticity in the complex mammalian brain. It is important and probably successful approach for studying the plasticity of the brain to investigate cellular bases of the plasticity. The basic process of modifications of nervous system is synaptic plasticity. The synaptic plasticity is divided into two categories; (A) axonal sprouting and formation of new synapses; (B) plasticity of synaptic transmission. Sprouting of new synapses has long-lasting effect, while plasticity of synaptic transmission which includes frequency potentiation, posttetanic potentiation and longterm potentiation has temporal effect within several hours. In our laboratory, axonal sprouting and formation of new synapses after chronic lesion of the contralateral nucleus interpositus (IP) of the cerebellum, frequency potentiation and posttetanic potentiation of the cerebellar synapses in the cat have been investigated in detail by Tsukahara and co-workers (Tsukahara et al., 1974, 1975; Murakami et al., 1977a,b).

This thesis focuses on the former synaptic plasticity of the sprouting of new synapses in the red nucleus (RN) in wider extent. Phenomena of sprouting of synapses are further divided into three sub-categories; (1) lesion-induced sprouting in the early developmental stage; (2) lesion-induced sprouting in the adult; (3) sprouting without lesions. In this thesis, axonal sprouting and formation of new synapses in above three sub-categories of the sprouting are investigated in RN cells. Fig.1 illustrates the results of this study diagrammatically.

Formation of functional synapses in RN neurons after cross-innervation of peripheral nerves where the inputs and outputs of RN cells are remained intact is investigated in chapter 2 and 3 (Fig.1G). In chapter 4, association cortex, secondary somatic sensory area, medial lemniscus and pretectal area inputs to RN other than the previously identified sensorimotor cortex and IP inputs are examined in the adult cat. Further, lesion-induced sproutings of the parietal association cortex- and medial lemniscal-RN synapses following the IP lesion will be shown. In the next chapter (chapter 5), lesion-induced sprouting in the kitten RN neurons after the cerebral or cerebellar input destruction are described (Fig. 1A-C). It will be shown that the extent and degree of sprouting

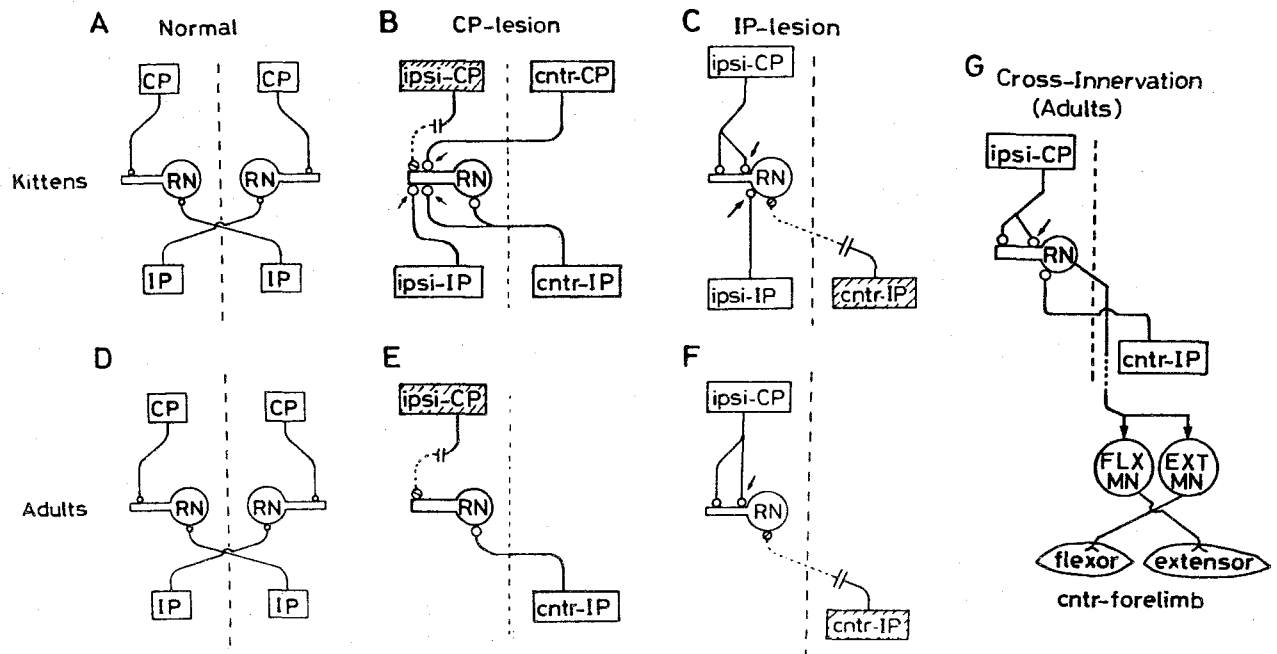


Fig.1 Diagram of synaptic connections of the red nucleus (RN).
A,B,C: Synaptic connections of kitten red nucleus neurons in normal (A), after chronic destruction of the ipsilateral cerebro-rubral input (CP-lesion) (B), and after chronic lesion of the contralateral nucleus interpositus (IP) of the cerebellum (C). D,E,F: Same as A,B,C but in adult cat red nucleus neurons. G: Synaptic connections in the adult cat red nucleus neurons after cross-innervation of the contralateral forelimb flexor and extensor nerves. CP: Cerebral peduncle. ipsi-CP, ipsi-IP: ipsilateral-CP and ipsilateral-IP. contr-IP, contr-CP: contralateral-IP and contralateral-CP. FLX MN: flexor motor neuron. EXT MN: extensor motor neuron. Arrows indicate the sprouting.

in RN neurons at the early developmental stage are remarkably higher than those of the adult cat. The detailed introduction of each succeeding chapter will be presented at the top of each chapter.

REFERENCES

- Blakemore C, Van Sluyters RC (1974) Reversal of the physiological effects of monocular deprivation in kittens: Further evidence for a sensitive period. *J Physiol (Lond)* 237: 195-216
- Hirsch HVB and Spinelli DN (1971) Modification of the distribution of receptive field orientation in cats by selective visual exposure during development. *Exp Brain Res* 12: 509-527
- Ito M (1980) Investigation of motor learning mechanisms in the cerebellar flocculus. In: *Integrative Control Functions of the Brain*. Ito M, Tsukahara N, Kubota K, Yagi K (ed) Vol. 3: pp. 351-367, Kodansha/Elsevier, Tokyo, Amsterdam
- Murakami F, Tsukahara N, Fujito Y (1977a) Analysis of unitary EPSPs mediated by the newly-formed cortico-rubral synapses after lesion of the nucleus interpositus of the cerebellum. *Exp Brain Res* 30: 233-243
- Murakami F, Tsukahara N, Fyjitto Y (1977b) Properties of synaptic transmission of the newly-formed cortico-rubral synapses after lesion of the nucleus interpositus of the cerebellum. *Exp Brain Res* 30: 245-258
- Tsukahara N, Hultborn H, Murakami F (1974) Sprouting of cortico-rubral synapses in red nucleus after destruction of the interpositus of the cerebellum. *Experientia* 30: 57-58
- Tsukahara N, Hultborn H, Murakami F, Fujito Y (1975) Electrophysiological study of the formation of new synapses and collateral sprouting in the red nucleus after partial denervation. *J Neurophysiol* 38: 1359-1372

CHAPTER II

FORMATION OF FUNCTIONAL SYNAPSES IN ADULT CAT RED NUCLEUS
FROM THE CEREBRUM FOLLOWING CROSS-INNervation OF FLEXOR
AND EXTENSOR NERVES. I. APPEARANCE OF NEW SYNAPTIC POTENTIALS.

INTRODUCTION

After partial denervation, sprouting occurs in some central neurons of adult and immature mammals (Cotman and Lynch, 1976; Lund, 1978; Raisman, 1977; Tsukahara, 1981). Furthermore, physiological investigations using extracellular (Wall and Egger, 1971; Lynch et al., 1973) and intracellular (Tsukahara et al., 1974; 1975a,b, Murakami et al., 1977a,b) recording techniques suggest that these newly-formed synapses are physiologically active. However, to what extent the formation of new synapses occurs under conditions other than partial denervation remains to be explored.

Sperry (1942, 1947) investigated the functional compensation in movement disorders after "cross-innervation" of nerves innervating the flexor and extensor muscles of various mammals and found that in monkeys motor relearning occurs, an observation which has never been made in similarly treated rats. Eccles et al. (1962) examined the possible change in the synaptic connections of spinal motoneurons after cross-innervation of hindlimb flexor and extensor nerves. Although they found evidence suggesting the formation of new synapses on motoneurons after cross-innervation, sprouting was restricted to a group of motoneurons which were axotomized. Furthermore, the degree of reorganization was very small. Since synaptic plasticity at higher levels of the nervous system is expected to be larger than in the spinal cord, it would be of great interest to know whether synaptic

connections of supraspinal neurons undergo some modification after cross-innervation of flexor and extensor nerves.

Regarding red nucleus (RN) neurons, after destruction of the cerebellar nucleus interpositus (IP), a fast-rising component appears in corticorubral EPSPs; this was taken to indicate that new synapses are formed at the proximal portion of the soma-dendritic membrane of RN cells (Tsukahara et al., 1974, 1975a,b; Murakami et al., 1977a,b). This interpretation has been partly supported by electron microscopic studies (Nakamura et al., 1974; Hanaway and Smith, 1978; Murakami et al., 1981).

In the present investigation we examined whether similar changes occur in cat RN neurons after cross-innervation of forelimb extensor and flexor nerves. In some RN neurons, a fast-rising component appeared in corticorubral EPSPs, as in the case of IP lesions, suggesting the occurrence of corticorubral sprouting at the proximal part of the RN cell membrane. A preliminary report has been made (Tsukahara and Fujito, 1976).

METHODS

Cross- or self-union surgery Adult cats were used; in 43 cross-innervation, and in 2 self-union surgery was performed under aseptic conditions. Only unilateral forelimbs were operated contralaterally to the intracellular recording of RN cells. The cats were anesthetized with pentobarbitone sodium, the musculocutaneous, median, ulnar, and radial nerves were dissected out at the axillary region and cut

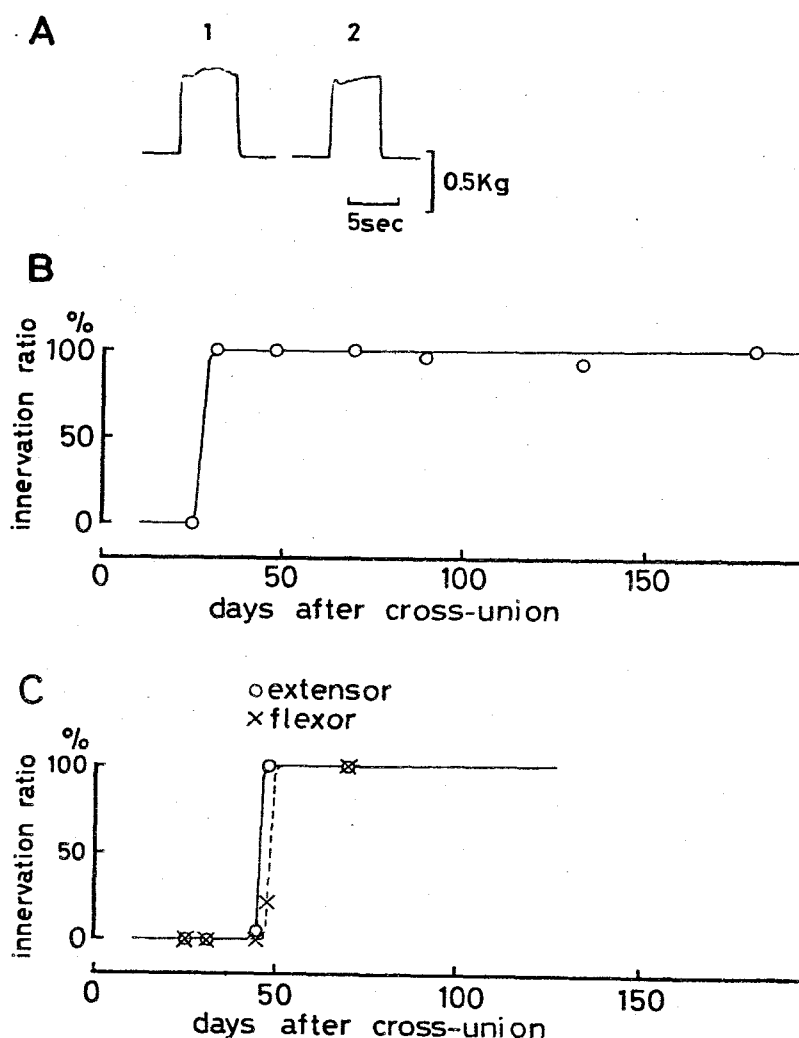


Fig.1 Time course of reinnervation

A: Isometric tension produced (1) by direct stimulation and (2) stimulation of the cross-innervated radial nerve in the biceps muscles 87 days after cross-innervation. B: Change in the innervation ratio after cross-innervation (m. biceps brachii) (ratio of isometric tension produced by nerve stimulation to that produced by direct muscle stimulation). C: Data as in Fig. B; (o), m. extensor digitorum communis; (x) m. flexor palmaris longus.

for cross- or self-union. The central stumps of the musculocutaneous, median and ulnar nerves were united to the peripheral stump of the radial nerve by suturing the nerve sheath with a fine nylon thread using a binocular microscope. The central stump of the radial nerve was similarly united to the peripheral stumps of the musculocutaneous, median and ulnar nerves. For self-union, the forelimb nerves were sectioned and re-united, without crossing, by suturing the nerve sheath.

To evaluate the degree of re-innervation, the distal tendon of m. triceps brachii, and m. biceps brachii, m. extensor digitorum communis, and m. flexor palmaris longus were cut, and the distal portion of each muscle was freed of the surrounding structure. The cut tendon was then attached to a tension transducer to measure the isometric tension induced by direct, as well as by nerve, stimulation. The degree of functional re-innervation was estimated by the ratio of maximal tension obtained by nerve stimulation (Fig.1A2) to that produced by direct muscle stimulation (Fig.1A1). Complete reinnervation required about one month for upperarm muscles, and two months for forearm muscles (Fig.1B,C).

Behavior after cross-innervation. Although we did not perform a systematic analysis of the behavior of cross-innervated cats, we have made some observations on the cross-innervated forelimbs of two cats. The movement of the elbow joint during voluntary goal-directed forelimb movement was observed by a television monitor system.

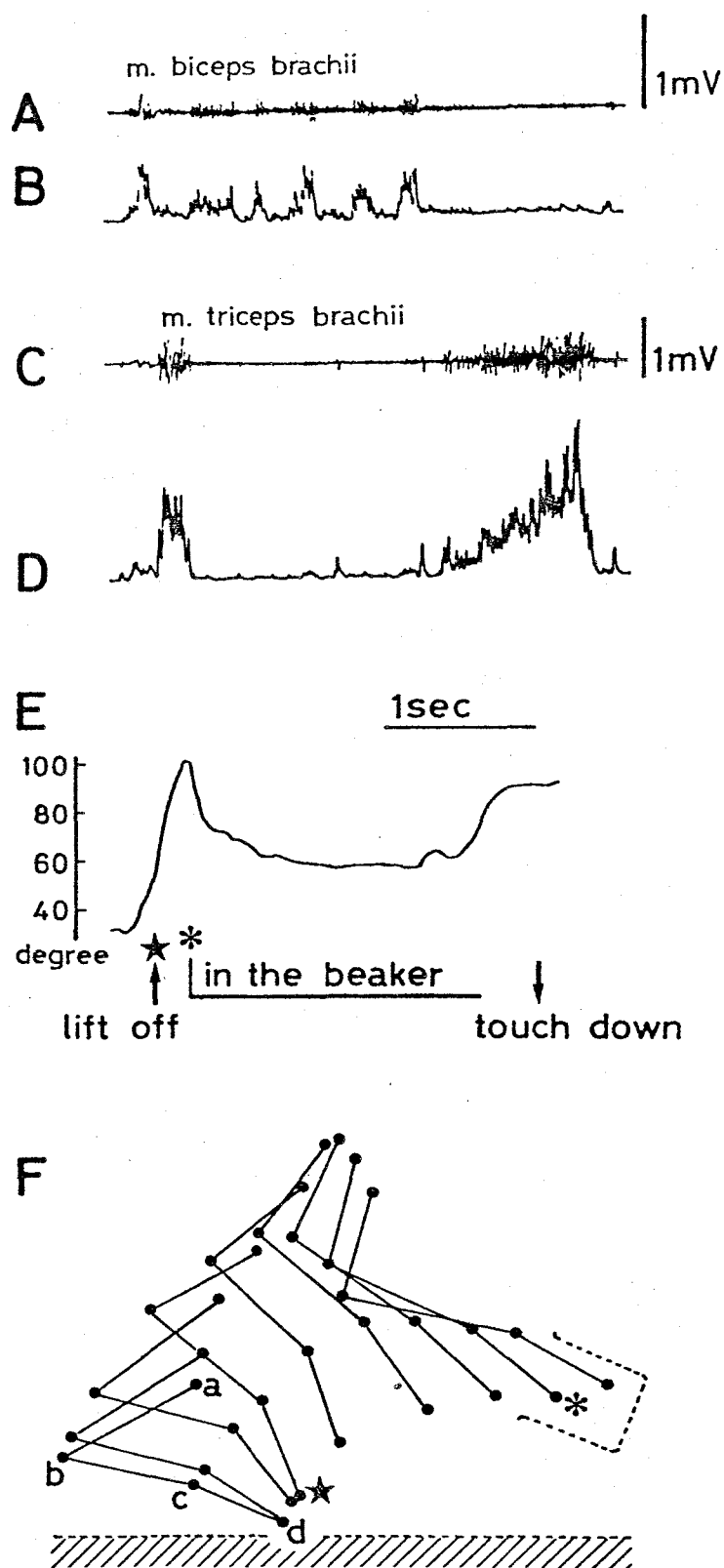


Fig.2

Fig.2 EMGs and joint movement of the cross-innervated forelimb during voluntary movement in a cat cross-innervated 99 days previously. In this and succeeding experiments involving behavioral observations, the musculocutaneous and radial nerve supplying the triceps brachii were cross-innervated.

A,B: EMG from the elbow flexor (m. biceps brachii). In A, the EMG has been passed through a high-pass filter (-3dB at 33 Hz). The EMG shown in A was integrated with a time constant of 10msec after full-wave rectification and the integrated EMG is shown in B. C: EMG from the elbow extensor (m. triceps brachii) after passage through the high-pass filter. D: the integrated EMG from C. E: Time course of elbow joint angle excursion as measured on the video-recorder display. The time calibration in E also applies to A-D. F: Stick diagram of the forelimb during the movement of lifting the forelimb and putting the paw into a beaker containing food. The time of lifting off and the time of putting the paw into the beaker are indicated by a star and asterisk respectively, in both E and F. In F, a,b,c and d represent the position of the shoulder, elbow, wrist and paw, respectively. Each stick was sampled at every 50 msec interval.

Electromyographic (EMG) recordings from the m.biceps brachii and m. triceps brachii of the cross-innervated forelimb were made simultaneously with cinematographic analysis of forelimb movement. The timing of the cinematographic and electromyographic recording was matched by the use of photodiode signals which were recorded simultaneously in the video recorder and electromyograms. Fig.2 illustrates the movement of a cross-innervated forelimb during food catching. This cat, which was cross-innervated three months previously, can flex and extend the forelimb freely, with active tension development registered on the electromyograms. Fig.2A and C show electromyographic recordings^g from the m. biceps brachii and m. triceps brachii, respectively. The corresponding integrated records are shown in Fig.2B and D. Elbow joint movement was measured from video records, and changes of elbow joint angle are plotted with the same time scale (Fig.2E). During goal-directed movement, elbow joint extension is associated with EMG activity in the triceps muscle and flexion with EMG activity in the biceps muscle. The trajectory of the forelimb during goal-directed movement is shown in Fig.2F. The forepaw reaches the target beaker smoothly without any oscillation. This suggests that coordination of the cross-innervated forelimb within the elbow, shoulder, and wrist joints is well developed.

In contrast to the smoothly coordinated movement of the cross-innervated forelimb during voluntary movement,

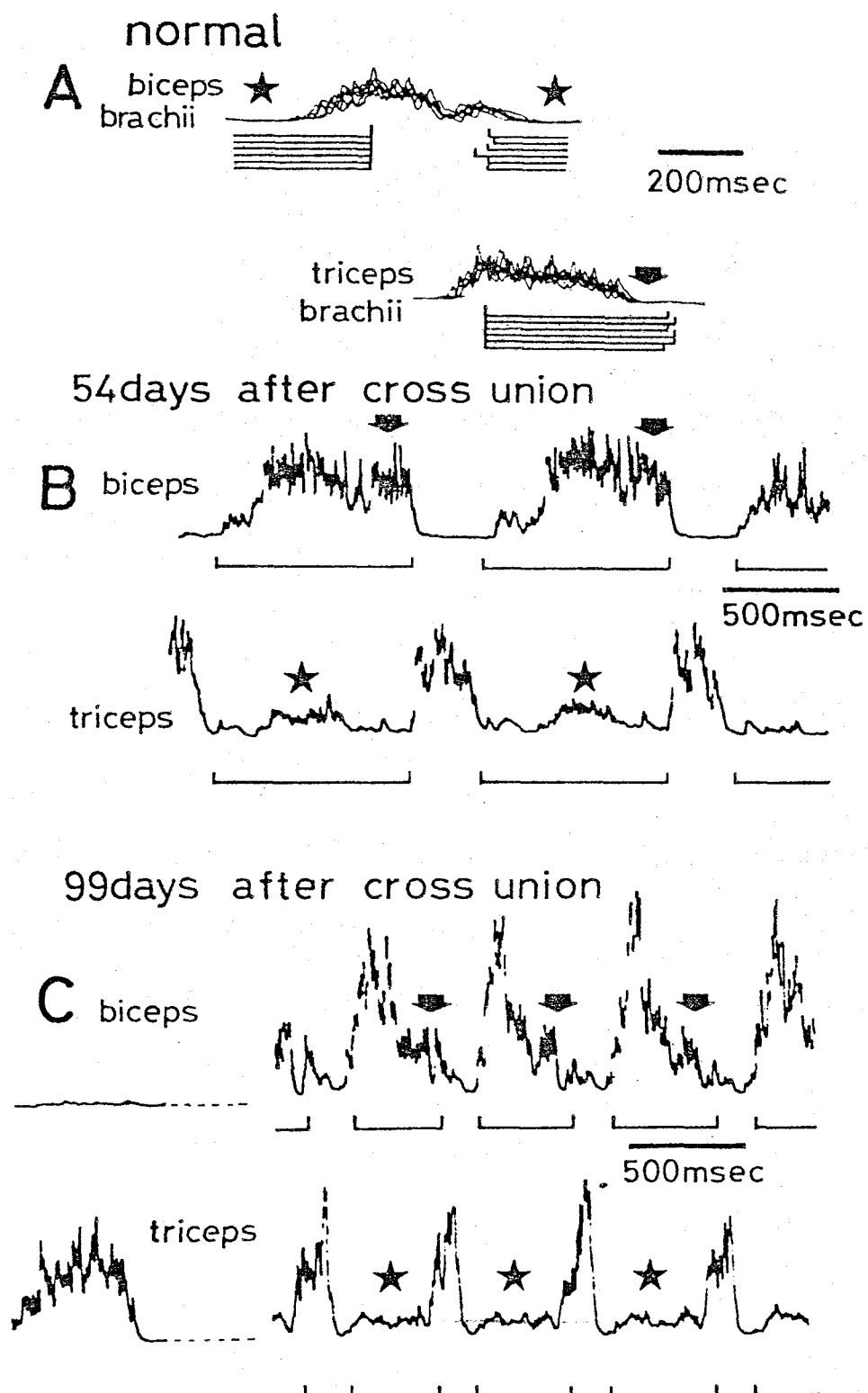


Fig.3

Fig.3 EMGs from the elbow flexor and extensor in normal and cross-innervated walking cats. EMGs have been passed thorough a high-pass filter and integrated as in Fig.2. A: superimposed traces of the integrated EMGs of a normal walking cat (from Udo et al., 1980 Fig.10). B: Integrated EMGs of a walking cat cross-innervated 54 days previously. C: Integrated EMGs of a walking cat cross-innervated 99 days previously. In A-C, upper traces are integrated EMGs from the elbow flexor (m. biceps brachii) and lower traces are integrated EMGs from the elbow extensor (m. triceps brachii). Horizontal bars indicate the stance phase. Stars indicate the middle of the stance phase and arrows mark the final one thirds of the stance phase. Note that in the normal cat, no muscle activity is evident at the stages marked by stars or arrows; whereas in cross-innervated cats muscle activity is evident at both these stages.

movement of the same forelimb during locomotion is not well-coordinated. In normal walking cats one cycle of locomotion can be divided into swing and stance phases (Engberg and Lundberg, 1969; Goslow et al, 1973; Udo et al., 1980). In normal animals flexor (biceps brachii) activity is enhanced in the swing phase and in the late stance phase, and there is no biceps activity in the early stance phase (Fig.3A). In contrast, extensor triceps activity is enhanced in the early stance phase, and there is no triceps activity in the late stance phase (Fig.3A).

In a cat cross-innervated between the nerves of m. triceps brachii and m. biceps brachii 54 days previously, the basic locomotor patterns of elbow joint movement are reversed (Fig.3B). However, superimposed upon these reversed EMG patterns, some compensating muscle activity is also evident. In this animal, flexor activity is enhanced during both the early and late part of the stance phase; while extensor activity is enhanced during both the swing phase and, less prominently, during the stance phase. Similar results were observed at 99 days after cross-innervation, as shown in Fig.3C. These results therefore suggest a partial compensation for the reversed movement, although locomotion was found to be dominated by reversed movements even after three months of cross-innervation.

Intracellular recording Procedures for intracellular recording from RN neurons were essentially as reported previously (Tsukahara et al., 1975a). RN neurons were identified antidromically by stimulating the contralateral C₁ and L₁

spinal segments; RN neurons activated from C_1 and L_1 were designated "L-cells", those activated only from C_1 , "C-cells" (Tsukahara and Kosaka, 1968). Corticorubral fibers were stimulated at two levels; within the sensorimotor cortex (SM) and the cerebral peduncle (CP).

RN cell population responses were produced by IP-stimulation conditioned by corticorubral excitation, which was induced by stimulating the cerebral peduncle (CP). Facilitation of the population responses was processed by a mini-computer equipped with a controlled stimulating and averaging system. The intervals between stimuli and the number of repetitions were controlled by a minicomputer; the field potentials were averaged, displayed on the oscilloscope and photographed automatically.

RESULTS

Intracellular records were obtained for 328 RN neurons from 43 cross-innervated cats and 28 RN neurons from 2 self-union cats. The RN neurons were identified antidromically by stimulation of C_1 and L_1 spinal cord.

1. Appearance of a fast-rising component in composite corticorubral EPSPs

Typical slow cerebral peduncle (CP)-EPSPs evoked in a RN cell by CP stimulation in a normal cat are illustrated in Fig.4A (Tsukahara and Kosaka, 1968). Figures 4B-E show the CP-EPSPs from a cat subjected 176 days earlier to cross-

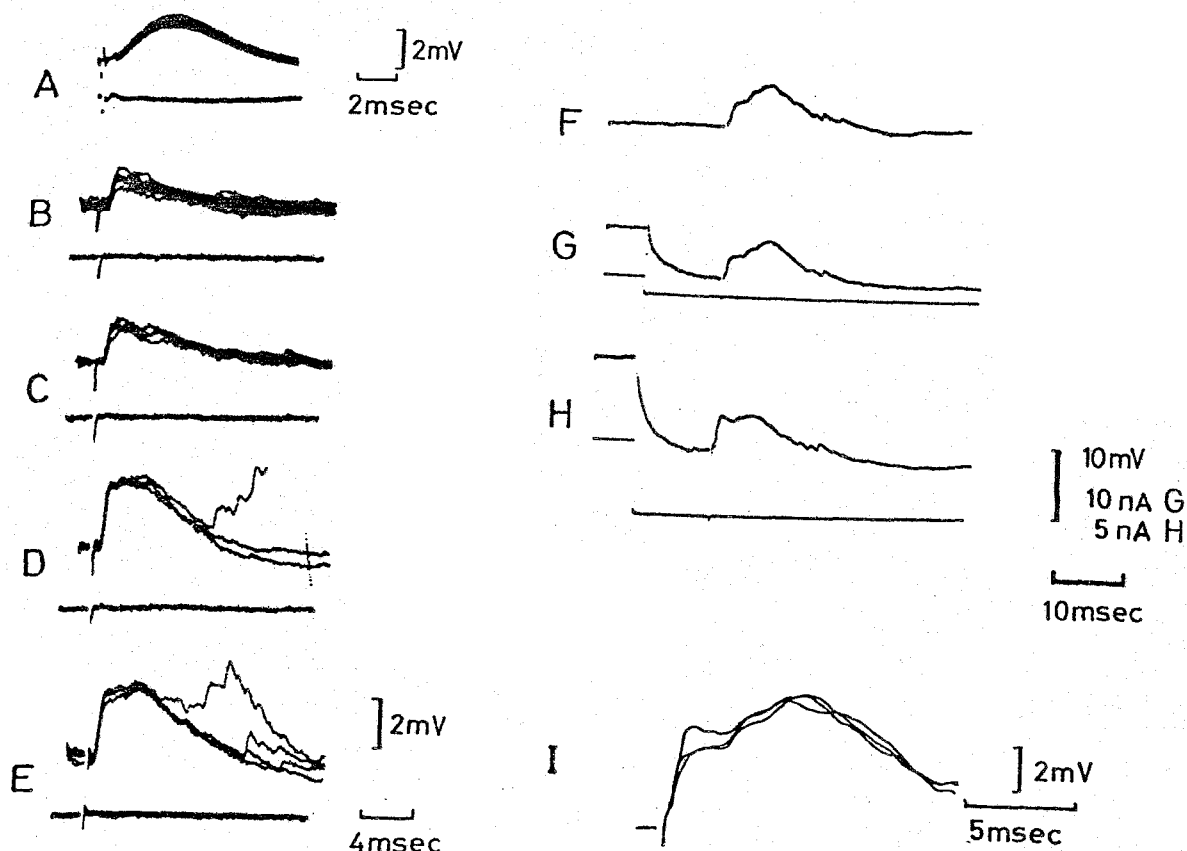


Fig.4 Corticorubral EPSPs in cross-innervated cats

A: CP-EPSP induced in a RN cell from a normal cat. B-H: CP-EPSPs in RN cells of cross-innervated cats. B-E, CP-EPSPs induced with increasing CP stimulus intensities from B to E in a RN cell innervating the upper spinal segments. Upper traces, intracellular potentials; Lower traces, extracellular records corresponding to upper traces. Voltage and time calibrations of E also apply to B, C, D. F-H: Records from a cat cross-innervated 147 days before intracellular recording. CP-EPSPs during membrane hyperpolarization; the current was applied in step-wise fashion as indicated in the lower traces of G and H. F: Control CP-EPSP. I: Superimposed tracings of CP-EPSPs shown in F-H. Voltage and time calibration of H also apply to F and G.

innervation of the forelimb flexor and extensor nerves. CP-EPSPs of a RN cell innervating the upper spinal segment had a fast-rising component superimposed on the slow-rising one. By changing the intensity of the stimulus, the fast-rising component could be graded in amplitude. The time-to-peak of the fast-rising component was about 1 msec; that of the slow rising component was about 3 msec. The latter value approximates that of normal CP-EPSPs (3.6 msec on the average for 100 RN cells; Tsukahara et al., 1975a).

The mean latency of the fast-rising component of the CP-EPSP was 0.96 ± 0.19 msec ($n=122$) for C-cells from cross-innervated cats. This value is not significantly different from that of normal cats (1.0 ± 0.2 msec, $n=100$). Therefore, we concluded that the fast-rising components are produced monosynaptically.

The sensitivity of the EPSPs to membrane polarization was tested by changing the membrane potential. As seen in Fig.4G-H and the superimposed trace in Fig.4 I, the fast-rising component increased in size, whereas the slow-rising component remained virtually unchanged. This indicates that the synapse producing the fast-rising component is located more proximally on the soma-dendritic membrane of RN cells than that producing the slow-rising component.

A similar fast-rising component with longer latency than that of the CP-EPSP (Fig.5A) could be induced by stimulating the cerebral sensorimotor cortex (SM) (Fig.5B). The conduction

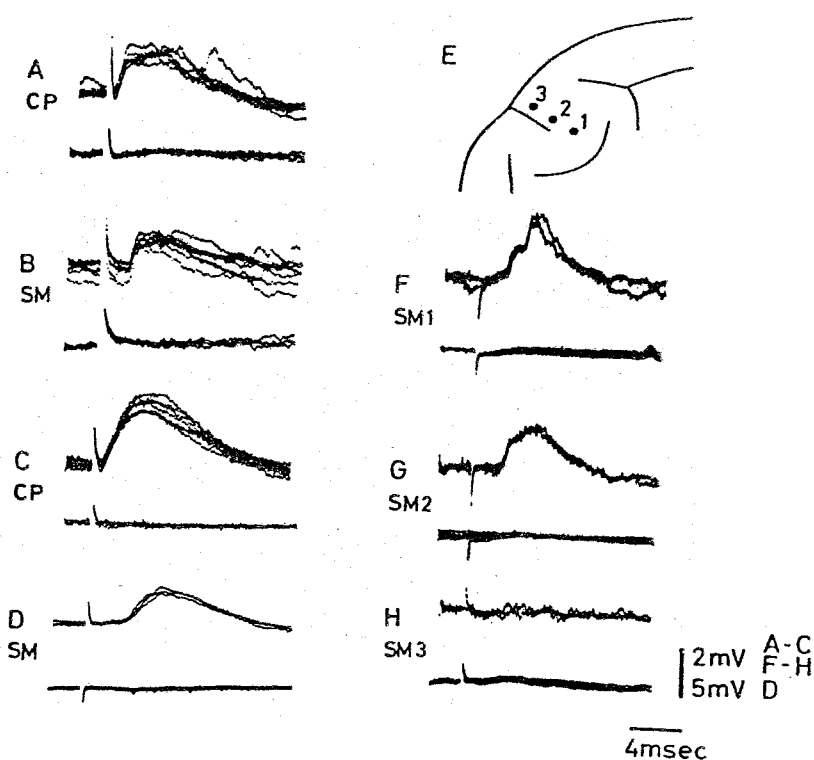


Fig.5 Somatotopical organization of the projective area of the newly-appeared corticorubral EPSPs after cross-union

A: CP-EPSPs produced in a RN cell (C-cell) 176 days after cross-innervation.

B: Sensorimotor cortex (SM)-EPSPs produced in the same cell as A.

C: CP-EPSPs produced in an L-cell 188 days after cross-innervation

D: SM-EPSPs produced in the same cell as C. E: Sites of SM stimulation.

F-H: SM-EPSPs produced in a C-cell by stimulating electrodes located in 1 (SM1), 2 (SM2), 3 (SM3) (E) 140 days after cross-innervation.

velocity of corticorubral fibers responsible for the fast-rising components was estimated as 16 m/sec; a value in the same range as that of corticorubral fibers mediating the slow rising component (20 m/sec, Tsukahara and Kosaka, 1968).

The corticorubral projection is organized somatotopically (Tsukahara and Kosaka, 1968; Padel et al., 1973). The cells innervating the lower spinal segments (L-cells) receive inputs from the medial part of the pericruciate cortex and parietal association cortex (Fujito et al., 1978). RN cells innervating the upper spinal segment (C-cells) receive cortical inputs from the lateral part of the pericruciate cortex. Figures 5F-H show the corticorubral EPSPs in a C-cell from a cross-innervated cat operated 140 days earlier. Stimulation of the lateral part of the pericruciate cortex (Fig. 5E) produced a fast-rising component superimposed on the slow-rising ones (Fig. 5F). Stimulation of the medial part of the postcruciate cortex, however, elicited no responses (Fig. 5H). It is likely that the fast-rising component of the corticorubral EPSPs is produced from a region similar to that from which the slow-rising component derives.

Times-to-peak of CP-EPSPs, corrected for extracellular field potentials, were measured for C- and L-cells in cross-innervated cats. If dual peaks occurred, the initial peak was used to determine the time-to-peak of the EPSPs. The frequency distribution of the time-to-peak is illustrated

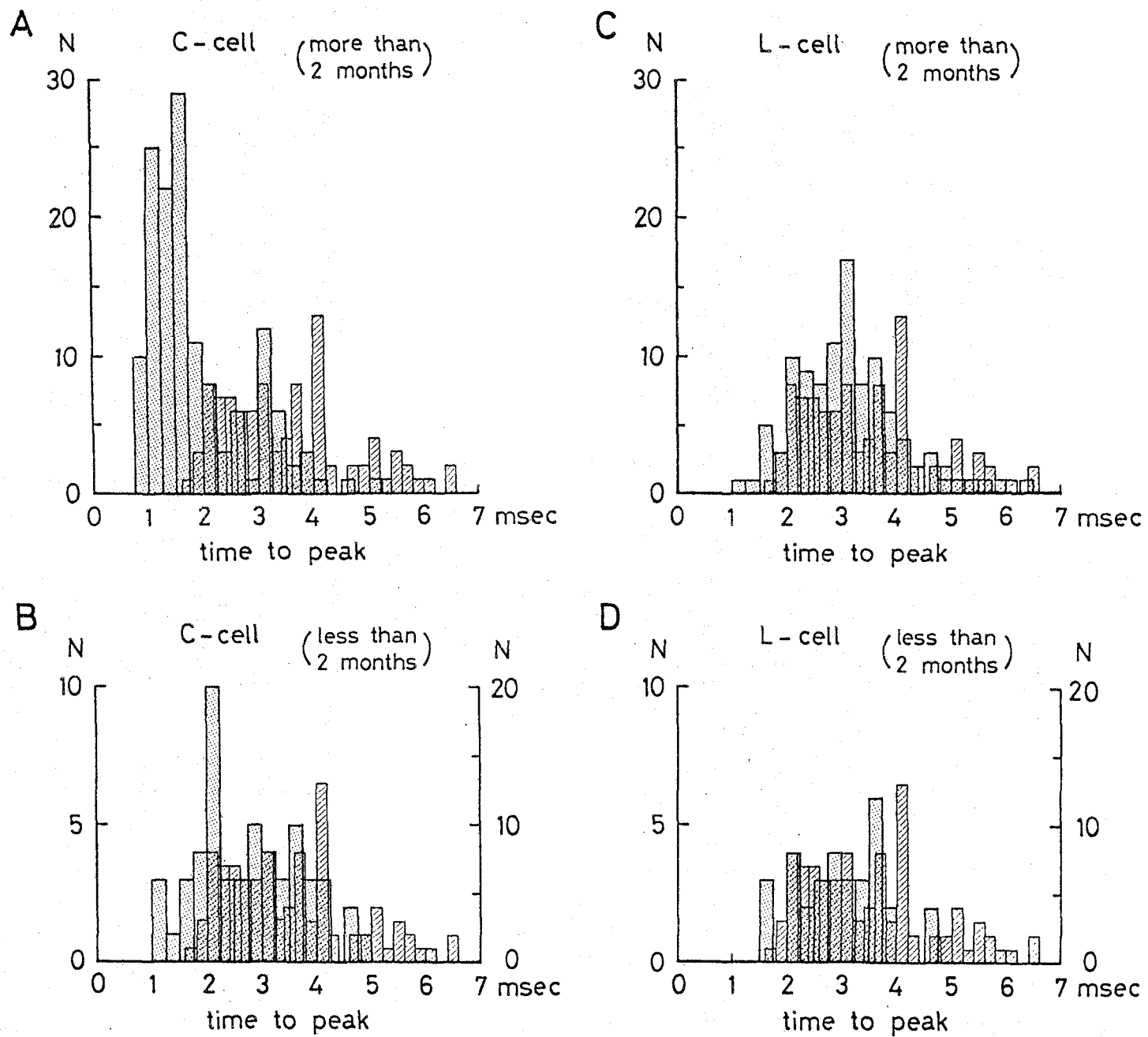


Fig. 6

Fig.6 Frequency distribution of time-to-peak of CP-EPSPs in cross-innervated cats. The number of cells is shown on the ordinate as dotted column, the time-to-peak of CP-EPSPs on the abscissa. The shaded columns in A-D illustrate the previously reported frequency distribution of time-to-peak in normal cats (Tsukahara et al., 1975a). The right-hand ordinate in Fig. B and D applies to normal cats, and common to A-D. The left-hand ordinate applies to cross-innervated cats. Data are from cats cross-innervated more (A,C) and less (B,D) than two months before the acute experiments.

in Fig.6. Since for complete re-innervation of the forearm muscles about 2 months are required (Fig.1), CP-EPSPs were divided into two groups; CP-EPSPs from cats operated less- and more than two months earlier. The mean time-to-peak of the CP-EPSPs for C-cells shown in Fig.6A was 1.9 ± 0.9 msec ($n=160$); this is significantly shorter ($p < 0.001$) than in normal cats (3.6 ± 1.4 msec, $n=100$; Tsukahara et al., 1975a). On the other hand, time-to-peak of the CP-EPSPs from C-cells shown in Fig.6B is much longer; the mean time-to-peak was 2.7 ± 1.0 msec ($n=53$). CP-EPSPs from most L-cells manifested a much longer time-to-peak than from C-cells (Fig.6C,D). The mean time-to-peak of CP-EPSPs from L-cells was 2.9 ± 0.9 msec ($n=115$).

CP-EPSPs with fast-rising components were recorded from a wide area in RN. We attempted to record RN cells from an area covering stereotaxic coordinates A.2.5 to A.5.5. The recording position was determined from the stereotaxic apparatus; readings of the rostrocaudal coordinates were plotted against the time-to-peak of CP-EPSPs from the respective RN cells (Fig.7). The sites were widely distributed in the RN region.

The time-to-peak of the CP-EPSPs of C-cells is plotted in Fig.7A. The slow-rising component of ^{dual-peaked} CP-EPSPs of C-cells is also plotted by open triangles in Fig.7A. The time-to-peak of CP-EPSPs of L-cells is plotted in Fig.7B.

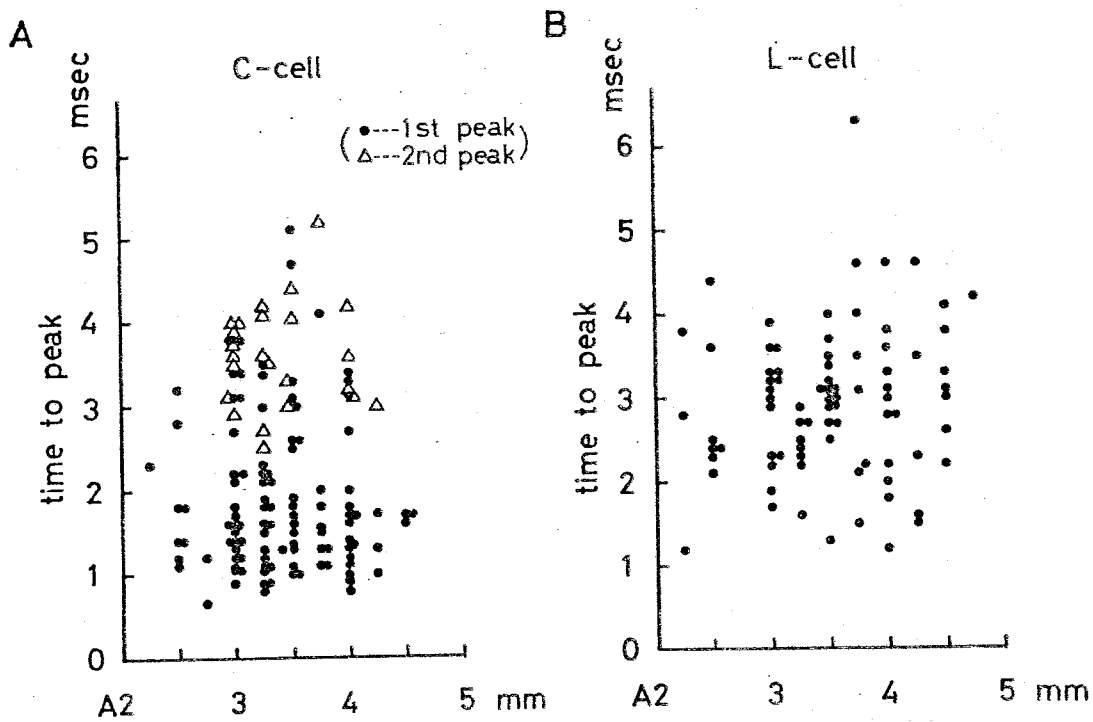


Fig.7 CP-EPSPs recorded at various sites along the rostro-caudal axis of the red nucleus.

A: Ordinate; time-to-peak of CP-EPSPs; abscissa, location of the RN cells (C-cells) in the anterior posterior coordinate of the stereotaxic coordinate. B; Same as in A, but for L-cells.

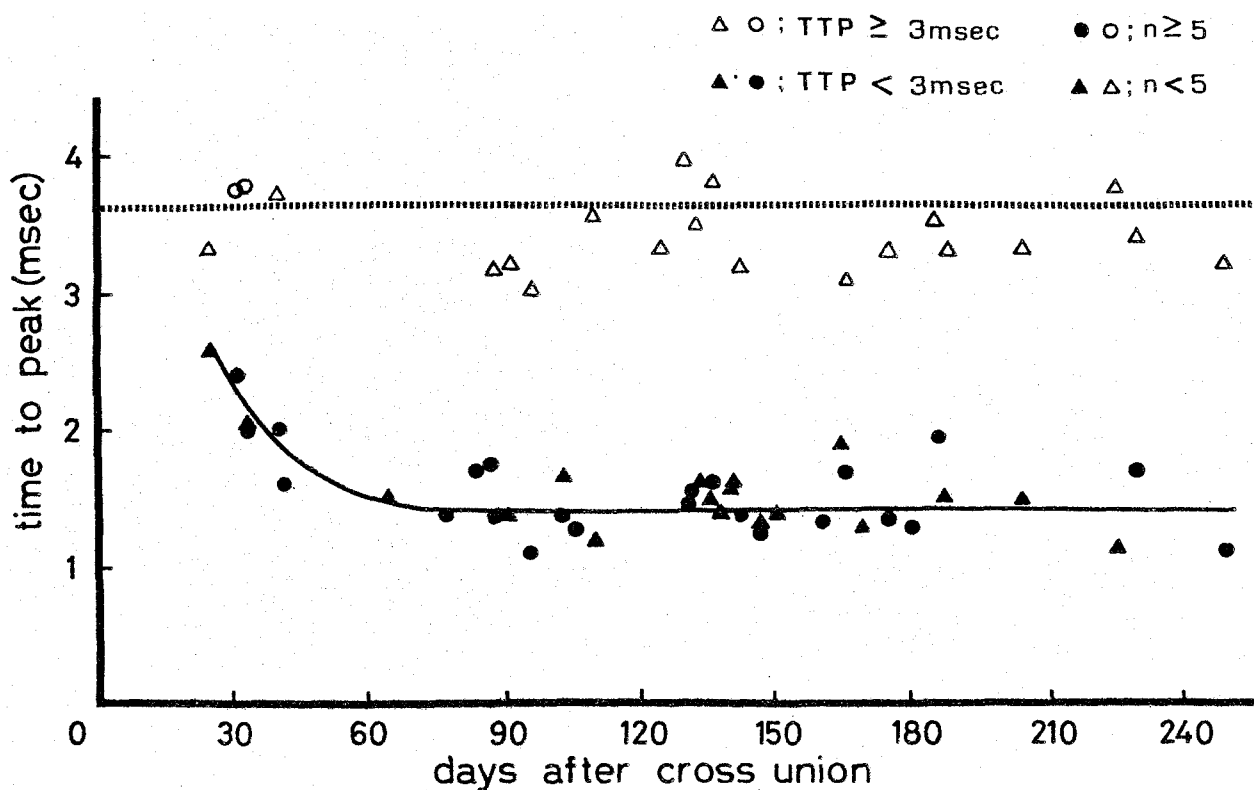


Fig.8 Time course of the change in the time-to-peak of CP-EPSPs after cross-innervation of forelimb nerves

Open circles and open triangles, the mean time to peak of the CP-EPSPs equal or more than 3 msec. Filled circles and filled triangles, mean time-to-peak of the CP-EPSPs less than 3 msec. From C-cells. Circles: average of more than 5 RN cells. Triangles: average of less than 5 RN cells.

Ordinate, time-to-peak of the CP-EPSPs. Abscissa, days after cross-innervation. Dotted line: mean time-to-peak of 100 CP-EPSPs in normal cats derived from Tsukahara et al., 1975a).

Time course of the change of time-to-peak of CP-EPSPs
after cross-innervation

To evaluate the time course of appearance of the fast-rising component ⁿis composite corticorubral EPSPs after cross-innervation, recordings were made at different periods after cross-innervation surgery. Fig.8 illustrates the relation between average time-to-peak and the days elapsed since cross-innervation. The CP-EPSPs of C-cells are divided into two arbitrary ⁿgroups; the one with time-to-peak less than 3 msec and the other with time-to-peak of CP-EPSPs equal and more than 3 msec. The mean time-to-peak of these two groups of CP-EPSPs was calculated in each cat and plotted in different symbols in Fig.8. Fast-rising components appeared within two months from cross-innervation.

CP-EPSP after self-union of forelimb nerves

The time course of corticorubral EPSPs was observed in cats subjected to self-union of the forelimb nerves. As shown in Fig.9, in most of the CP-EPSPs from C-cells, time-to-peak was within the normal range (3.2 ± 0.9 msec, n=28).

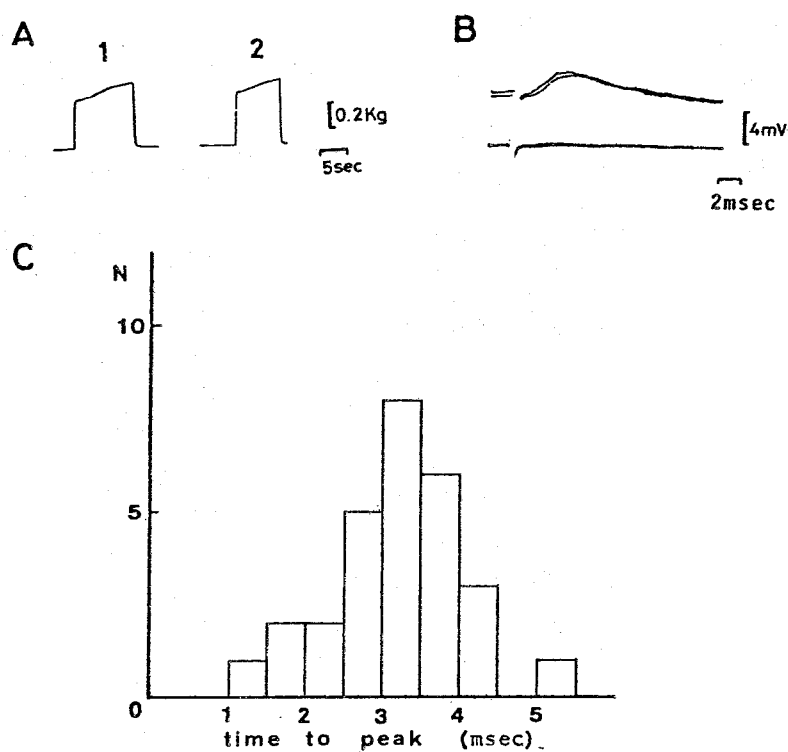


Fig.9 CP-EPSPs after self-union of forelimb nerves.

A: Isometric tension induced in the biceps muscle by direct (A1) and musculocutaneous nerve (A2) stimulation after 84 days of self union. B: Upper traces represent the intracellular responses in C-cell; lower traces show the extracellular controls. C: Frequency distribution of time-to-peak of CP-EPSPs from C-cells. The number of cells is shown on the ordinate.

Facilitation of RN population responses by conditioning
CP stimuli

As reported previously (Tsukahara et al., 1967), IP stimulation yields prominent field potentials in the RN region consisting of a presynaptic and postsynaptic component (Fig.10 A). When IP stimulation was preceded by CP stimulation, the amplitude of the postsynaptic component increased (Fig.10C) whereas that of the presynaptic component remained unchanged. In normal animals, the amplitudes increased gradually, peaked at about 3 msec interval and slowly returned to the control value. If the amplitudes of the postsynaptic components are averaged and plotted in terms of percent of the control values against stimulus intervals, the time course of the facilitation is similar to that of CP-EPSPs (Fig.10D). The interval for the maximal facilitation was measured in normal cats; the frequency distribution of this optimal interval is plotted in Fig.10E. The distribution was in good agreement with that of the time-to-peak of CP-EPSPs recorded intracellularly in normal cats.

Similar experiments were performed in cats subjected to cross-innervation (Fig.11). IP-induced field potentials were recorded from RN C- or L-cell regions, identified by antidromic field potentials evoked by C₁ and L₁ spinal segments. In the C-cell region, the facilitation curve revealed an additional early peak (Fig.11A-D,I) which was not noted in the L-cell region (Fig.11E-H,J).

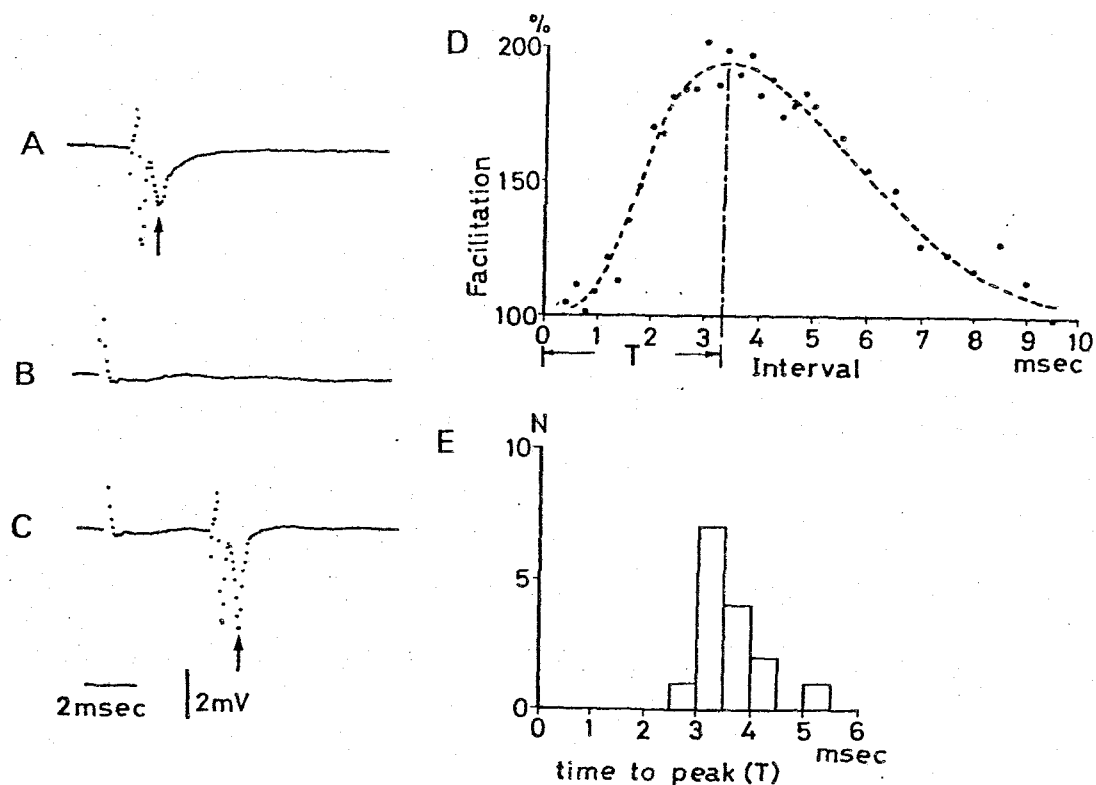


Fig.10 Facilitation of IP-induced field potentials by preceding CP stimuli in normal cats. A-C represent average field potentials in the red nucleus. Sixteen averagings were performed; the sampling time was 50 microseconds. A: IP-induced field potential in the control. B: CP-induced field potential as the background field potential for measuring the amplitude of subsequent IP-induced field potentials. C: The amplitude of the postsynaptic IP-induced field potential was facilitated by the preceding CP stimulation. D: Time course of the facilitation partly shown in A-C. The ordinate represents the amplitude of the postsynaptic component of the IP field potential, normalized in terms of percent of the control value. Abscissa: Interval between CP and IP stimulation. T shows the interval for peak facilitation. E: Frequency distribution of interval times for peak facilitation in normal cats. Upward arrows mark the peak of the postsynaptic field potentials.

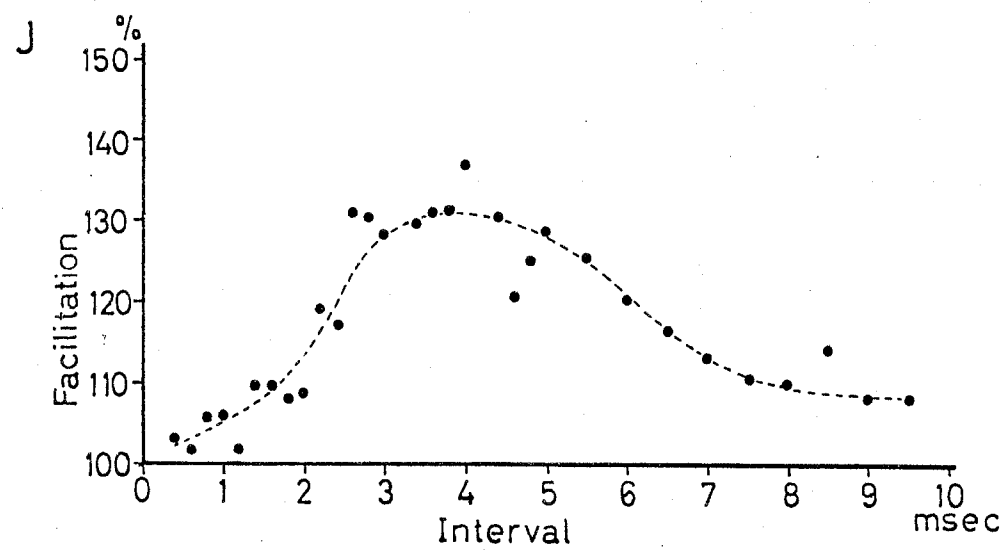
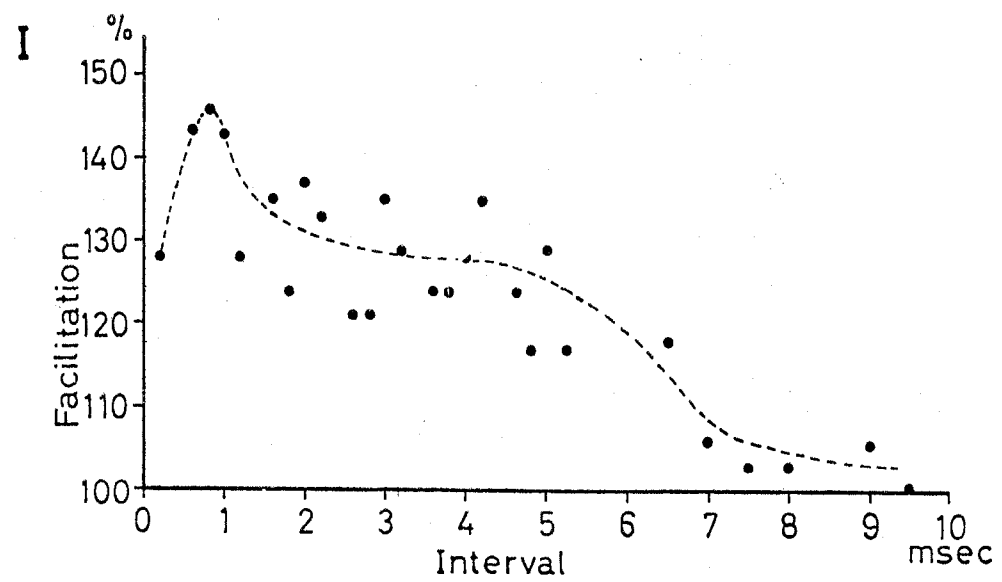
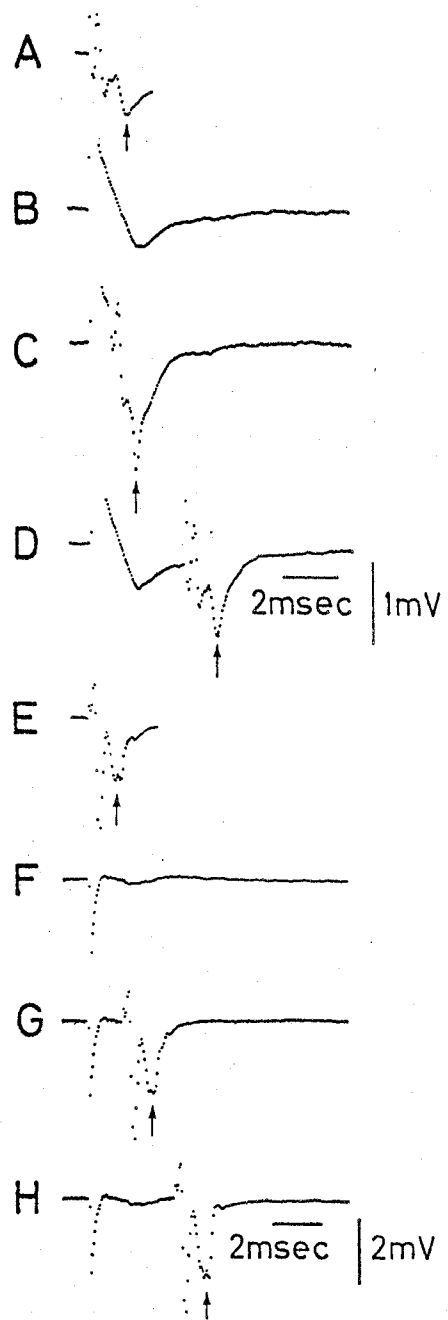


Fig. 11

Fig.11 Facilitation of IP-induced field potentials by conditioning CP stimulation on cross-innervated cats. A-H: Average field potentials in the red nucleus. A-D, facilitation of the IP-induced field potentials by preceding CP stimulation, recorded from the C-cell region. A: IP-induced field potential in the control. B; CP-induced field potential. C and D: Facilitation of the IP-induced field by the preceding CP stimulation. E-H: Facilitation recorded from the L-cell region of RN. E: IP induced field potential. F: CP-induced field potential. G and H: Facilitation of the IP-induced field potential by conditioning CP stimulation. I and J : Time course of the facilitation partly shown in A-D and E-H , respectively. Upward arrows mark the peak of postsynaptic field potentials.

Although assessing the time course of the facilitation of IP-induced RN population responses is an indirect method for evaluating the time course of the CP-EPSPs, it has a certain advantage in that it represents the activity of a population of RN cells, and further, the results obtained by this methods are from intact cells whose behaviour is not distorted by microelectrode impalement. Therefore, the time course of facilitation of IP-field potentials which was characterized by a rapid rise time, represents additional supportive evidence for the changing time course of CP-EPSPs in C-cells after cross-innervation. The frequency distributions of optimal intervals for facilitation of IP-field potential in the C- and L-cell region are shown in Fig.12A and B, respectively.

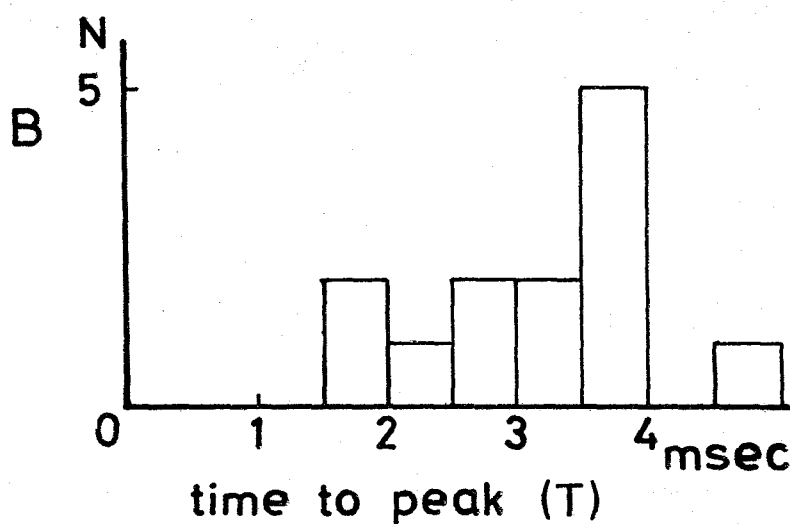
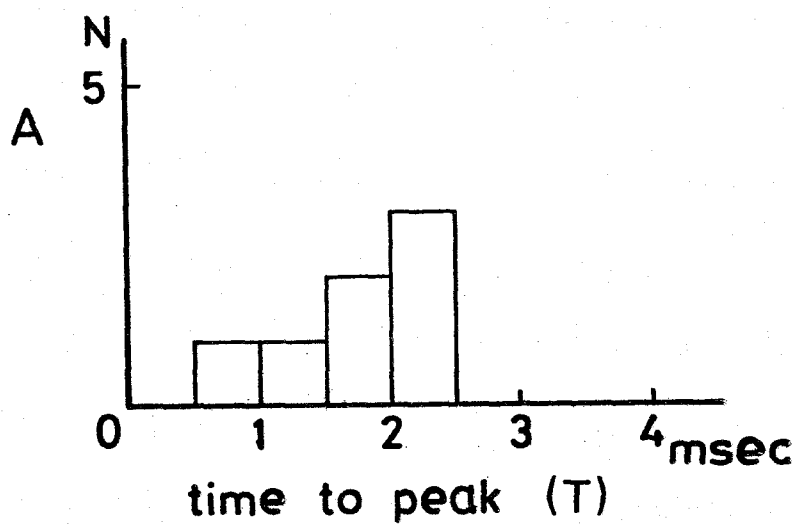


Fig.12 Frequency distribution of interval times for peak facilitation of cross-innervated cats. A: C-cell region of RN.
B: L-cell region of RN.

DISCUSSION

Sprouting is primarily found after the occurrence of lesions in central synaptic inputs (lesion-induced sprouting) and it is especially remarkable in the early developmental stages (Cotman and Lynch, 1976; Lund, 1978; Raisman, 1977; Tsukahara, 1981). Our present results suggest that sprouting also occurs in the absence of lesions in the direct synaptic inputs. This hypothesis is based on the observations that a fast-rising component appears superimposed on the original slow-rising corticorubral dendritic EPSPs after cross-innervation surgery. This is supplemented by additional data of the unitary corticorubral EPSPs and dendritic cable properties of RN cells after cross-innervation (Fujito et al., 1981). On analogy with the previous experiments (Tsukahara et al., 1974; 1975a) changing properties of corticorubral EPSPs after cross-innervation can be accounted for in terms of the formation of functional synapses at the proximal portion of the RN cell dendrites. This interpretation is supported by the results of electronmicroscopic studies on IP lesions (Nakamura et al., 1974; Hanaway and Smith, 1978; Murakami et al., 1981).

In the present experimental model, neither the synaptic inputs nor the axons of RN cells were destroyed and our present and previously reported results (Tsukahara and Fujito, 1976) may represent the first experimental demonstration suggesting the formation of functional synapses on intact central neurons of adult mammals. In peripheral nervous

system, Brown and Ironton (1977) showed that a few days of muscle inactivity act as a stimulus to sprouting at the neuromuscular junction. Rotshenker and McMahan (1976) and Rotshenker (1979) reported that in frogs with intact innervated muscles, the crushing of the motor nerve of one cutaneous pectoris muscle gives rise to sprouting on the contralateral side.

Changes in the time course of corticorubral EPSPs were found primarily in RN cells innervating the upper spinal segments (C-cells), although similar changes were observed in some L-cells. This is not surprising, as some L-cells extend collaterals to the upper spinal segments (Shinoda et al., 1977).

About two months after cross-innervation are required for the full establishment of the modification; this period corresponds with completion of forearm muscle re-innervation. This suggests that the mere dissection of the peripheral nerves is not the main factor in the induction of sprouting.

The remarkable coordination of the cross-innervated forelimb during voluntary goal-directed movement implies that reorganization of motor control has taken place somewhere in the brain. This idea is supported by the difference in motor performance between voluntary movements and stereotyped movements such as those involved in locomotion. A full interpretation of the behavioral adaptation observed after cross-innervation (Brinkman and Porter, 1977) or cross-connection of muscles (Yumiya et al., 1979) is a

tremendous tasks and remains to be explored. Nonetheless it is of some interest to speculate about the correlation between behavioral changes and the cellular changes in RN neurons which are observed after cross-innervation. The sprouting of corticorubral neurons onto the proximal portion of RN dendrites indicates a switching of control from cerebellar to cerebral predominance after cross-innervation, because the corticorubral synapses are located closer to the neuronal trigger zone. If these observed cellular changes are indeed part of the neuronal reorganization responsible for behavioral adaptation, the cerebral motor commands would be expected to be most effectively transmitted to the spinal cord during voluntary movements. If, in contrast, the stereotyped movements of locomotion are controlled mainly by cerebellar pathways, the disorders of locomotive movement should not show any improvement after cross-innervation, since no plastic change in the interpositorubra pathway was observed. Viewed in this context, the difference between behavioral adaptation during voluntary and involuntary movements becomes understandable.

Tsukahara et al. (1981) have reported that classical conditioning can be established by pairing an electric shock to the cerebral peduncle (conditioned stimulus) and the forelimb (unconditioned stimulus). Mediation of this conditioned response may be via the corticorubrospinal pathway and a possible site of the conditioned change may be the corticorubral synapses, since no appreciable change takes place along the interpositorubrospinal pathway after

the establishment of the conditioned responses. Therefore, the question of whether sprouting of the corticorubral synapses represents the neuronal basis of the conditioned change in classical conditioning, is an interesting topic for future studies.

SUMMARY. We investigated the effects of cross-innervating the peripheral forelimb flexor and extensor nerves of adult cats on the time course of corticorubral EPSPs. Red nucleus neurons were identified by antidromic invasion from C₁ or L₁ spinal segments as innervating the upper spinal segments (C-cells) or sending axons to the lumbosacral cord (L-cells).

In C-cells, a fast-rising component, superimposed on the slow-rising corticorubral EPSPs induced by cerebral sensorimotor cortex or the cerebral peduncle (CP) stimulation, was noted. The mean time-to-peak of this component in cross-innervated cats operated more than two months earlier was 1.9 ± 0.9 msec ($n=160$), shorter than in normal cats (3.6 ± 1.4 msec, $n=100$). The same value in cats cross-innervated less than two months before was 2.7 ± 1.0 msec ($n=53$). The mean time-to-peak of CP-EPSPs from L cells was 2.9 ± 0.9 msec ($n=115$).

The fast-rising component had a latency of 0.96 ± 0.19 msec ($n=122$), and it was mediated by fibers with conduction velocities of less than 20 m/sec. The projective area of the fast-rising component is organized somatotopically. Since it is more sensitive to membrane hyperpolarization than slow rising corticorubral EPSPs, it is mediated by synapses located more proximally than the corticorubral synapses of normal cats.

The time course of facilitation by preceding cerebral peduncle stimulation of the nucleus interpositus (IP)-induced RN population responses was measured. It was characterized by a rapid, followed by a slower rise time in the RN region where C-cells are concentrated. In contrast, the L-cell region was

characterized by a slow rise time.

In cats subjected to self-union of the peripheral flexor and extensor nerves, the majority of C-cells had CP-EPSPs with a time-to-peak within the normal range.

Our results suggest that after cross-innervation, sprouting and formation of functional synapses occur on the proximal portion of the soma-dendritic membrane of red nucleus neurons.

Key Words: Sprouting--Corticorubral Synapse---Red Nucleus
----Cross-Innervation--Sprouting Without Degeneration

REFERENCES

- Brinkman J , Porter, R (1977) Plasticity of motor behavior in monkeys with crossed forelimb nerves. Proc. Int. Congr. Physiol. Sci. 13: 96
- Brown M C, Ironton R (1977) Motor neuron sprouting induced by prolonged tetrodotoxin block of nerve action potentials. Nature 265:459-461
- Cotman C W , Lynch G S (1976) Reactive synaptogenesis in the adult nervous system: the effects of partial deafferentation on new synapses formation. In: Barondes S (ed) Neuronal Recognition , pp. 69-108, Plenum, New York.
- Eccles J C, Eccles R M, Shealey C N, Willis W D (1962) Experiments utilizing monosynaptic excitatory action on motoneurons for testing hypothesis relating to specificity of neuronal connection. J. Neurophysiol. 25: 559-579
- Engberg I , Lundberg A (1969) An electromyographic analysis of muscular activity in the hindlimb of the cat during unrestrained locomotion. Acta Physiol Scand , 75:614-630
- Fujito Y, Oda Y, Maeda J, Tsukahara N (1978) Synaptic inputs of the red nucleus neurons in the cat--a further study. Proc. Jap. Acad 54: Ser B. 65-68
- Fujito Y, Tsukahara N, Oda Y, Yoshida M (1982) Formation of functional synapses in adult cat red nucleus from the cerebrum following cross-innervation of forelimb flexor and extensor nerves. II. Analysis of newly-appeared synaptic potentials. Exp Brain Res

- Goslow G E , Reinking R.M , Stuart D G (1973) The cat step cycle:hindlimb joint angles and muscle lengths during unrestrained locomotion. J Morphol 141:11-42
- Hanaway J, Smith J (1978) Sprouting of corticorubral terminals in the cerebellar deafferented cat red nucleus. Soc. Neurosci Abstr 4: 1507
- Lund, R D (1978) Development and Plasticity of the Brain. Oxford, New York
- Lynch G, Deadwyler S, Cotman C W (1973) Postlesion axonal growth produces permanent functional connections. Science 180: 1364-1366
- Murakami F, Katsumaru H, Saito K, Tsukahara N (1981) An electron-microscopic study of corticorubral projections to red nucleus neurons identified by intracellular injection of HRP. Neurosci Lett Suppl (in press)
- Murakami F, Tsukahara N, Fujito Y (1977a) Analysis of unitary EPSPs mediated by the newly-formed corticorubral synapses after lesion of the nucleus interpositus of the cerebellum. Exp Brain Res 30:233-243
- Murakami F, Tsukahara N, Fujito Y (1977b) Properties of ^{the} synaptic transmission of the newly-formed corticorubral synapses after lesion of the nucleus interpositus of the cerebellum. Exp Brain Res 30:245-258
- Nakamura Y, Mizuno N, Konishi A, Sato M (1974) Synaptic reorganization of the red nucleus after chronic deafferentation from cerebellorubral fibers: an electron microscop study in the cat. Brain Res 82:298-301
- Padel Y, Smith A M, Armand J (1973) Topography of projections from the motor cortex to rubrospinal units in the cat. Exp Brain Res 17:315-332

- Raisman G (1977) Formation of synapses in the adult rat after injury: similarities and differences between a peripheral and a central nervous site. *Phil Trans Roy Soc London* 278:349-359
- Rotshenker S (1979) Synapse formation in intact innervated cutaneous pectoris muscles of the frog following denervation of the opposite muscle. *J Physiol* 292:535-547
- Rotshenker S, McMahan U J (1976) Altered pattern^s of innervation in frog muscle after denervation. *J. Neurocytol.* 5:719-730
- Shinoda Y, Chez C, Arnold A (1977) Spinal branching of rubrospinal axons in the cat. *Exp Brain Res* 30: 203-218
- Sperry, R W (1942) Transplantation of motor nerves and muscles in the forelimb of the rat. *J Comp Neurol* 76: 283-321
- Sperry, R W (1947) Effect of crossing nerves to antagonistic limb muscles in the monkey. *Arch Neurol Psychiatry* 58: 452-473
- Tsukahara N (1978) Synaptic plasticity in the red nucleus. In: Cotman C W (ed) *Neuronal Plasticity*. Raven, New York, pp 113-130
- Tsukahara N (1981) Synaptic plasticity in the central nervous system. *Ann Rev Neurosci* 4: 351-380
- Tsukahara N, Fujito Y (1976) Physiological evidence of formation of new synapses from cerebrum in the red nucleus neurons following cross-union of forelimb nerves. *Brain Res* 106:184-188

Tsukahara N, Hultborn H, Murakami F (1974) Sprouting of cortico-rubral synapses in red nucleus neurons after destruction of the nucleus interpositus of the cerebellum, *Experientia* 30: 57-58

Tsukahara N, Hultborn H, Murakami F, Fujito Y (1975a) Electrophysiological study of formation of new synapses and collateral sprouting in red nucleus neurons after partial denervation. *J. Neurophysiol.* 38: 1359-1372

Tsukahara N, Hultborn H, Murakami F, Fujito Y (1975b) Physiological evidence of collateral sprouting and formation of new synapses in the red nucleus following partial denervation In: Santini M (ed) *Golgi Centennial Symposium Proceedings*, Raven, New York, pp.299-303

Tsukahara N, Kosaka K (1968) The mode of cerebral excitation of red nucleus neurons. *Exp. Brain Res.* 5:102-117

Tsukahara N, Oda Y, Notsu T (1981) Classical conditioning mediated by the red nucleus in the cat. *J. Neurosci.* 1: 72-79

Udo M, Matsukawa K, Kamei H, Oda Y (1980) Cerebellar control of locomotion: effects of cooling cerebellar intermediate cortex in high decerebrate and awake walking cats. *J. Neurophysiol.* 44:119-134

- Wall P D, Egger M D (1971) Formation of new connexions in adult rat brains after partial deafferentation. Nature 232: 542-545
- Yumiya H, Larsen K D, Asanuma H (1979) Motor readjustment and input-output relationship of motor cortex following cross-connection of forearm muscles in cats. Brain Res. 117: 566-570

CHAPTER III

FORMATION OF FUNCTIONAL SYNAPSES IN ADULT CAT RED NUCLEUS
FROM THE CEREBRUM FOLLOWING CROSS-INNervation OF FORELIMB
FLEXOR AND EXTENSOR NERVES. II. ANALYSIS OF NEWLY-APPEARED
SYNAPTIC POTENTIALS.

INTRODUCTION

We previously reported the appearance of a new fast-rising component in composite corticorubral EPSPs after cross-innervation of cat forelimb flexor and extensor nerves (Tsukahara and Fujito, 1976; Tsukahara et al., 1982). This phenomenon is similar to that found after lesion of the cerebellar nucleus interpositus (IP) (Tsukahara et al., 1974; 1975a,b; Murakami et al., 1977a,b) and was interpreted to be due to formation of new synapses on the proximal portion of soma-dendritic membrane of red nucleus (RN) neurons. However, our previous studies did not determine whether, after cross-innervation, a similar fast-rising component appears in the corticorubral unitary EPSPs or whether some changes occur in the cable property of dendrites. Furthermore, a question remains as to whether there is a drastic loss in interpositorubral synapses after cross-innervation, because loss of these synapses induces sprouting as reported previously (Tsukahara et al., 1974; 1975a,b; Murakami et al., 1977a,b).

In the present study we attempted to answer these questions.

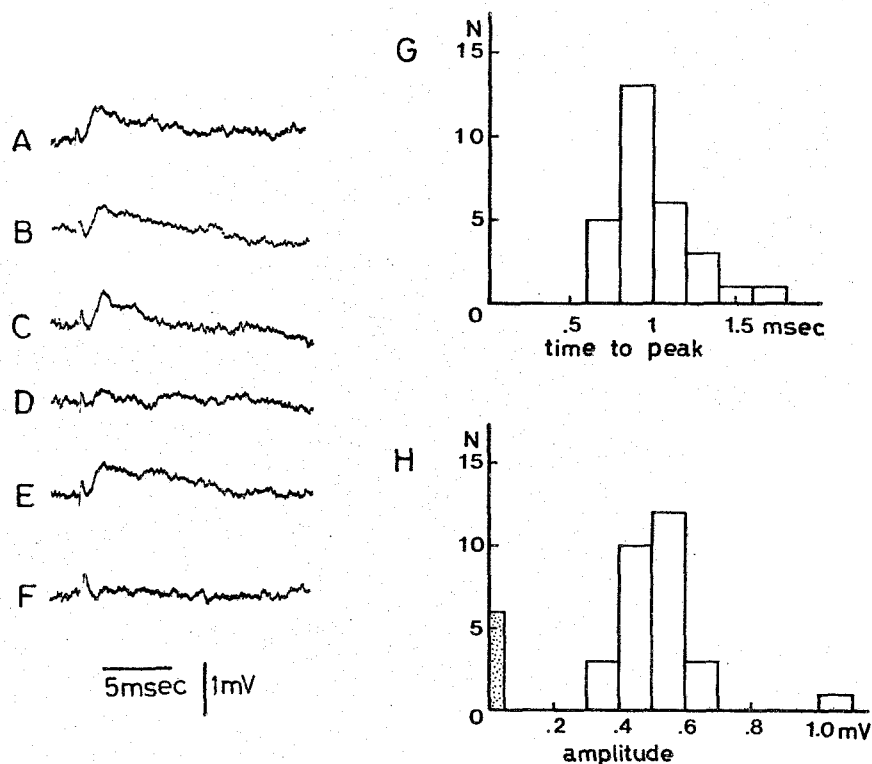


Fig. 1. Corticorubral unitary EPSPs, produced by applying identical stimulation intensity to the cerebral peduncle of an RN cell from a cat cross-innervated 161 days earlier. A-E: Examples of intracellular recordings of unitary EPSPs; in D there was no response. F: extracellular recording just outside the cell. Voltage and time calibrations below F also apply to A-E. G and H: Frequency distribution of the time-to-peak (G) and the amplitude (H) measured from each of the consecutive EPSP traces partially shown in A-E. The shaded area in H represents the number of response failures.

METHODS

The experimental procedures were essentially the same as those reported previously (Tsukahara et al., 1981).

RESULTS

The present results are based on intracellular recordings of RN cells identified antidromically as innervating the upper spinal segments (C-cells; Tsukahara and Kosaka, 1968) from the same animals as used in the previous paper (Tsukahara et al., 1981). Stable intracellular records with spikes greater than 50 mV were selected. These records were obtained from adult cats cross-innervated from 60 to 250 days earlier.

Unitary nature of corticorubral EPSPs after cross-innervation experiments

Figs. 1A-E show examples of the corticorubral EPSPs induced in an RN cell from a cat cross-innervated 161 days earlier. During threshold cerebral peduncle (CP) or sensorimotor cortex (SM) stimulation, unitary EPSPs appeared in an all-or-nothing manner and varied in amplitude. These EPSPs are thought to be due to activation of a single cortical fiber or, less likely, a group of cortical fibers, behaving in an all or none manner with this stimulus, projected onto the RN cell used for recording. The responses are designated corticorubral unitary EPSPs (Murakami et al., 1977a). Failure is demonstrated in Fig. 1D. The extracellular

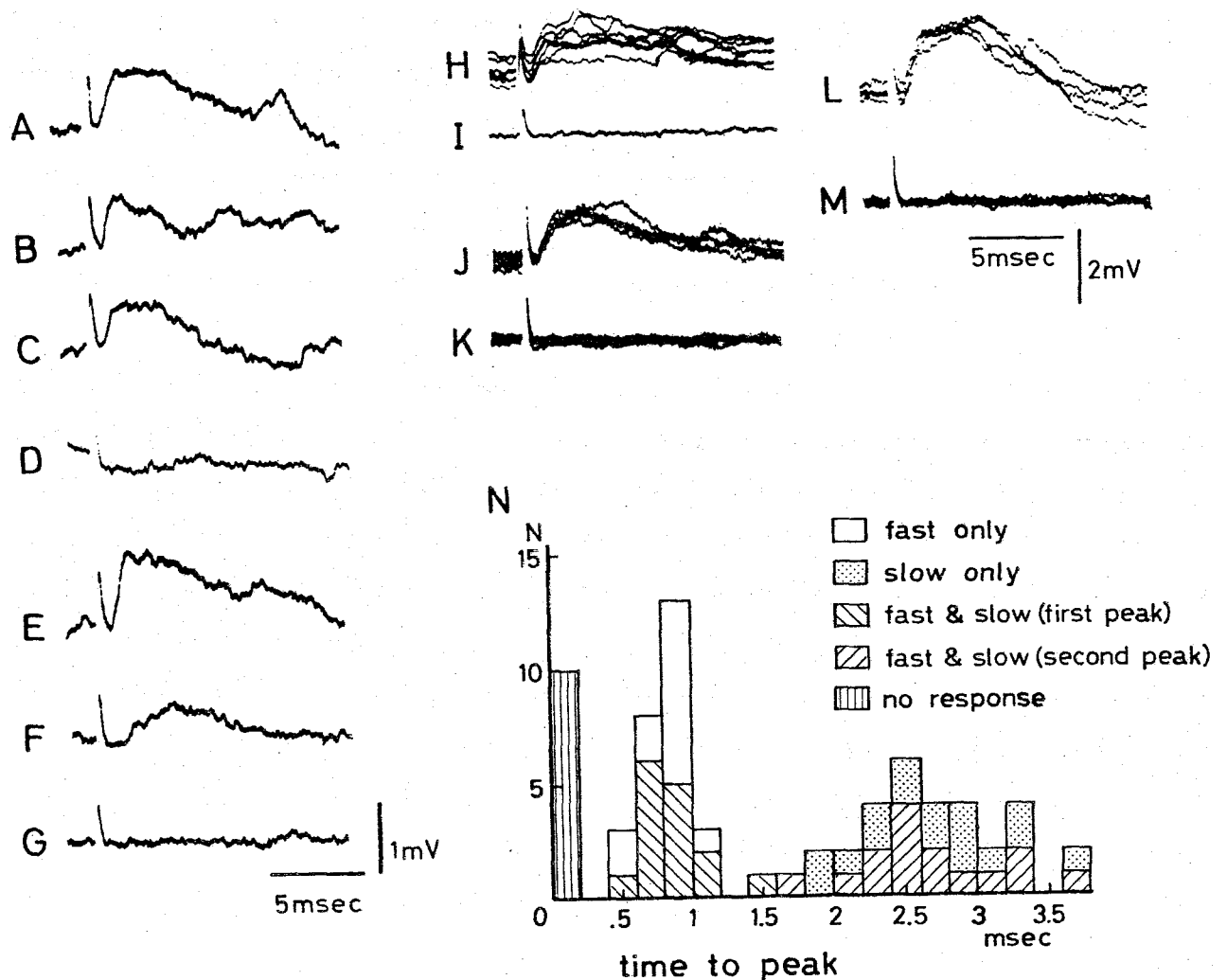


Fig. 2. Double peaked cerebral peduncle (CP) induced unitary EPSPs and CP-EPSPs in an RN cell from a cat cross-innervated 250 days earlier. A-F: Examples of intracellular recordings of unitary EPSPs induced by applying identical stimulation intensity to the CP; in D there is no response. The unitary EPSPs sometimes have both fast and slow peaks, as shown in A and C. Unitary EPSPs in B and E have only fast peaks while that in F has only slow peak. G shows an extracellular recording made just outside the cell. Voltage and time calibrations in G also apply to A-F. H is superimposed CP-unitary-EPSPs and I is the extracellular recording for H. J and L: Intracellular recordings of CP-EPSPs. K and M show the extracellular recordings corresponding to J and L. Stimulus intensity was increased from H to L. Voltage and time scales below M also apply to H-L.

N represents the frequency distribution of the time-to-peak of CP-unitary-EPSPs measured from each of the consecutive EPSP traces illustrated^d in A-F. Each symbol in columns represents the variation of time course of the CP-unitary-EPSPs. Open columns show the time-to-peaks of unimodal CP-unitary-EPSPs with fast peak; dots, time-to-peak^s of unimodal EPSPs with slow peak; left-up oblique lines, time-to-peaks of first peak in double peaked unitary-EPSPs; right-up oblique lines, time-to-peaks of second peak in double peaked EPSPs. Vertical lined column represents the number of failures.

field potential is shown in Fig. 1F. The mean time-to-peak and amplitude of 18 averaged corticorubral unitary EPSPs from 30-40 consecutive traces of C-cells from cross-innervated cats was measured, the mean amplitude was 0.41 ± 0.11 mV, and the mean time-to-peak was 1.14 ± 0.51 msec. These values are significantly different from normal cats (0.33 ± 0.09 mV, $n=22$; $p<0.01$ and 2.68 ± 0.61 msec, $n=22$; $p<0.001$) (Murakami et al., 1977a).

As illustrated in Fig. 1, corticorubral unitary EPSPs are characterized by a fast-rising time course and a large amplitude. In a few cases the corticorubral unitary EPSPs are followed by an additional slow component. This is prominent at times, but usually obscured by the fluctuating falling phase of the EPSPs. Fig. 2A-F represent examples of CP-unitary-EPSPs with both fast and slow time course. Double peaked EPSPs are shown in Fig. 2A and C; while unimodal peakes are shown in Fig. 2B and E (fast peak) and 2F (slow peak). The double peaked CP-EPSPs becomes gradually larger in size with increasing stimulus intensity from threshold stimulation (Fig. 2H, J and L). The bimodal distribution of the time-to-peak of CP-unitary-EPSPs is presented in Fig. 2N. In case of double-peaked unitary EPSPs the amplitude and time-to-peak were measured for the first peak.

Fig. 3 shows the relation between the time-to-peak and amplitudes of these corticorubral unitary EPSPs. we noted a

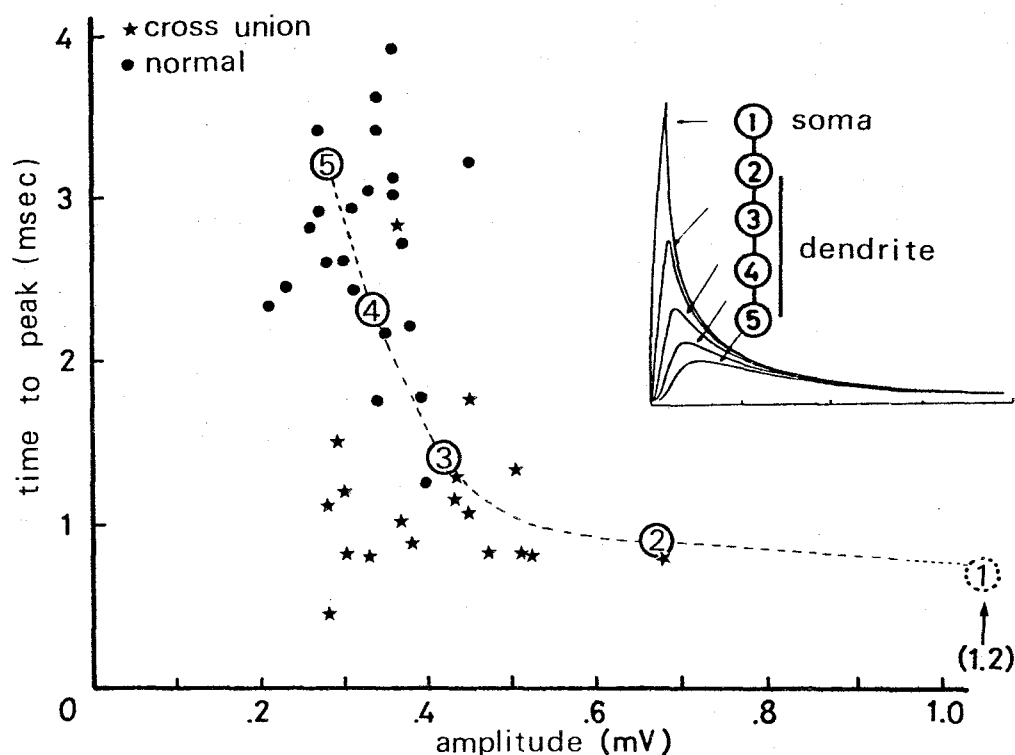


Fig. 3. Relation between time-to-peak and peak amplitude in corticorubral unitary EPSPs. (●), unitary EPSPs of normal cats as reported by Murakami et al. (1977a); (*), unitary EPSPs of our cross-innervated cats. Each point represents the average time-to-peak and the average amplitude of 30-40 consecutive traces obtained for each unitary EPSP. The large open circles labelled 1-5 represent the time-to-peak and amplitude of theoretical EPSPs, derived by applying the compartment model of Rall (1964) to typical RN cells at each of a chain of five compartments (Murakami et al., 1977a). The circled numbers correspond to the compartments. The inset shows the relative time course and amplitude of theoretical EPSPs generated in those compartments.

tendency for unitary EPSPs with shorter time-to-peak values to have larger amplitudes. This relation is predicted theoretically by Rall's compartment model, as schematically illustrated in the inset of Fig.3. It has been reported that Rall's model is applicable to RN cells (Tsukahara et al., 1975c; Sato and Tsukahara, 1976). There was good agreement between the theoretical curve and our experimental findings. These results suggest that the new synapses formed, after cross-innervation experiments developed on the proximal dendrites of RN cells. The finding that some corticorubral unitary EPSPs have both fast and slow components indicates that axonal sprouting may occur in a proximal direction from axons previously connected to the RN cells at distal sites.

Cable properties of RN cells after cross-innervation

We investigated whether peripheral cross-innervation produced a change of the cable properties of RN cells. Fig.4A illustrates the membrane potential change induced by a step current in an RN cell from a cat cross-innervated 110 days earlier. The voltage transient thus obtained were measured at 0.2 or 0.5 msec intervals and plotted on the semilogarithmic coordinates. Voltage points could be fitted by a straight line except during the initial 2 msec. This straight line gives the membrane time constant; $\tau_0 = 5.3$ msec. If the difference between this straight line and the deviated data points of the initial 2 msec are plotted on a semilogarithmic scale, they could be fitted by another straight line, the slope of which gives a time constant of a second exponential function, $\tau_1 = 0.7$ msec. The mean time constant, τ_0 , was 5.2 ± 0.7 msec ($n=10$); in normal cats it was 5.6 ± 1.0 msec ($n=25$) (Tsukahara et al., 1975c); τ_1 was 0.69 ± 0.19 msec ($n=10$); in normal cats it was 0.6 ± 0.2 msec ($n=25$) (Tsukahara et al., 1975c). The mean membrane resistance of RN cells was 2.5 ± 0.8 M Ω , not significantly different from that of normal cats (2.5 ± 0.9 M Ω) (Tsukahara et al., 1975c). From the ratio of τ_1 and τ_0 , it was possible to estimate the electrotonic length of RN cells L , using the equation of Rall (1969) $L = \pi / \sqrt{\tau_0 / \tau_1 - 1}$. In Fig.4B, the electrotonic length was plotted against the respective input resistance of RN cells. The mean electrotonic length was somewhat

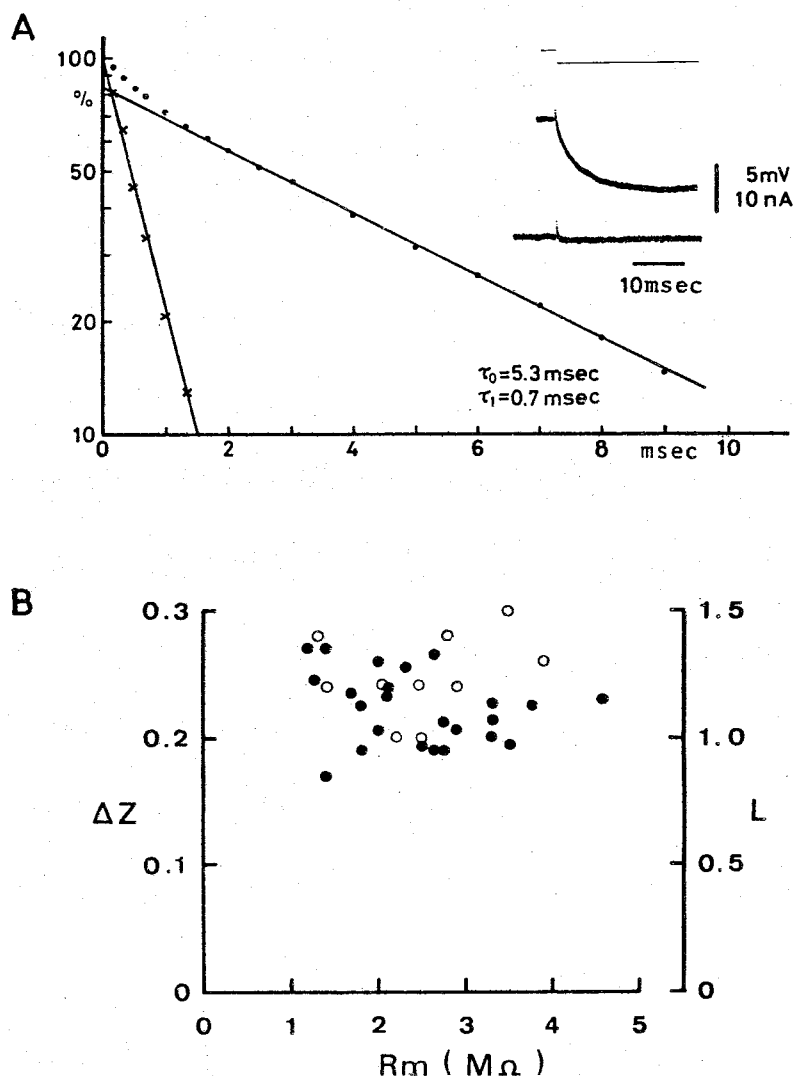


Fig.4. Membrane potential change induced by a step current in an RN cell from a cross-innervated cat, and cable parameters of RN cells. A: Semilogarithmic plot of the membrane transient response at the onset of the hyperpolarizing current pulse. Inset recordes: Intracellular (middle trace) and extracellular (lower trace) potential changes induced by a hyperpolarizing current'step (upper trace). The straight tail portion of the curve at times larger than 2 msec represents the first time constant, $\tau_0 = 5.3 \text{ msec}$. The difference between the experimental data (●) and the extrapolated line at times shorter than 2 msec was plotted on a semilogarithmic scale (x). The line

through the crosses represents the second equalizing time constant, $\tau_1 = 0.7$ msec. B: Plot of electrotonic length, L , or the increment of L in the five compartments model, ΔZ , (ordinate) of RN cells against input membrane resistance (abscissa). (o), data from cats with cross-innervation; (●), data from normal cats (Tsukahara et al., 1975c).

larger in cross-innervated cats, 1.2 ± 0.2 ($n=10$) (versus 1.1 ± 0.15 , $n=25$; Tsukahara et al., 1975c). These data were obtained from the C-cell of cats subjected to cross-innervation between 110 and 250 days earlier.

Convergence number of interposito-rubral synapses

One of the possible mechanisms underlying the induction of sprouting after cross-innervation may be the degeneration of IP neurons, resulting in lesion-induced sprouting in RN cells. This hypothesis can be tested by determining the extent of convergence of IP axons onto RN neurons before and after cross-innervation.

The rising slope of IP-induced EPSPs was measured from intracellular records from which the extracellular field potentials at different stimulus intensities were subtracted (Toyama et al., 1970). Fig. 5E plots the rising slope of the IP-EPSP as a function of stimulus intensity. Saturation occurs above 20 volts of IP stimulation. This would indicate that all the IP axons converging onto the cell are excited. Therefore, the steepest rising slope of the maximum IP-EPSP would indicate that all IP axons converging onto the RN cells are excited in this experimental condition. The unitary EPSPs of the same cell at threshold stimulus intensity, were recorded (Fig. 5A) and the mean rate of the rise of unitary EPSPs was measured. The difference of the ratio of the slope between the maximum EPSP and the unitary IP-EPSPs gives the number of IP axons

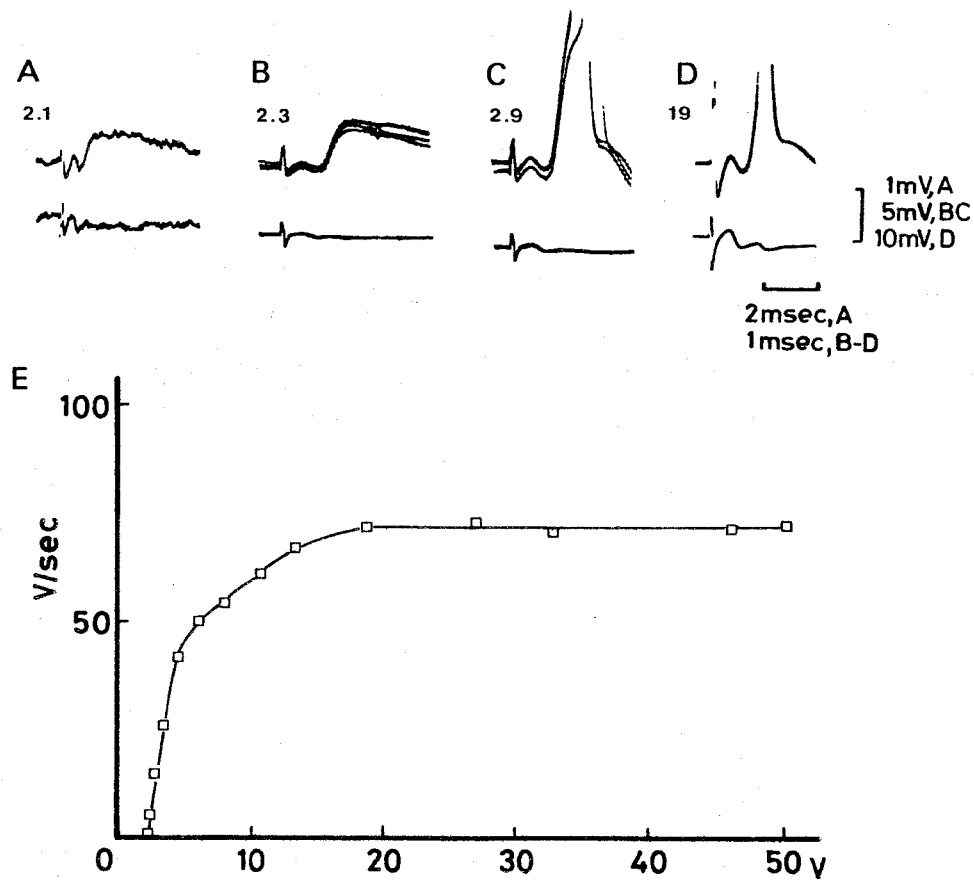


Fig. 5. Effect of increasing the intensity of IP stimulation.

A-D: EPSPs and spikes evoked by IP stimuli with various intensities (indicated in volts, upper traces). Lower traces represent the extracellular controls. Application of time and voltage calibrations in D are indicated by labels in A-D.

E: Maximum rate of IP-EPSP rises plotted against IP stimulation intensities.

converging onto the RN cells (Toyama et al., 1970). In the experiment shown in Fig. 5, the mean rate of rise of the unitary IP-EPSPs was 1.5 volt/sec, the maximum rate of rise was 72 volt/sec. Therefore, the convergence number of IP axons onto this RN cell was measured to be 48.

The convergence number of interposito-rubral synapses, obtained for 8 C-cells from cats cross-innervated from 102 to 147 days earlier ranged from 37 to 57, (48 ± 6 , $n=8$). This value is similar that obtained in normal cats (47 ± 1 , $n=3$, Toyama et al., 1970).

DISCUSSION

The present investigation shows that, as in composite EPSPs (Tsukahara et al., 1981), a new fast-rising component appeared in the unitary corticorubral EPSPs after cross-innervation of the cat peripheral nerves. Similar findings have been reported after the destruction of the nucleus interpositus of the cerebellum, suggesting that functional synapses are formed on the proximal portion of the soma-dendritic membrane of RN cells. However, there are several other possibilities which need to be considered.

First, shrinkage of RN neurons which may occur after cross-innervation, would result in a shortening of the electrotonic length. However, this possibility is unlikely since the electrotonic length was actually slightly longer. Moreover, it is not possible to explain the dual peaks of the corticorubral EPSPs after cross-innervation by a change in the

electrotonic length of RN cells. Therefore, the formation of new synapses at different locations is a reasonable hypothesis.

The present paper provides additional evidence supporting the formation of new synapses. Analysis of the corticorubral unitary EPSPs revealed a change in amplitude and time-to-peak, as would be expected if new synapses are formed at the proximal portion of the RN cell dendrites.

The second question we asked in undertaking the present investigation was whether the formation of new synapses occurs without a major change in the input from the nucleus interpositus. Previous studies have shown that after lesion of the nucleus interpositus, sprouting and formation of new functional synapses occur from the corticorubral fibers (Tsukahara et al., 1975a,b; Murakami et al., 1977a, b). Therefore, the possibility exists that after cross-innervation, degeneration of the IP neurons took place, leading to the sprouting of corticorubral fibers. However, this possibility is unlikely because, according to our physiological estimate of interposito-rubral convergence, there is no large-scale degeneration of the interposito-rubral synapses after cross-innervation.

The time course of the EPSPs is determined by a number of factors; 1) the time course of the synaptic current; 2) the location of the synapses on the neuronal soma-dendritic membrane (Rall, 1964; Tsukahara et al 1975c) 3) the dendritic and electrical properties of the neurons, such as time constant,

electrotonic length and soma-dendritic conductance ratio (Jack et al., 1971; Tsukahara et al., 1975c), 4) the temporal dispersion of impulses during conduction of presynaptic fibers (Tsukahara and Kosaka, 1968). Although the last factor can be excluded in the case of unitary EPSPs, it is not clear whether the appearance of the fast-rising components of the corticorubral EPSPs is exclusively due to relocation of the synapses. The variation on the shape and amplitude of unitary EPSPs may well be due to variations in the amount and time course of synaptic currents. Nevertheless, the observed tendency of fast-rising corticorubral unitary EPSPs to be larger in amplitude, in the manner expected from the theoretical prediction, is in accord with the hypothesis that the fast-rising unitary EPSPs are generated at a site closer to the soma than the slower ones. Furthermore, the fast-rising component is more sensitive to membrane potential displacement than the slow-rising components (Tsukahara et al., 1981); this also supports the view that fast-rising EPSPs are produced by synapses closer to the soma than slow-rising ones. Electron microscopic studies may answer the question as to whether the synapses are produced from cortical fibers on the proximal portion of the dendrites of RN cells, as is suggested by physiological data.

SUMMARY

The effects of cross-innervation of peripheral flexor and extensor nerves on the time course and properties of red nucleus (RN) neurons were studied in adult cats.

Time course of corticorubral unitary EPSPs was examined. In operated cats, RN neurons innervating upper spinal segments (C-cells) manifested corticorubral unitary EPSPs with shorter time-to-peak and larger amplitude than in normal cats. The mean amplitude of these EPSPs was 0.41 ± 0.11 mV; the mean time-to-peak was 1.14 ± 0.51 msec ($n=18$). These values differ from normal cats (0.33 ± 0.09 mV, and 2.68 ± 0.61 msec, $n=22$).

RN neuron membrane properties were examined in cross-innervated cats. The main time constant was 5.2 ± 0.7 msec ($n=10$), the shorter equalizing time constant, 0.69 ± 0.19 msec ($n=10$), the input resistance, 2.5 ± 0.8 M Ω . These values were not significantly different from those of normal cats. The electrotonic length was 1.2 ($n=10$), somewhat larger than in normal cats.

The number of converging interposito-rubral synapses, estimated in 8 cells from cross-innervated cats, ranged from 37 to 57. This was not significantly different from normal cats, and indicated that there is no large-scale degeneration of interpositorubral synapses after cross-innervation.

These results suggest that sprouting and formation of functional synapses occur after cross-innervation of peripheral flexor and extensor nerves.

Key Words : Sprouting--Red Nucleus--Cross-Innervation--
Unitary Corticorubral EPSPs--Cable Properties.

References

- Jack JJB, Miller S, Porter R, Redman SJ (1971) The time course of minimal excitatory post-synaptic potentials evoked in spinal motoneurons by group Ia afferent fibers. *J Physiol* 215: 353-380
- Murakami F, Tsukahara N, Fujito Y (1977a) Analysis of unitary EPSPs mediated by the newly-formed cortico-rubral synapses after lesion of the nucleus interpositus of the cerebellum. *Exp Brain Res* 30: 233-243
- Murakami F, Tsukahara N, Fujito Y (1977b) Properties of the synaptic transmission of the newly formed cortico-rubral synapses after lesion of the nucleus interpositus of the cerebellum. *Exp Brain Res* 30: 245-258
- Rall W (1964) Theoretical significance of dendritic trees for neuronal input-output relations. In: Reiss RF (ed) *Neuronal theory and modeling*, Stanford Univ Press, Stanford, pp 73-97
- Rall W (1969) Time constants and electrotonic length of membrane cylinders and neurons. *Biophys J* 9: 1483-1508
- Sato S, Tsukahara N (1976) Some properties of the theoretical membrane transients in Rall's neuron model. *J Theo Biol* 63: 151-163
- Toyama K, Tsukahara N, Kosaka K, Matsunami K (1970) Synaptic excitation of red nucleus neurons by fibers from interpositus nucleus. *Exp Brain Res* 11: 187-198
- Tsukahara N, Fujito Y (1976) Physiological evidence of formation of new synapses from cerebrum in the red nucleus neurons following cross-union of forelimb nerves. *Brain Res* 106: 184-188
- Tsukahara N, Fujito Y, Oda Y, Maeda J (1982) Formation of

functional synapses in the adult cat red nucleus from the cerebrum following cross-innervation of flexor and extensor nerves. I. Appearance of new synaptic potential. Exp Brain Res, in press

Tsukahara N, Hultborn H, Murakami F (1974) Sprouting of cortico-rubral synapses in red nucleus neurones after destruction of the nucleus interpositus of the cerebellum. *Experientia*, Basel 30: 57-58

Tsukahara N, Hultborn H, Murakami F, Fujito Y (1975a) Physiological evidence of collateral sprouting and formation of new synapses in the red nucleus following partial denervation. In: Santini M. (ed) Golgi centennial symposium proceedings, Raven Press, New York, pp299-303

Tsukahara N, Hultborn H, Murakami F, Fujito Y (1975b) Electrophysiological study of formation of new synapses and collateral sprouting in red nucleus neurons after partial denervation. *J Neurophysiol* 38: 1359-1372

Tsukahara N, Kosaka K (1968) The mode of cerebral excitation of red nucleus neurons. *Exp Brain Res* 5: 102-117

Tsukahara N, Murakami F, Hultborn H (1975c) Electrical constants of neurons of the red nucleus. *Exp Brain Res* 23: 49-64

Tsukahara N, Toyama k, Kosaka K (1967) Electrical activity of red nucleus neurones investigated with intracellular microelectrodes. *Exp Brain Res* 4: 18-33

CHAPTER IV

SYNAPTIC INPUTS OF RUBROSPINAL NEURONS FROM ASSOCIATION CORTEX,
PRETECTUM, MEDIAL LEMNISCUS IN THE CAT AND THEIR PLASTICITY.

INTRODUCTION

The rubrospinal neurons (RN neurons) receive synaptic inputs from the ipsilateral sensorimotor cortex (SM) and the contralateral nucleus interpositus (IP) of the cerebellum. (Tsukahara and Kosaka, 1968; Toyama et al., 1970; Tsukahara et al., 1975b). Electrophysiological and histological investigations have shown that synapses from SM are located on the distal dendrites of RN neurons while those of IP are terminated on the soma (Tsukahara and Kosaka, 1968; Tsukahara et al., 1975b; Toyama et al. 1970; Brown, 1974; King et al., 1972 and 1973; Nakamura and Mizuno, 1971; Murakami et al., 1982). In recent studies it has been reported that after IP lesions or cross-innervation of peripheral nerves, sprouting of cortico-rubral fibers occurs and new synapses are formed at the proximal portion of the dendrites of RN neurons (Tsukahara et al., 1975a; Murakami et al., 1977a, 1982; Tsukahara et al., 1982; Fujito et al., 1982).

In several studies, it has been suggested that there are other synaptic inputs to RN neurons which terminate on somewhere between the soma and distal dendrites (Tsukahara et al., 1975b; Nishioka and Nakahama, 1973; Massion, 1961; Eccles et al., 1975a). Anatomical observations have shown that there are other cortical inputs from the parietal association cortex and secondary sensory area (Rinvik, 1965; Mabuchi and Kusama, 1966; Mizuno et al., 1973). Furthermore, Cajal described that lemniscal fibers

project to the RN nucleus, and recent anatomical investigations have shown that pretectal fibers terminate in RN nucleus (Graybiel, 1974; Itoh, 1977).

The present study attempted to identify synaptic inputs of RN neurons other than IP and SM and characterize the properties of the synaptic potentials produced by these new inputs in some detail. Attempts are also made to clarify the possible change of these synaptic inputs after destruction of the major synaptic input of the RN cells, nucleus interpositus of the cerebellum (IP). It will be shown that association cortex, pretectal area and the medial lemniscus give excitatory and inhibitory inputs to RN neurons. Furthermore, after destruction of the IP, the lemniscal and association cortical inputs increase the transmission efficacy possibly by sprouting .

Some of the present findings have been reported in brief (Fujito et al., 1978).

MATERIALS AND METHODS

Five types of preparations were used; Normal (n=28), both SM and IP destructed (n=6), IP lesioned (n=1), IP and dorsal column nuclei (DCN) lesioned (n=1) and decerebrated (n=1) cats.

Chronic operation

Cats were anesthetized with pentobarbitone sodium injected intraperitoneally (35 mg/kg) in chronic operations. In case of IP lesion, DCN lesion or decerebration, both the right IP and dentate nucleus, the right DCN or caudal part of the left internal capsule was destroyed stereotaxically. Ablation of the left SM was performed by suction under direct vision. Each chronic destruction was performed more than two weeks before the acute experiment.

Stimulation and recording

In acute experiments cats were an^sthetized with pentobarbitone sodium (35 mg/kg), immobilized by gallamine triethiodide and artificially respired. Supplement doses of pentobarbitone and gallamine were injected intravenously as required. The methods of stimulation and recording from RN neurons were essentially the same as those employed previously (Tsukahara et al., 1975a). Bipolar stimulating electrodes made of acupuncture needles, insulated except at the tips were inserted stereotaxically for stimulation of several sites. The left cerebral cortex was stimulated by those bipolar acupuncture electrodes inserted into the depth of 1.0-1.5 mm from the cortical surface. The

arrangement of electrodes for stimulation of cerebrum are shown diagrammatically in Fig. 1A. RN neurons were identified antidromically by stimulating the contralateral surface of spinal cord at C₁ and L₁ segments; RN neurons activated only from C₁ were designated as "C-cells". those activated from C₁ and L₁, as "L-cells" (Tsukahara and Kosaka, 1968). Glass microelectrode, filled with 2M NaCl or 2M K-citrate and having an electric resistance of 6-16 MΩ were used. Intracellular recording was performed from the left RN neurons. In some animals, recording from RN neurons in the right was done for testing the crossed cerebro-rubral projection. The degree of lesions and the locations of stimulating electrodes were verified by histological examination after the acute experiments. Following abbreviations were used in the text as well as in the figures:

AC: anterior cruciate gyrus

AES: anterior ectosylvian gyrus

ASS: anterior suprasylvian gyrus

C₁: first cervical segment of spinal cord

CP: cerebral peduncle

IP: nucleus interpositus of the cerebellum

LAT: lateral gyrus

L₁: first lumbar segment of spinal cord

ML: medial lemniscus

MSS: medial suprasylvian gyrus

M_{II}: supplementary motor area

PASC: parietal association cortex

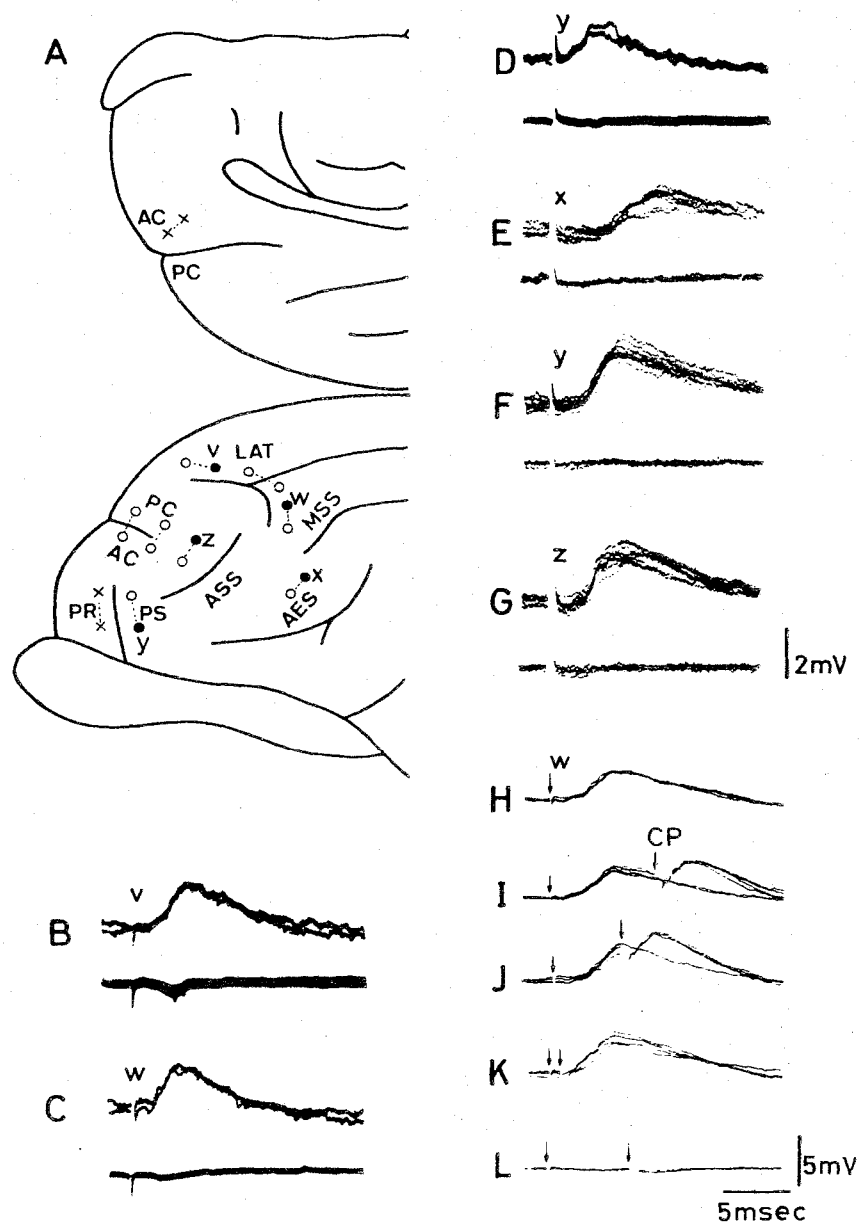


Fig.1

Fig.1 EPSPs induced by cerebral cortex.

A: Arrangement of electrodes for stimulation of cerebral cortex. open and filled circles represent effective positions of stimuli for inducing corticorubral EPSPs. No EPSP was recorded by stimulating the loci indicated by crosses. Dotted line which links adjacent stimulation points indicate pairs of bipolar electrodes. B-G exemplify corticorubral EPSPs induced by cathodal stimulating current via electrodes labelled by v, w, x, y and z in A. B-D represent corticorubral EPSPs in a RN cell, E-G: Corticorubral EPSPs induced in other RN cell. Upper traces, intracellular records; Lower traces, corresponding extracellular records in B-G. H-K show a collision experiment of EPSPs induced from PASC and CP. CP stimuli were applied at various time intervals after preceding PASC stimuli. Downward arrows in H-L indicate the onsets of PASC and CP stimuli. L shows the extracellular control. Time calibration in L also applies to B-K. Voltage calibration in G also applies to B-F. Voltage calibration in L also applies to H-K.

PC: posterior cruciate gyrus

PCC: pericruciate gyrus

PRT: pretectal area

PS: presylvian gyrus

PR: proreus gyrus

PY; pyramidal tract

SM: sensorimotor cortex

S_{II}: secondary sensory area

RN: red nucleus

RESULTS

RN neurons were identified by their antidromic activation from the C₁ spinal segment. RN neurons with spike amplitude of more than 50 mV were selected for the following analysis.

1. Cerebral inputs of RN neurons

Cerebrorubral projections were investigated in 26 normal cats. Fig. 1B-G illustrate examples of cerebrally-induced EPSPs in two RN cells by stimulating six different cortical areas; rostral portion of the parietal association cortex (PASC, anterior part of lateral gyrus, posterior part of anterior suprasylvian gyrus and anterior part of middle suprasylvian gyrus); secondary sensory area (S_{II}, anterior ectosylvian gyrus), presylvian gyrus (PS), proreus gyrus, supplementary motor area (M_{II}, medial surface of anterior cruciate gyrus) and pericruciate gyrus (PCC, limb and trunk area of sensorimotor

cortex). By stimulation of the ipsilateral PASC, S_{II} , PS and PCC(filled or open circles in Fig. 1A) EPSPs were produced in RN neurons. The EPSPs were occasionally followed by membrane hyperpolarization (not illustrated). EPSPs could not be produced by stimulating the proreus gyrus and M_{II} (crosses in Fig. 1A). No responses was observed by stimulating the contralateral cerebral cortex.

Cortically-induced EPSPs had a slow rise time similar to that reported previously for the PCC-EPSPs (Tsukahara et al., 1967; Tsukahara and Kosaka, 1968). The mean and S.D. of latencies of the EPSPs induced from PASC, PS, S_{II} and PCC were 2.1 ± 0.6 msec (n=51), 2.1 ± 0.8 msec (m=29), 2.6 ± 0.8 msec (n=31) and 1.8 ± 0.4 msec (n=77), respectively. The mean and S.D. of times to peak of the EPSPs from PASC, PS, S_{II} and PCC were 3.4 ± 1.1 msec (n=51), 3.3 ± 0.9 msec (n=29), 3.9 ± 1.5 msec (n=31) and 3.9 ± 1.2 msec (n=77), respectively. PASC and S_{II} -induced EPSPs were found in cats where PCC, PS and anterior suprasylvian gyrus were ablated two weeks previously. (SM ablated cat). This indicates that PASC and S_{II} -induced EPSPs are at least partly produced through independent pathway other than that mediated by SM. Furthermore the PASC, PS and S_{II} -induced EPSPs interfered with CP-EPSPs at short intervals (within 1.5 msec), (partly shown in Fig. 1H-L) by the impulse collision. Therefore, PASC, PS and S_{II} -rubral fibers pass through the CP. In view of the

short latency of CP-EPSPs with chronic ablation of the SM, these PASC, PS and S_{II} -induced EPSPs were considered to be produced monosynaptically.

Topographical organization of cerebro-rubral projections

As shown in Fig. 1B-G, each RN cell receives cerebral inputs from different cortical areas and effective sites to produce the EPSPs were varied in individual RN cells. We investigated whether there are some characteristics of cerebral projection pattern, such as somatotopy or topography, or not. According to the histological (Rinvik and Walberg, 1964; Mabuchi and Kusama, 1966; Pompeiano and Brodal, 1957; Martin et al., 1974) and physiological (Tshukahara and Kosaka, 1968; Padel et al., 1972, 1973) observations, the SM-RN projection is arranged in a somatotopical manner; the lateral part of SM, forelimb area, projects to the C-cells which are located in the dorsomedial portion of RN, and the medial part of SM projects to the L-cells located in the ventrolateral portion of RN. Here, RN neurons were divided into two groups; neurons innervating the cervico-thoracic segments were referred to as C-cells and neurons innervating the lumbosacral segments were referred to as L-cells (see methods). Stimulation of the medial part of PASC induced EPSPs predominantly in L-cell (27 L-cells) and some in C-cells (5 C-cells). Stimulation of the lateral part of PASC induced EPSPs in C-cells (19 C-cells) (Fig. 2A). Therefore, there was a tendency of somatotopy that C-cells receive inputs from the lateral part

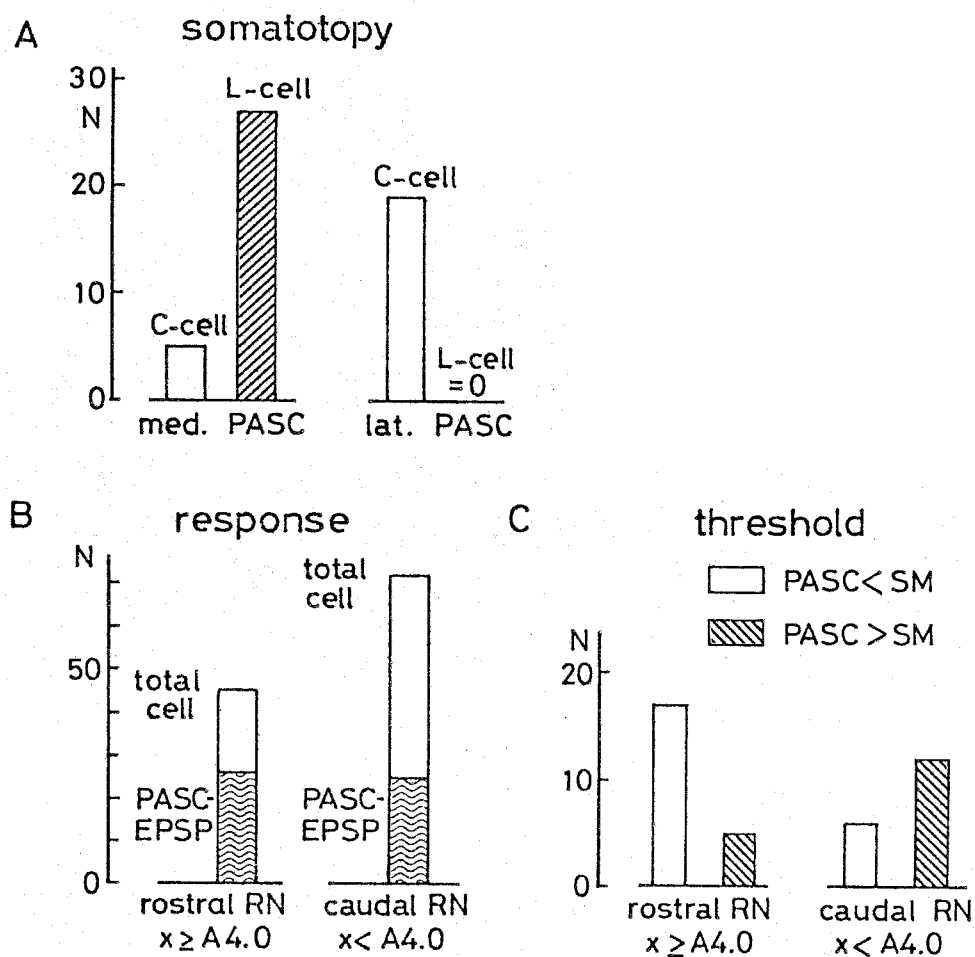


Fig.2 topographical arrangements of PASC-rubral projection.

A: Frequency distribution of effective sites^s to produce PASC-induced EPSP in each RN neuron. Ordinate, number of RN cells. In the left group, medial part of PASC was effective site, while the right group represents the RN cells where lateral part of PASC was effective site. Open columns represent C-cells; Dashed column, L-cells. B: Comparison of probability of appearance

of PASC-induced EPSPs in the rostrally-located RN and the caudally-located RN cells. Shaded columns represent the number of RN cells in which PASC-induced EPSPs were observed and open columns represent RN cells in which PASC-induced EPSPs were not found.

C: Comparison of threshold stimulating currents for evokeing PASC- and SM-induced EPSPs. Open column: RN cells in which threshold currents of PASC-induce EPSPs were lower than those of SM-EPSPs. Hatched column: RN cells where threshold currents of PASC-induced EPSPs were higher than those of SM-EPSPs.

of PASC whereas L-cells receive projection from the medial part of it, although there is some overlaps. PS-induced EPSPs were found in 20 C-cells and 9 L-cells. S_{II} -induced EPSPs were observed in 18 C-cells and in 13 L-cells.

Topographical organization of PASC-rubral projection in rostro-caudal orientation was also examined. RN neurons were divided into two arbitrary groups by their locations of the stereotaxic coordinates; the one at equal or anterior than A 4.0 and the other posterior than A4.0. 26 out of total 45 cells of the rostral RN cell group received PASC-induced EPSPs, while 25 out of 72 cells of the caudal group received PASC-induced EPSPs (Fig. 2B). Therefore, it appears that there was a tendency that PASC-rubral projection was more evident in the rostral group than in the caudal group ($p < 0.05$). Furthermore, threshold currents to produce PASC-induced EPSP and PCC-induced EPSP were compared in 40 RN neurons. In the rostral RN cell group, PASC was more effective for inducing EPSPs than SM. In contrast, PASC was less effective in the caudal group than SM (Fig. 2C). The tendency that PASC input was more predominant than SM input in the rostral group was statistically significant ($p < 0.01$). As to PS-rubral and S_{II} -rubral projections, no significant topographical organizations were revealed in this study. Because the somatotopical arrangement of PASC-rubral projection was similar in both the rostral and caudal RN cell group, it was concluded that the medial part of PASC projects predominantly

to L-cells in the rostral part of RN and the lateral part of PASC projects predominantly to C-cells in the rostral part of it.

Appearance of new fast-rising component in PASC-induced EPSPs following chronic IP lesion.

It has been reported that SM-rubral fibers sprout and form new synapses on the proximal portion of soma-dendritic membrane of RN neurons and new fast-rising SM-EPSPs appear following chronic IP lesion (Tsukahara et al., 1974, 1975a; Murakami et al., 1977, 1982). Sprouting phenomenon of the PASC-rubral projection was examined after chronic destruction of the contralateral IP and dentate nucleus in this section. Fig. 3 shows CP- and PASC-induced EPSPs in a cat IP lesioned 11 months before. In this cat, CP-EPSPs had dual peaks of a fast-rising component superimposed on the normal slow-rising component as reported in the previous reports (Fig. 3C) (Tsukahara et al., 1974, 1975a; Murakami et al., 1977). Fig. 3D-F illustrate PASC-induced EPSPs having a new fast-rising component of rise time of about 1 msec and EPSPs from the lateral part were most predominant. On analogy with similar finding of SM-EPSPs after destruction of IP, it is likely that the newly-appeared fast-rising component of PASC-induced EPSPs are due to the sprouting of new synapses formed on the proximal portion of the soma-dendritic membrane of RN neurons.

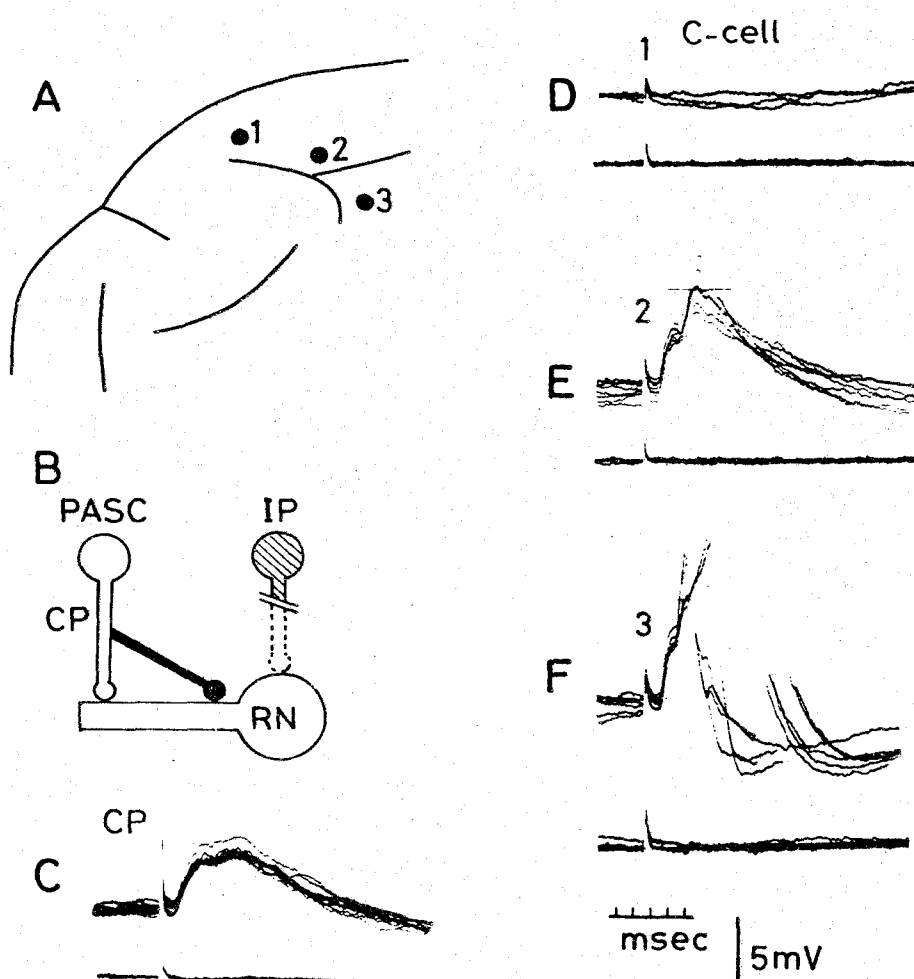


Fig. 3 Appearance of fast-rising component in PASC-induced EPSPs after chronic IP lesion. A illustrates the sites of PASC stimulation. B: Diagram of PASC-rubral connections following the IP destruction. Sprouting of this new collaterals is indicated in black. Shaded neuron indicates the lesion. C: CP-EPSPs in a RN neuron from a cat with the IP lesion. D-F: PASC-induced EPSPs produced in a C-cell from the same cat by stimulating the cortical sites labelled by 1, 2, 3 in A. Upper traces show intracellular recording and lower traces indicate the extracellular controls in C-F.

2. Brain stem inputs to the RN neurons

In this section, synaptic inputs from the pretectal area (PRT, in 7 cats) and the medial lemniscus fibers (ML, in 5 cats) were investigated. Fig. 4A exemplifies the EPSP induced by the ipsilateral PRT stimulation having a short time to peak of 1.0 msec and a latency of 0.8 msec. The mean and S.D. of the latencies of the PRT-induced EPSPs were 1.1 ± 0.3 msec ($n=18$) and those of times to peak were 1.0 ± 0.4 msec ($n=18$). Judging from their short latency, these EPSPs were produced monosynaptically. The mean time to peak of PRT-induced EPSPs was significantly shorter than that of the CP-EPSPs ($p < 0.0005$), and slightly but significantly longer than that of the IP-EPSPs (0.71 ± 0.23 msec, $n=32$) ($p < 0.005$). The PRT-induced EPSPs were frequently followed by the membrane hyperpolarization and the membrane hyperpolarization could be inverted to the depolarizing potential by injecting the hyperpolarizing current (Fig. 4B,C). Therefore, the membrane hyperpolarizations were IPSPs. The latency of the IPSP in Fig. 4B was 2.2 msec.

Fig. 5A represents the EPSPs evoked by ML stimulation. The latency of the ML-induced EPSPs ranged from 1.0 msec to 1.9 msec and the mean and S.D. of the latencies were 1.3 ± 0.2 msec ($n=17$). Judging from their short latencies, it is likely that the shortest part of the ML-EPSPs were produced monosynaptically. The mean time to peak of ML-EPSPs, 1.6 ± 0.5 msec, was significantly shorter than that of the CP-EPSPs ($p < 0.0005$) and

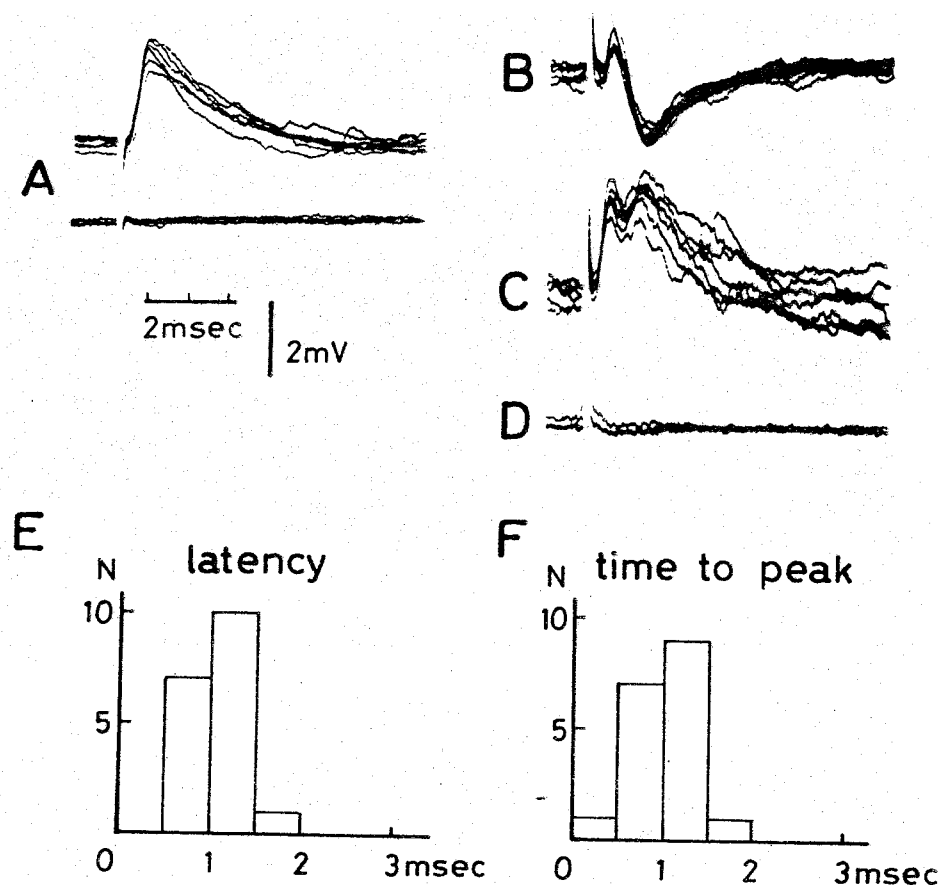


Fig.4 PRT-induced EPSPs and IPSPs. A: PRT-induced EPSPs (upper traces) and extracellular potentials (lower traces). B: PRT-induced EPSPs and succeeding hyperpolarizing potentials. C: The inverted depolarizing potentials by injecting the hyperpolarizing current in the same cell to B.

D : the extracellular controls just outside the cell. Voltage and time calibrations below A also apply to B-D. E, F: Frequency distribution of the latency(E) and the time-to-peak (F) of PRT-induced EPSPs.

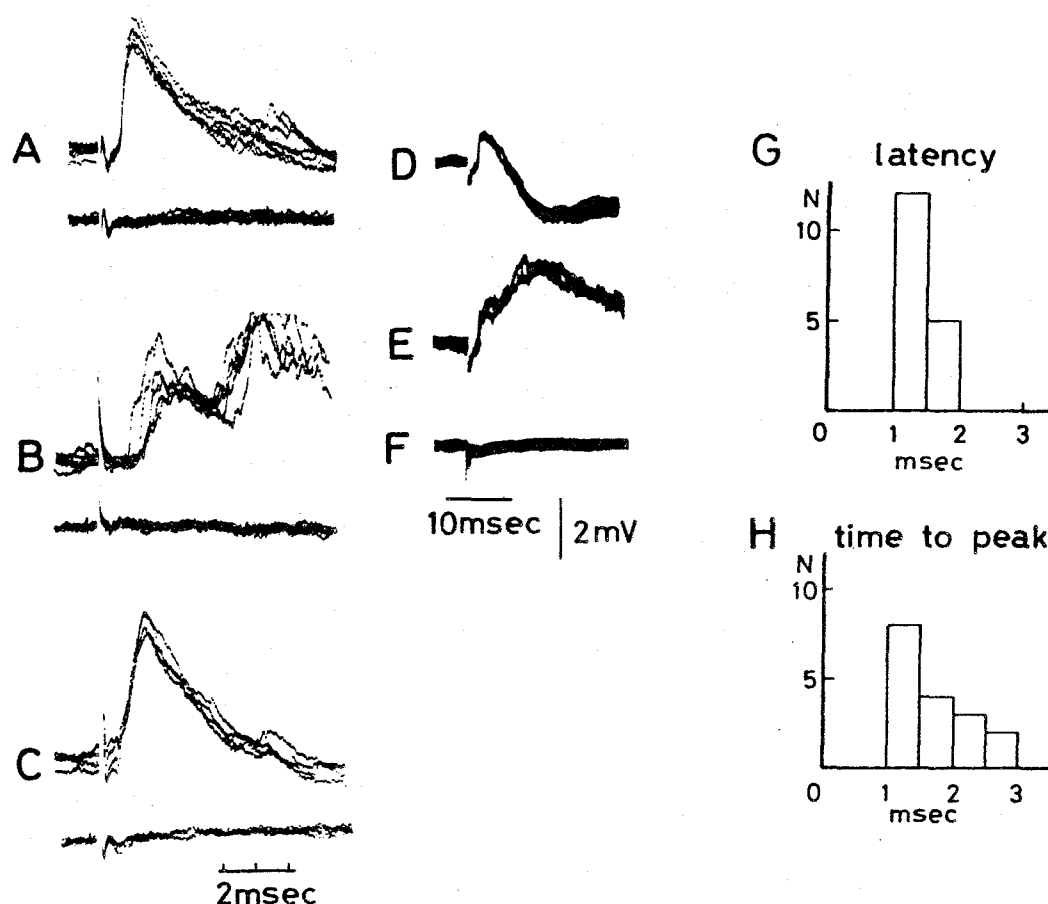


Fig.5 Medial lemniscal input to RN cells. A: ML-induced EPSPs. B: DCN-induced EPSPs in normal cats. C: ML-induced EPSPs in the chronically decerebrated cat. D: ML-induced EPSPs and following hyperpolarizations. In E, the hyperpolarizations were inverted to depolarizing potentials by injecting hyperpolarizing currents. F: Extracellular control for D, E. G, H: Frequency distributions of the latency (G) and the time-to-peak (H) of ML-induced EPSPs. Time and voltage calibrations in F also applies to A-E.

significantly longer than that of the IP-EPSPs ($p < 0.0005$).

ML-induced EPSPs were also frequently followed by membrane hyperpolarizations and they could be inverted to depolarizing potentials by injecting the hyperpolarizing current (Fig. 5D,E). Therefore these membrane hyperpolarizations were IPSPs. In two cats stimulating electrodes were placed in the contralateral dorsal column nuclei (DCN) which are origin of the ML fibers. Stimulation of the DCN produced EPSPs (Fig. 5B) and evoked the succeeding hyperpolarizations similar to ML-induced PSPs (not illustrated).

In order to examine whether the PRT- and ML-induced EPSPs were produced by different sources from those of the IP- and the cerebral-induced EPSPs, both the contralateral IP and the ipsilateral SM were destroyed chronically in 4 cats, the contralateral IP was destroyed in one cat, and the ipsilateral decerebration was performed in one cat. In these chronic cats the PRT-induced and the ML-induced EPSPs were produced in RN cells. This indicates that the PRT- and ML-induced EPSPs originated from the different synaptic sources other than the cerebellum and the cerebral cortex.

It has been reported that the sensitivity of the CP-EPSPs to membrane polarization is less sensitive than that of the IP-EPSPs (Tsukahara and Kosaka, 1968; Tsukahara et al., 1975b). The normalized amplitudes of EPSPs to membrane potential displacements were defined as $V_i/V_o \times 100\%$ where V_i represents

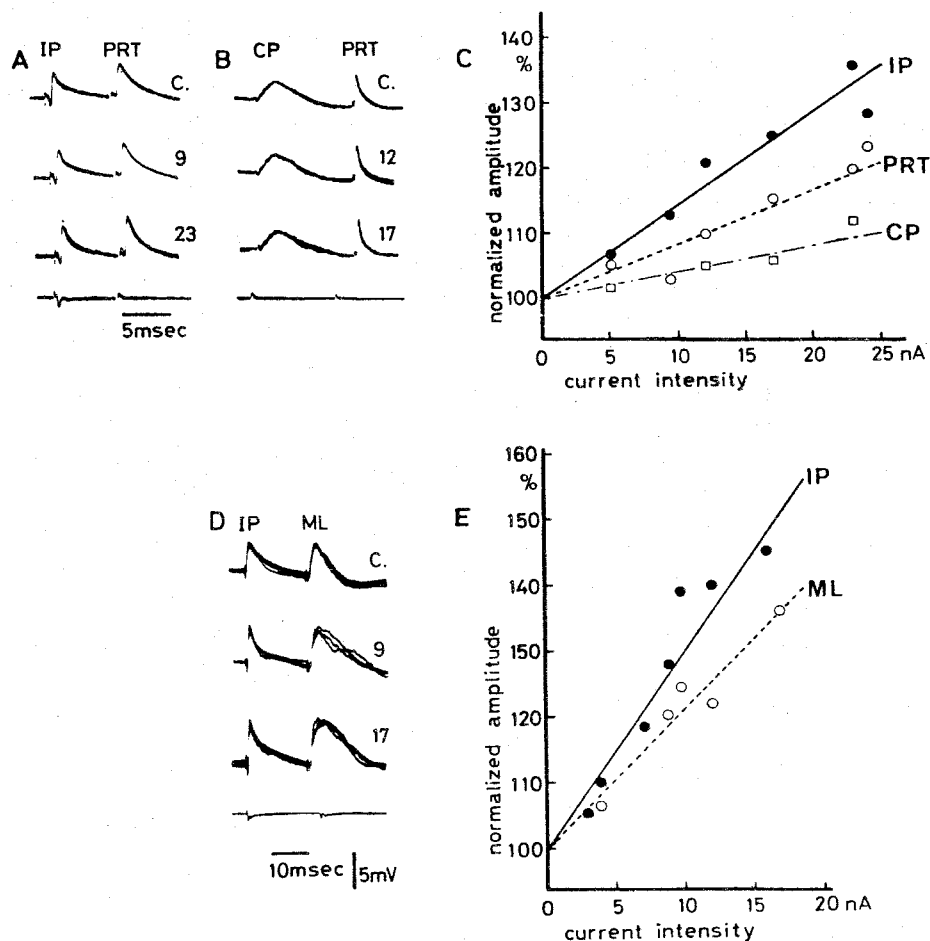


Fig.6 Sensitivity of PRT- and ML-induced EPSPs to membrane hyperpolarization. A-C represent the effect of membrane hyperpolarization on the IP-, CP- and PRT-induced EPSPs in a RN cell. A, B: Specimen records of EPSPs for C before (C.) and during membrane hyperpolarization by injecting the amount of current labelled on each trace (nA). The lowermost traces show the extracellular controls corresponding to upper traces. C: Plot of the normalized amplitudes of these EPSPs from the experiment partly shown in A and B against intensities of currents injected.

Open circles, data of PRT-induced EPSPs; closed circles, data of IP-EPSPs; open squares, data of CP-EPSPs. D,E: Comparison of the sensitivities between IP-EPSPs and ML-induced EPSPs in another RN cell. D illustrates the effect of membrane potential displacement on IP-and ML-induced EPSPs. Uppermost traces represent the control record with no current injection. Middle two traces show records during membrane hyperpolarization by passage of the amount of current labelled on each trace (nA). Lowermost trace is corresponding extracellular field potentials. E: Comparison between the IP- (filled circles) and ML-induced (open circles) EPSPs from experiment partly shown in D. Normalized amplitudes of EPSPs are plotted against the respective current intensities. Time calibrations in D also applies to B. Voltage calibration in D also applies to A and B.

the amplitude of EPSP with current injection and V_0 represents the mean amplitude of EPSPs with no current injection, and the current sensitivities of EPSPs were defined as $(V_i - V_0) / V_0 I \times 100 \%$ where I represents the intensity or injected current. Fig.6A-C represent the effects of membrane potential change on the IP-, CP- and PRT-induced EPSPs in a RN cell. Fig.6C plots the normalized amplitudes of these EPSPs against the intensities of the current injections. The slopes of lines labelled by IP, PRT and CP represent the respective mean ratios of the sensitivities of these EPSPs to membrane hyperpolarization. The sensitivity of the PRT-induced EPSPs was significantly smaller than that of the IP-EPSPs ($p < 0.005$), and significantly larger than that of the CP-EPSPs ($p < 0.0005$). This result suggests that the PRT-rubral synapses located at more proximal portion of the dendrites than the corticorubral synapses and more distal portion of the dendrites than the IP-rubral synapses in the RN cell represented in Fig. 6A-C. Fig. 6D,E show similar experiment for the ML-induced EPSPs against the IP-EPSPs in another RN cell. In this cell the ratio of sensitivity of the ML-induced EPSPs was significantly smaller than that of the IP-EPSPs ($p < 0.0005$). Therefore, it is indicated that the ML-rubral synapses are located at more distal dendrites than the IP-rubral synapses in the RN cell. The PRT-induced EPSPs were produced in both C-cells (10 cells) and L-cells (8 cells), and the ML-induced

EPSPs were also produced in both C-cells (9 cells) and L-cells (8 cells).

Sprouting of ML-rubral synapses after the chronic IP lesion

It was shown that ML-rubral synapses are located on the dendrites of RN cells in the above section. We examined the possibility that ML fibers sprout and form new synapses after the chronic IP destruction as corticorubral fibers. Fig. 7C,D show ML-induced EPSPs in a RN cell of the cat with IP lesion which were characterized with a shorter time to peak of 1 msec. Since the normal ML-induce EPSPs (Fig. 7B) have a relative short time to peak (1.6 msec in the mean value), and there is some overlap in the time to peak of ML- and IP-EPSPs, the small difference of rise time of ML-induced EPSPs between the intact and the IP-lesioned cats was difficult to evaluate. However, effectiveness of ML stimulation to induce the extracellular unit spike of RN cells was clearly increased in the IP lesioned cats than that in normal cats. Single shock stimulations of ML excited only 5 RN units out of 112 RN units in 3 normal cats. In contrast, 50 RN cells out of 56 RN cells were excited in 3 both IP and SM lesioned cats. One of the mechanisms is that ML-rubral fibers sprout and form new synapses following chronic IP destruction (Fig. 7A).

Sprouting of the corticorubral synapses following the IP lesion has been reported previously by Tsukahara et al. (1974, 1975a). However, sprouting of collateral fibers of the pyramidal

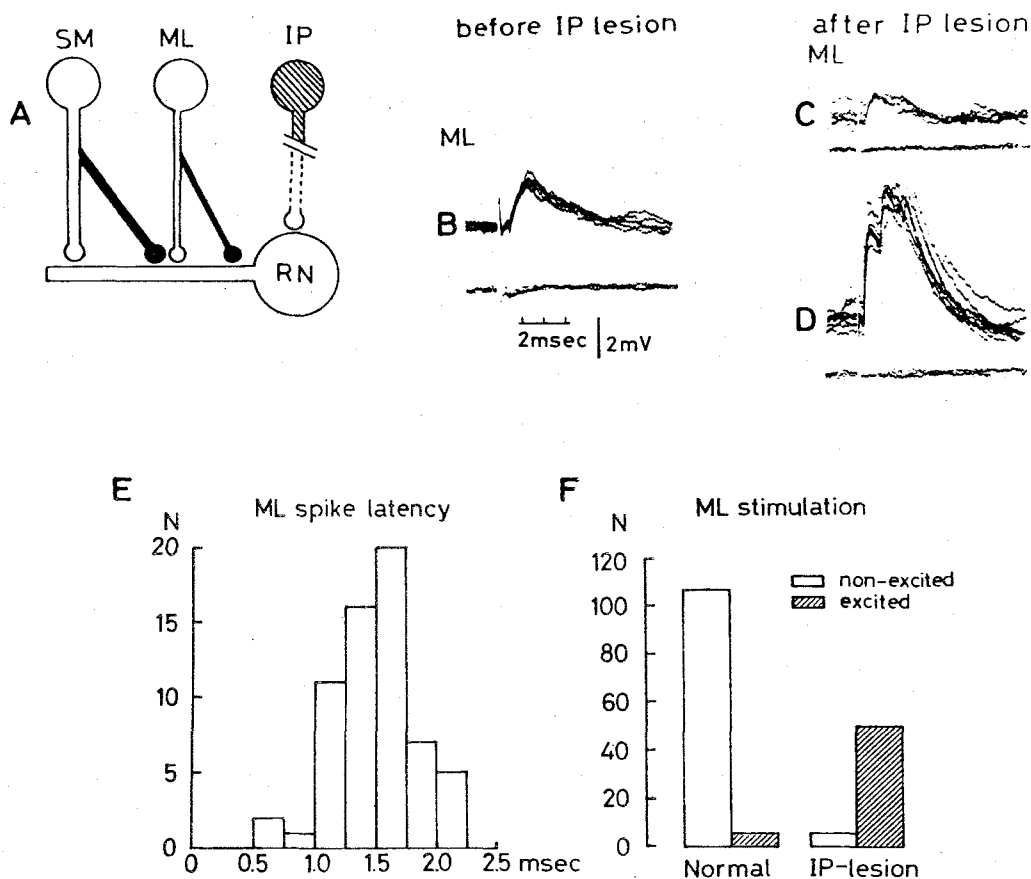


Fig.7 Medial lemniscal input after the chronic IP lesion. A: Diagram of synaptic connection of SM- and ML-rubral input in cats with the IP lesion. B: ML-induced EPSPs in a RN cell from a normal cat. C,D: ML-induced EPSPs in a RN cell from the cat with the IP lesion. Intensity of stimulation was increased from C to D. Lower traces of B-D show the extracellular controls corresponding to upper traces. Voltage and time calibrations in B also applies to C,D. E: Frequency distribution of latencies of unit spikes activated by ML stimulation in cats with IP and SM destructions. F: Number of RN unit spikes in normal cats and the chronic cats with IP and SM lesions. Open columns indicate RN units which were not excited by single shock ML stimulations. Shaded columns represent RN units excited by the single shock ML stimulations.

tract in RN neurons of cats with IP lesion has been remained unasked. The lemniscal input was also destroyed by chronically destroying the contralateral DCN. EPSPs induced by the pyramidal tract stimulation in Fig. 8B, from a cat with both IP and DCN lesions, had a fast-rising component superimposed on the normal slow-rising one and similar shape to CP-EPSPs in the same cat (Fig. 8A). In view of the appearance of the dual peaked CP-EPSPs in the IP lesioned cats, it appears that the collateral fibers to RN nucleus of the pyramidal tract also sprout and form new synapses at the proximal portion of soma-dendritic membrane of RN cells following IP and DCN lesions.

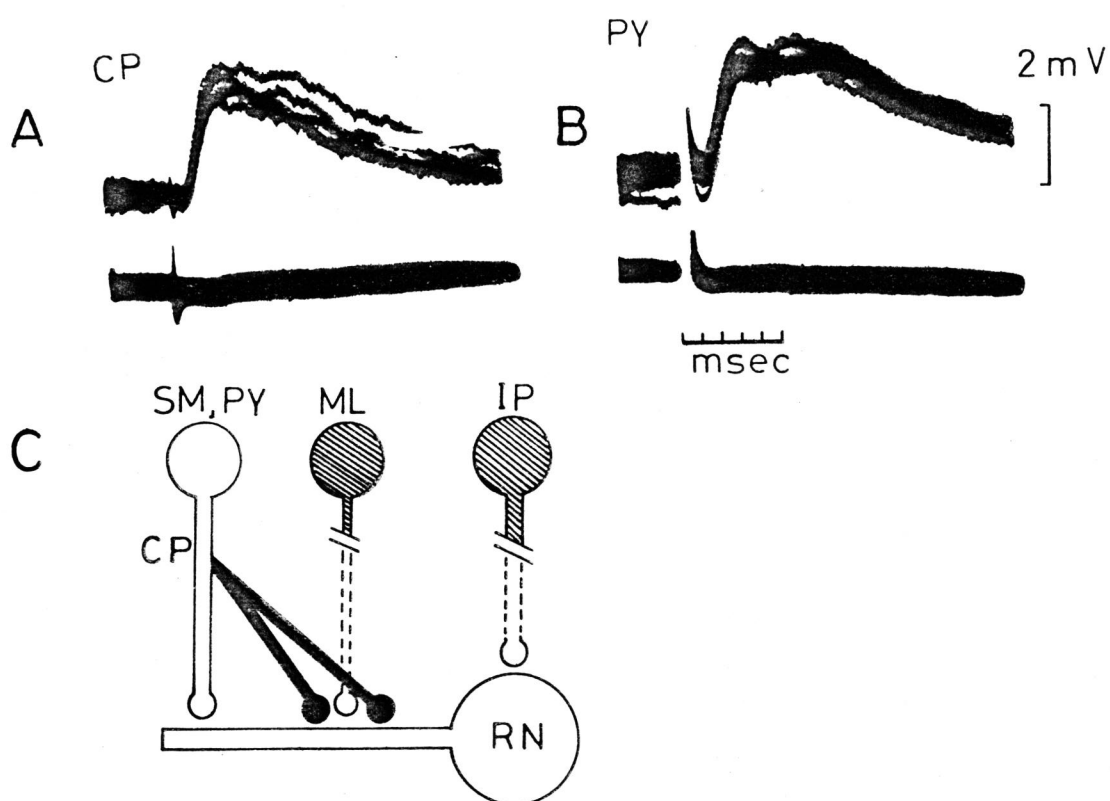


Fig.8 Appearance of fast-rising component in EPSPs induced by stimulation of the pyramidal tract following chronic IP and DCN destructions. A: CP-EPSPs in a cat with IP and DCN lesions. B: Dual peaked PY-induced EPSPs in the same cat. Upper traces in A and B represent intracellular records. Lower traces in A, B show the extracellular controls. C: Diagram of connections of SM-rubral and PY-rubral synapses after IP and DCN lesions.

DISCUSSION

Cortical inputs

In agreement with the histological results, present results show that PASC projects to the rubrospinal (RN) neurons. Oka et al. (1979) have shown that PASC projects to parvocellular red nucleus. The present results extend their finding to the red nucleus neurons which send their axons to the spinal cord. It has been shown that the lateral portion of PASC projects to the dorsomedial portion of the predominantly rostral part of RN and the medial portion of PASC projects to the ventrolateral portion of the predominantly rostral part of RN (Mabuchi and Kusama, 1966; Mizuno et al., 1973). Since C-cells are located in the dorsomedial portion and L-cells in the ventrolateral portion of RN (Padel et al., 1972; Pompeiano and Brodal, 1957; Eccles et al., 1975a,b), these observations are in good accordance with the present results that stimulation of the lateral part of PASC produced predominantly EPSPs in C-cells and stimulation of the medial part of PASC induced EPSPs predominantly in L-cells. These PASC-induced EPSPs were more frequently recorded in the rostral half of RN than in the caudal half.

Since PASC corresponds to area 5 of Hassler and Muhs-Clement (1964) and connected reciprocally with the pericruciate cortex (PCC) (Kawamura, 1973; Heath and Jones, 1971), a possibility remains that some of the PASC-induced EPSPs are mediated via the PCC. However, PASC-induced EPSPs were still

observed in cats with chronic ablation of PCC. Therefore, it is unlikely that PASC-induced EPSPs ^{were} mediated by PCC. Similarly, S_{II} -induced EPSPs were also produced in cats with chronic SM ablation. Our result that PS-induced EPSPs were predominantly produced in C-cells makes sense because PS corresponds to motor area of face (Woolsey, 1958). Rinvik (1965) showed that proreus gyrus and M_{II} project their fibers to the bilateral RN. However, proreus-induced and M_{II} -induced EPSPs could not be recorded from both sides. Thus proreus-rubral and M_{II} -rubral projections may not exist or are very sparse if they exist.

Typical slow rise time (about 3 msec) of the cortically-induced EPSPs suggests that PASC-, PS-, S_{II} -induced EPSPs were produced by synapses located on the distal dendrites as SM-rubral synapses.

Brain stem inputs

Our results that stimulation of PRT produced PSPs are in good accordance with the histological observations (Graybiel, 1974; Itoh, 1977). Furthermore, in agreement with previous physiological studies (Massion, 1961; Nishioka and Nakahama, 1973; Eccles et al., 1975a), there is peripheral inputs to the red nucleus which are not mediated by the cerebellum or cerebral cortex. Our result has shown that ML is the monosynaptic input to the red nucleus in agreement with the histological and physiological studies (Cajal, 1909-1911; Hazlett et al., 1972; Hand and Liu, 1966; Padel, personal communication).

The mean rise time of PRT- and ML-induced EPSPs is intermediate to those of CP-EPSPs and IP-EPSPs. Furthermore, sensitivity of these PRT- and ML-induced EPSPs to membrane hyperpolarization is also intermediate to those of CP- and IP-EPSPs. Therefore, it is likely that synapses of PRT and ML fibers terminated on the dendrites between distal part where SM fibers terminate and the soma where IP fibers terminate. This is in agreement with the previous suggestion (Tsukahara et al., 1975b) that some unidentified synaptic inputs exist which terminate between the soma and terminal dendrites.

The PRT is one of the key structure of extrageniculate visual system (Kawamura, 1974) and receives visual inputs. RN neurons receive short latency excitation by photic stimulation (Massion, 1967, in review). It is likely that this visually-evoked responses are mediated via the PRT. Similarly, RN neurons receive lemniscal input is consistent with the previous finding that after cerebellectomy, stimulation of the peripheral nerve produced short latency evoked responses in RN (Nishioka and Nakahama, 1973). However, it must be noted that the PRT- and ML-induced EPSPs are less powerful than that of IP-EPSPs. Therefore, the main traffic of signals to RN is considered to be mediated by the IP.

Bromberg and Gilman (1978) reported that multiunit activities in the red nucleus show an initial decrease of responses and a subsequently show recovery after lesions of the contralateral IP. To evaluate whether the restoration of activity depends upon intact corticofugal fibers, ipsilateral PCC was ablated

six weeks after the contralateral IP lesion. After the ablation, there was an immediate drop in amplitude of the activity.

However, there is a slow restoration, indicating that other inputs substitute the function of the destroyed IP and PCC.

The present study has supplemented that one of the mechanisms of the slow restoration after both IP and SM lesion is sprouting and formation of functional synapses from PASC and possibly from ML inputs.

SUMMARY

Synaptic inputs of rubrospinal (RN) neurons from the cerebral cortex, pretectal area (PRT) and medial lemniscus (ML) were investigated physiologically. Stimulation of the ipsilateral parietal association cortex (PASC) and secondary sensory area (S_{II}) produced slow-rising monosynaptic EPSPs of 3 msec's rise time and, in some cases, succeeding hyperpolarizations similar to the sensorimotor cortex (SM)-induced PSPs which have been previously shown. Stimulation of the contralateral cerebral cortex never produced detectable PSPs. It was shown that PASC- and S_{II} -rubral projections pass through independent pathway other than that mediated by SM and through the cerebral peduncle (CP). Topographical arrangement of PASC-rubral projection was found. Stimulation of the lateral part of PASC produced predominantly EPSPs in RN cells which innervated the upper spinal segments, while stimulation of the medial part of PASC induced EPSPs predominantly in RN cells innervating the lumbosacral cord. Further, PASC-induced EPSPs were more frequently recorded in the rostral half of RN than in the caudal half.

Monosynaptic EPSPs and multisynaptic IPSPs were induced by stimulation of the ipsilateral PRT, ML and its origin of the contralateral dorsal column nuclei. PRT- and ML-induced EPSPs had relatively fast mean time-to-peak and S,D, of 1.0 ± 0.4 msec ($n=18$) and 1.6 ± 0.5 msec ($n=17$), respectively. These mean rise times were intermediate to those of CP-EPSPs and IP-EPSPs. Furthermore, sensitivity of amplitudes of PRT-induced EPSPs

to membrane hyperpolarization was intermediate to those of CP- and IP-EPSPs, and that of ML-induced EPSPs was lower than that of IP-EPSPs. Therefore, it is likely that synapses of PRT and ML fibers terminate on the dendrites between distal where CP-rubral synapses terminate and soma where IP-rubral synapses terminate.

PASC-induced EPSPs after the chronic IP lesion had new fast-rising component and effectiveness of ML stimulation to induce the unit spike of RN cells was clearly increased in the IP and SM lesioned cat. Thus it was indicated that PASC- and ML-rubral fibers sprouted and formed new synapses after chronic IP destruction.

REFERENCES

- Bromberg, M. B., and Gilman, S. (1978) Changes om rubral multiunit activity after lesions in the interpositus nucleus of the cat. *Brain Res.*, 152: 353-357.
- Brown, L. T. (1974) Corticorubral projections in the rat. *J. Comp. Neurol.*, 154: 149-168.
- Cajal, S. Ramon y. (1909-1911) *Histologie du Système Nerveux de L'Home et des Vertébrés*. Maloine, Paris, 2 vols.
- Eccles, J. C., Scheid, P., and Táboříková, H. (1975a) Responses of red nucleus neurons to antidromic and synaptic activation. *J. Neurophysiolo.* 38: 947-964.
- Eccles J. C., Rantucci, T., Scheid, P., and Táboříková, H. (1975b) Somatotopic studies on red nucleus: Spinal projection level and respective receptive fields. *J Neurophysiolo.* 38: 965-980.
- Fujito, Y., Oda, Y., Maeda, J., and Tsukahara, N. (1978) synaptic inputs of the red nucleus neurons in the cat, A further study. *Proc. Japan Acad.*, 54, Ser. B: 65-68.
- Fujito, Y., Tsukahara, N., Oda, Y., and Yoshida, M. (1982) Formation of functional synapses in the adult cat red nucleus from the cerebrum following cross-innervation of forelimb flexor and extensor nerves. II. Analysis of newly appeared synaptic potentials. *Exp. Brain Res.* in press.
- Graybiel, A. M. (1974) Some efferents of the pretectal region in the cat. *Anat. Rec.*, 173: 365.
- Hanaway, J., and Smith, J. (1978) Sprouting of corticorubral terminals in the cerebellar deafferented cat red nucleus. *Soc. Neurosci . Abst.*, 4:1607.

- Hand, P. J., and Liu, C. N. (1966) Efferent projections of the nucleus gracilis. *Anat. Rec.*, 154: 353.
- Hassler, R., und Muhs-Clement, K. (1964) Architectonischer Aufbau des sensomotorischen und parietalen Cortex der Katze. *J. Hirnforsch.*, 6: 377-420.
- Hazlett, J. C., Dom, R., and Martin, G. F. (1972) Spino-bulbar, spino-thalamic and medial lemniscal connections in the american opossum, Didelphis marsupialis virginiana. *J. Com. Neurol.*, 146: 95-118.
- Heath, C. J. and Jones, E. G. (1971) The anatomical organization of the suprasylvian gyrus of the cat. *Ergebn, Anat. Entwickl.-Gesch.*, 45: 3-64.
- Itoh, K. (1977). Efferent projections of the pretectum in the cat. *Exp. Brain Res.*, 30: 89-105.
- Kawamura, K. (1973) Corticocortical fiber connections of the cat cerebrum. II. The parietal region. *Brain Res.*, 51: 23-40.
- Kawamura, S. (1974) Topical organization of the extrageniculate visual system in the cat *Exp. Neurol.*, 45: 451-461.
- King, J. S., Dom, R. M., Conner, J. B., and Martin, G. F. (1973) An experimental light and electron microscopic study of cerebellorubral projections in the opossum, Didelphis marsupialis virginiana. *Brain Res.*, 52: 61-78.
- King, J. S., Martin, G. F. and Conner, J. B. (1972) A light and electron microscopic study of corticorubral projections

- in the opossum, Didelphis marsupialis virginiana. Brain Res. 38: 251-265.
- Mabuchi, M., and Kusama, T. (1966) The cortico-rubral projection in the cat. Brain Res. 2: 254-273.
- Martin, G. F., Dom, R., Kattz, S., and King, J. S. (1974) The organization of projection neurons in the opossum red nucleus. Brain Res., 78: 17-34.
- Massion, J. (1961) Contribution a l'étude de la régulation cérébelluse du système extrapyramidal. Contrôle réflexe et tonique de la voie rubro-spinale par le cerevelet. ed. by Aracia, S. A. Masson, Paris.
- Massion, J. (1967) The mammalian red nucleus. Physiol. Rev. 47: 383-436.
- Mizuno, N., Mochizuki, K., Akimoto, C., Matsushima, R., and Sasaki, K. (1973) Projection from the parietal cortex to the brain stem nuclei in the cat, with spetial reference to the parietal cerebro-cerebellar system. J. Comp. Neurol. 147: 511-522.
- Murakami, F., Tsukahara, N., and Fujito, Y. (1977) Analysis of unitary EPSPs mediated by the newly-formed corticorubral synapses after lesion of the nucleus interpositus of the cerebellum. Exp. Brain Res. 30: 233-243.

Murakami, F., Katsumaru, H., Saito, K., and Tsukahara, N. (1982)

A quantitative study of synaptic reorganization in red nucleus neurons after lesion of nucleus interpositus of the cat: an electron microscopic study combined with intracellular injection of horse radish peroxidase. Brain Res. in press.

Nakamura, Y., and Mizuno, N. (1971) An electron microscopic study of the interpositorubral connections of the cat and the rabbit. Brain Res., 35: 283-286.

Nakamura, Y., Mizuno, N., Konishi, A., and Sato, M. (1974)

Synaptic reorganization of the red nucleus after chronic deafferentation from cerebellorubral fibers: an electron-microscopic study in the cat. Brain Res., 82: 298-301.

Nishioka, S., and Nakahama, H. (1973) Peripheral somatic activation of neurons in the cat red nucleus. J. Neurophysiol. 36: 296-307.

Oka, H., Jinnai, K., and Yamamoto, T. (1979) The parieto-rubro-olivary pathway in the cat. Exp. Brain Res., 37: 115-127.

Padel, Y., Armand, J., and Smith, A. M. (1972) Topography of rubrospinal units in the cat. Exp. Brain Res., 14: 363-371.

Padel, Y., Smith, A. M., and Armand, J. (1973) Topography of projections from the motor cortex to rubrospinal units in the cat. Exp. Brain Res., 17: 315-332.

Pompeiano, O., and Brodal, A. (1957) Experimental demonstration of a somatotopical origin of rubrospinal fibers in the cat. J. Comp. Neurol. 108: 225-251.

Rinvik, E. (1965) The corticorubral projection in the cat.

Further observations. *Exp. Neurol.* 12: 278-291.

Rinvik, E., and Walberg, F. (1963) Demonstration of a somatotopically arranged cortico-rubral projection in the cat. An experimental study with silver methods. *J. Comp. Neurol.* 120: 393-408.

Toyama, K., Tsukahara, N., Kosaka, K., and Matsunami, K. (1970) Synaptic excitation of red nucleus neurones by fibers from interpositus nucleus. *Exp. Brain Res.* 11: 187-198.

Tsukahara, N., and Fujito, Y. (1976) Physiological evidence of formation of new synapses from cerebrum in the red nucleus following cross-union of forelimb nerves. *Brain Res.*, 106: 184-188.

Tsukahara, N., Fujito, Y., Oda, Y., and Maeda, J. (1982) Formation of functional synapses in the adult cat red nucleus from the cerebrum following cross-innervation of flexor and extensor nerves. I. Appearance of new synaptic potentials. *Exp. Brain Res.* in press.

Tsukahara, N., Hultborn, H., and Murakami, F. (1974) Sprouting of corticorubral synapses in red nucleus neurons after destruction of the nucleus interpositus of the cerebellum. *Experientia*, 30: 57-58.

Tsukahara, N., Hultborn, H., Murakami, F., and Fujito, Y. (1975a) Electrophysiological study of formation of new synapses and collateral sprouting in red nucleus neurons after partial denervation. *J. Neurophysiol.* 38: 1359-1372.

- Tsukahara, N. and Kosaka, K. (1968) The mode of cerebral excitation of red nucleus neurons. *Exp. Brain Res.*, 5: 102-117.
- Tsukahara, N., Murakami, F., and Hultborn, H. (1975b) Electrical constants of neurons of the red nucleus. *Exp. Brain Res.*, 23: 49-64.
- Tsukahara, N., Toyama, K. and Kosaka, K. (1967) Electrical activity of red nucleus neurons investigated with intracellular microelectrodes. *Exp. Brain Res.*, 4: 18-33.
- Woolsey, C. N. (1958) Organization of somatic sensory and motor areas of the cerebral cortex. In: *Biological and Biochemical Basis of Behavior*, ed. by Horlow, H., and Woolsey, C. N. Univ of Wisconsin Press, Madison, pp63-81.

CHAPTER V

LESION-INDUCED SPROUTING IN THE KITTEN RED NUCLEUS

INTRODUCTION

Although axonal sprouting and formation of new synapses was first demonstrated in the 1950s (Edds, 1953), it has been difficult to demonstrate sprouting of central axonal connections unequivocally. However, recent studies have provided convincing evidence that sprouting does occur at central synapses and also that the newly-formed synapses are functionally active (Raisman, 1969; Moore et al., 1971; Steward et al., 1973; Cotman and Lynch, 1978; Lund, 1978; Tsukahara et al., 1974; Tsukahara, 1981).

Feline red nucleus (RN) neurons have proved a particularly felicitous substrate to demonstrate whether new, functional synaptic connections form following lesions, due to the ease of identifying their synaptic input. The rubrospinal neurons receive two kinds of synaptic input, one from the contralateral nucleus interpositus (IP) of the cerebellum on the somatic portion of the cells, and the other from the ipsilateral cerebral cortex on the distal dendrites. The physical segregation of the two types of input determines the characteristics of postsynaptic potentials as recorded in the RN cells (Tsukahara and Kosaka, 1968; Tsukahara et al., 1975b). By taking advantage of this synaptic organization, it has been possible to demonstrate that sprouting and formation of functional synapses occurs in the adult cat RN after destruction of the nucleus interpositus of the cerebellum (Tsukahara et al., 1974, 1975a). The newly-formed corticorubral synaptic transmission is

characterized by facilitation and posttetanic potentiation as in normal corticorubral synapses (Murakami et al., 1977). There is also evidence to suggest that sprouting and formation of functional synapses occurs in the cat after cross-innervation of peripheral flexor and extensor nerves (Tsukahara and Fujito, 1976; Tsukahara et al., in press; Fujito et al., in press).

In this study we have investigated neuronal sprouting in the kitten red nucleus following lesions of the ipsilateral cerebral cortex and contralateral IP. Young cats were used for these experiments because it is generally agreed that the degree and extent of neuronal sprouting is more remarkable after denervation in the neonatal stage than in the adult stage (see Cotman and Lynch, 1976; Lund, 1978; Tsukahara, 1981 for reviews). The histological work of Nah and Leong (1976a, and b) has previously demonstrated that, in rats, crossed corticorubral projections do appear after lesions of the ipsilateral cerebral cortex.

We have used physiological techniques to explore neuronal sprouting in the kitten RN and have, in particular, attempted to answer the following questions; 1) Do functional crossed cortico-rubral projections form after lesions to the ipsilateral cerebral cortex? 2) Are the inhibitory and excitatory component of newly formed crossed-rubral projections organized as in normal ipsilateral corticorubral projections? In the normal animal fast-conducting pyramidal tract fibers inhibit RN neurons postsynaptically, while slow-conducting pyramidal tract and corticorubral fibers excite monosynaptically via

synapses on the distal dendrites. 3) Are crossed corticorubral projections somatotopically organized as in the normal animal? In normal cats the forelimb cortical area projects onto RN cells innervating the upper spinal segments, whereas the hindlimb cortical area projects onto RN cells innervating the lower spinal segments.

preliminary reports of some of our results have already been published (Fujito et al., 1980; Tsukahara, 1980; Tsukahara and Fujito, 1981).

METHODS

Kittens from 17-149 days after birth were used. Kittens were anesthetized with pentobarbitone sodium and ablation of the left cerebral cortex was performed under direct vision in aseptic conditions (22 kittens). In 7 kittens hemispherectomy was performed also under direct vision. Procedures for intracellular recording from RN neurons were the same as those reported previously (Tsukahara et al., 1975), although the size of the brain in the young animal necessitated a recalibration of stereotaxic coordinates. RN neurons were identified antidromically by stimulating the contralateral C₁ and L₁ spinal segments; RN neurons activated from C₁ and L₁ were designated "L-cells", those activated only from C₁, "C-cells" (Tsukahara and Kosaka, 1968). Corticorubral fibers were stimulated at two levels; within the sensorimotor cortex (SM) and at the cerebral peduncle (CP).

The degree of ablation of the cerebral cortex and the

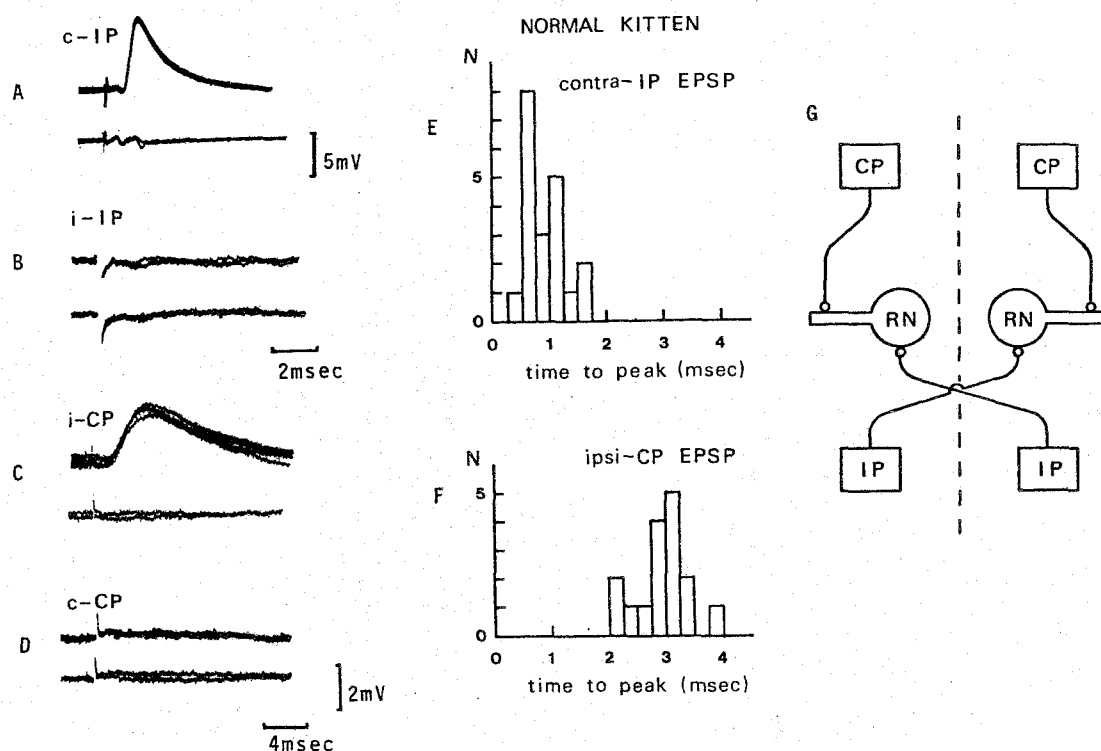


Fig.1 EPSPs produced in normal kitten red nucleus neurons

A: EPSPs elicited in a RN cell by stimulating the contralateral nucleus interpositus of the cerebellum (c-IP) (upper trace). The lower traces of A-D are corresponding extracellular traces as recorded just outside the cells. B: EPSPs induced by stimulating the ipsilateral IP (i-IP). C: EPSPs induced by stimulation of the ipsilateral cerebral peduncle (i-CP). D: EPSPs induced by stimulating the contralateral cerebral peduncle (c-CP). E,F: Frequency distribution of the time-to-peak of the EPSPs elicited in 80 day old kitten red nucleus. E: c-IP, F: i-CP. G: Diagram of the RN neuronal connections. Dashed line indicates the midline.

hemocerebellectomy were checked histologically after physiological experiments were completed.

RESULTS

Intracellular records were obtained from 263 RN cells from 34 kittens 37-302 days old. The RN cells were identified antidromically by stimulation of C₁ and L₁ spinal cord.

1. Synaptic organization of kitten red nucleus

Fig1. shows synaptic potentials recorded intracellularly in normal kitten RN cells. Synaptic potentials produced in RN neurons from 5 kittens 37 to 132 day old are virtually the same as those previously recorded in adults. Stimulation of the contralateral nucleus interpositus (IP) of the cerebellum produces fast-rising EPSPs (Fig.1A,E) with a mean latency of 1.0 ± 0.2 msec (n=39) and time-to-peak of 0.75 ± 0.3 msec (n=39) as in adult red nucleus (Tsukahara, Toyama, and Kosaka, 1967). Such EPSPs were only produced by stimulating the contralateral IP and not the ipsilateral IP, as shown in Fig.1B. Stimulation of the ipsilateral cerebral sensorimotor cortex (SM), or its fibers at the cerebral peduncle (CP), produces slow-rising dendritic EPSPs (Fig.1C,F) as in normal adult cats. These CP-EPSPs are sometimes followed by an IPSP as in the adult (see below). Stimulation of the contralateral CP does not produce any postsynaptic potentials in the majority of RN cells,

IPSILATERAL HEMISPHERECTOMIZED KITTEN

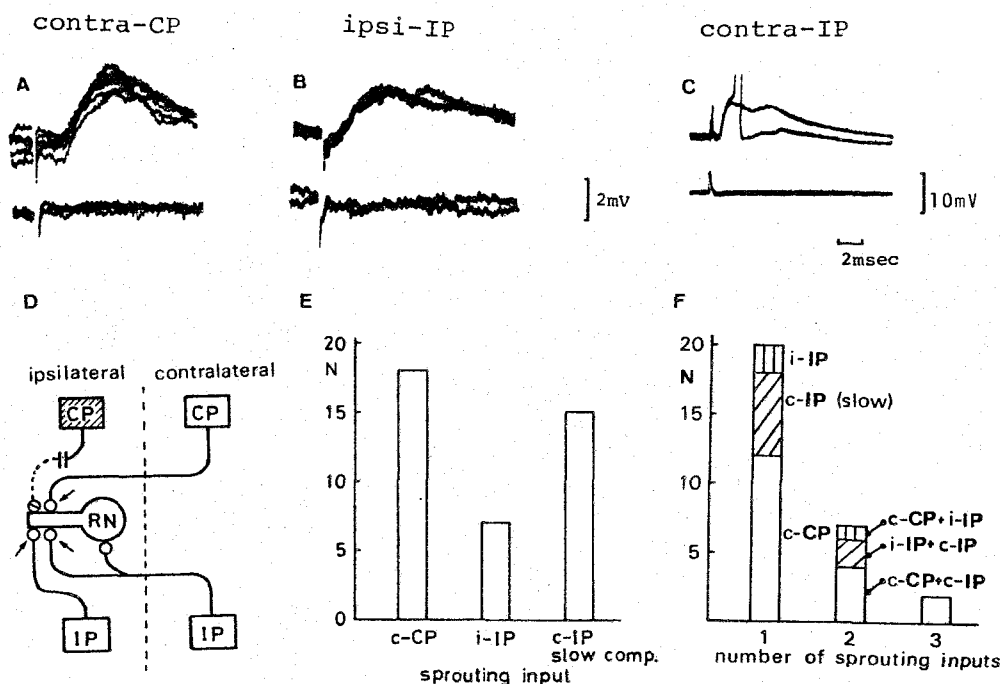


Fig.2 Newly-appeared EPSPs in kitten RN after destruction of the ipsilateral cerebro-rubral input

A: Newly-appeared EPSPs induced in a RN cell by stimulation of the contralateral cerebral peduncle (c-CP) (upper trace). Corresponding extracellular records are illustrated by the lower traces in A-C. B: EPSPs induced by stimulating the ipsilateral interpositus nucleus (i-IP) of the cerebellum. C: Newly-appeared dual-peaked EPSPs induced by stimulation of the contralateral IP (c-IP). Voltage calibration in B also applies to A. Time calibration in C also applies to A and B. D: Diagram illustrating sprouting in the kitten red nucleus (RN) after destruction of the ipsilateral cerebral cortex. Arrows indicate newly-formed synapses. Dashed line shows the

midline. E: Frequency distribution of appearance of each source of sprouting. Ordinate, number of RN cells. Left column, RN cells in which c-CP-EPSPs were recorded, middle column, RN cells in which c-CP-EPSPs were recorded, right column, RN cells in which a slow-rising component of c-IP EPSPs was recorded. F: Frequency distribution of numbers of sprouting sources in each RN cell. Ordinate, number of RN neurons. Left column indicates RN cells where only one source of sprouting was recorded. Open column, RN cells where only c-CP-EPSPs were recorded, oblique lined column, RN cells where only double peaked c-IP-EPSPs were recorded, vertical column, RN cells where only i-IP-EPSPs appeared. Middle column shows RN cells in which two sprouting sources were simultaneously recorded. Open column, RN cells where c-CP and dual-peaked c-IP-EPSPs were induced. oblique lined column, RN cells in which i-IP and dual-peaked c-IP-EPSPs were elicited, vertical lined column, RN cells where c-CP and i-IP-EPSPs were induced. Right column: RN cells where all three new inputs were simultaneously recorded.

as shown in Fig.1D. The latency of the CP-EPSPs is 1.4 ± 0.4 msec (n=40) and time-to-peak is 3.4 ± 0.8 msec (n=40). Although the latency of the CP-EPSPs is somewhat larger than that of normal adult ctas (1.0 ± 0.2 msec, n=100, Tsukahara et al., 1975), these data indicate that the synaptic organization of the kitten red nucleus is virtually the same as that of the adult.

2. Appearance of the postsynaptic potentials in RN cells after lesion of the ipsilateral corticorubral input

Typical slow CP-EPSPs evoked in a RN cell by stimulating the contralateral CP are illustrated in Fig.2A. In some cases, slow-rising EPSPs were also produced by stimulating the ipsilateral IP (Fig.2B), and further stimulation of the contralateral IP produced fast-rising IP-EPSPs followed by a slow-rising component, as shown in Fig.2C. The mean latency of the CP-EPSPs induced by stimulating the contralateral CP was $1.7 \text{ msec} \pm 0.5 \text{ msec}$ (n=77), and that of the IP-EPSPs induced by stimulating the ipsilateral IP was $1.5 \text{ msec} \pm 0.5 \text{ msec}$ (n=11). The time-to-peak of the CP-EPSPs was $3.4 \text{ msec} \pm 0.9 \text{ msec}$ (n=77), that of the IP-EPSPs induced from the ipsilateral IP was $2.9 \text{ msec} \pm 1.2 \text{ msec}$ (n=11), and the time-to-peak of the lateral component of the contralateral-IP-EPSPs was $2.8 \text{ msec} \pm 0.6 \text{ msec}$ (n=15).

The slow-rising CP-EPSPs induced from the contralateral CP are less sensitive to membrane potential displacement than the contralateral-IP-EPSPs (Fig.3A). Therefore, the newly-formed synapses are located on dendrites remote from the soma. Similarly, newly-appeared IP-EPSPs are less sensitive to membrane potential displacement than fast-rising IP-EPSPs, suggesting that

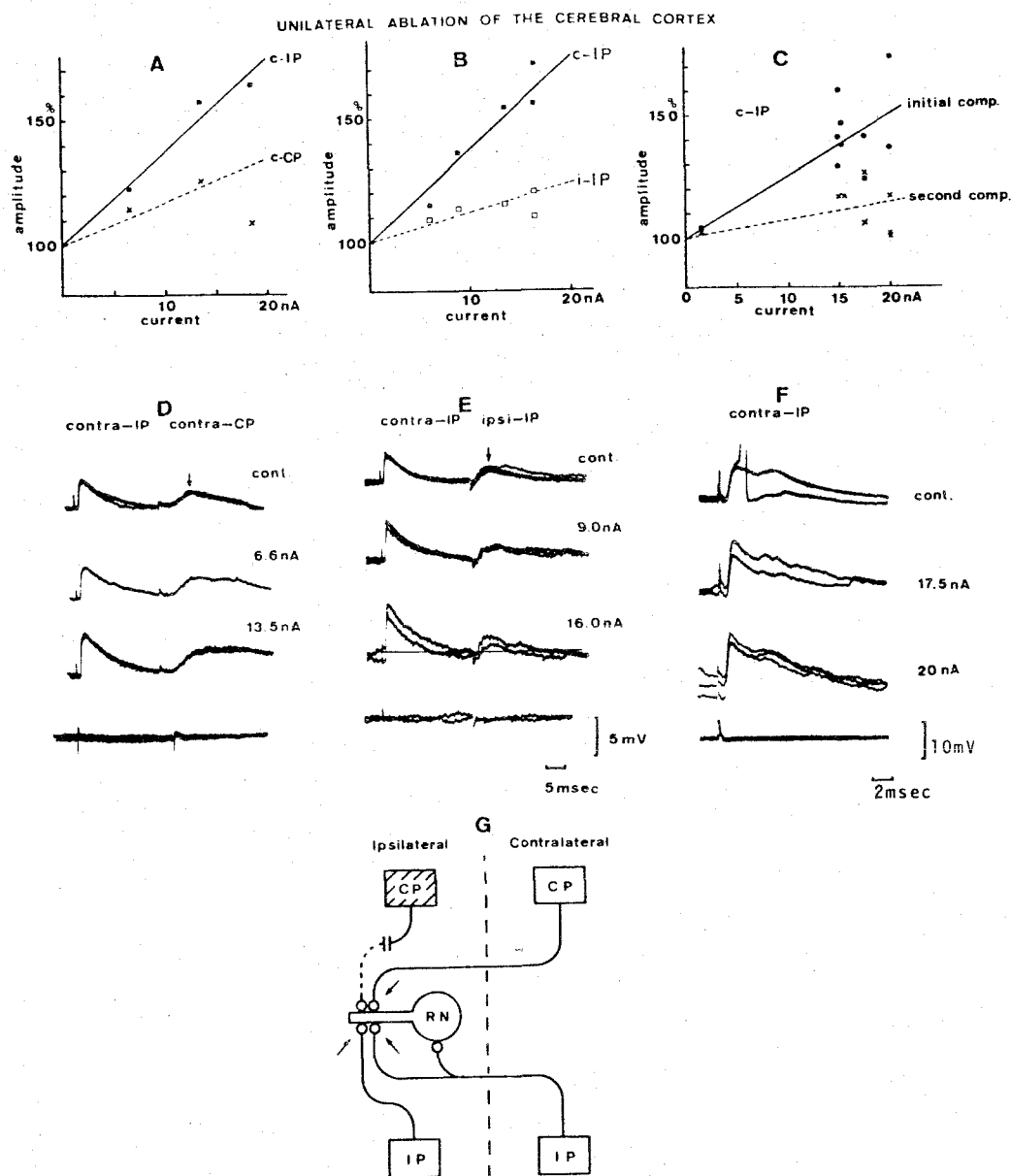


Fig.3 Sensitivity of newly-appeared EPSPs to membrane polarization in a kitten with cerebral lesions

A,B,C: Relationship between the amplitude of EPSPs and hyperpolarizing current. A: comparison between c-IP-EPSPs (filled squares) and c-CP-EPSPs (crosses) from experiments illustrated in D. Normalized amplitudes as a percentage of the control amplitudes (ordinate) are plotted against applied polarizing current (abscissa). B: Comparison between c-IP-EPSPs (filled squares) and i-IP-EPSPs

(open squares) from experiments illustrated in E. C: Comparison between the amplitudes of the initial fast-rising component (filled circles) and the second slow-rising component of c-IP-EPSPs (crosses) from experiments illustrated in F.

D,E,F: Specimen records of the EPSPs before (cont.) and during membrane hyperpolarization by passage of the amount of current labelled on each trace. The lowermost traces are corresponding extracellular field potentials. Voltage and time calibration in E also apply to D. Data from a cat with an ipsilateral SM lesion at the 67 th day postnatally.

G: Diagram illustrating sprouting in the kitten red nucleus (RN) after destruction of the ipsilateral cerebral cortex. arrows indicate newly-formed synapses. Dashed line shows the midline.

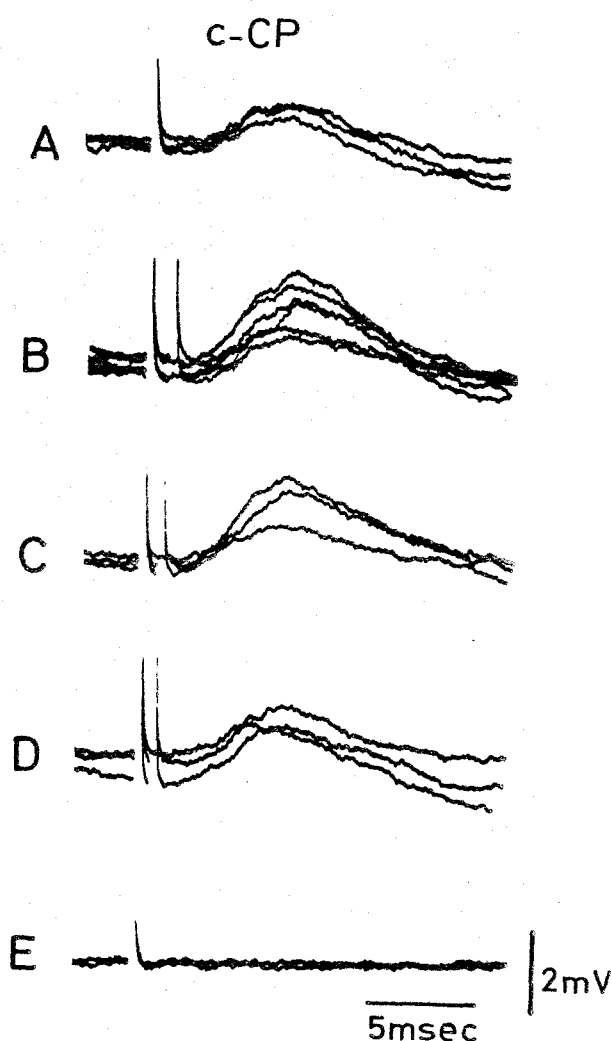


Fig.4 Double shock stimulation of the contralateral cerebral peduncle (c-CP) in a kitten with an ipsilateral cerebral lesion
 A-D: Newly-appeared EPSPs induced in a RN cell by stimulating the c-CP. A: EPSPs elicited by a single shock at the c-CP. B-D: EPSPs induced by double shocks at the c-CP. Intervals between double shocks were gradually shortened from B to D. In D, the second CP-EPSP was abolished. E: Corresponding extracellular control. Time and voltage calibration in E also apply to A-D. Data from a kitten with a chronic operation performed at 30th days postnatally.

they are produced at the distal dendrites.

The monosynaptic nature of the newly-appeared contralateral CP-EPSPs was tested by double stimulation experiments, and it was found that a second CP-EPSP was abolished abruptly at stimulus intervals of about 0.5 msec (Fig.4).

There are interesting features on the possible sources of sprouting following cerebral lesions in kittens. Although three possible sources of sprouting exist as described above, sprouting does not seem to take place from all three sources simultaneously at any given cell. Most frequently, 20 out of 29 RN cells tested, only one source gives sprouting (see Fig.2F).

Similar slow-rising EPSPs to those produced by CP stimulation (Fig.5A) was also produced by stimulating the contralateral sensorimotor cortex (c-SM), but with a longer latency (Fig.5B). Assuming the conduction distance from SM to CP to be 21 mm, the conduction velocities of the fibers responsible for producing the newly-appeared EPSPs can be calculated to be about 14 m/sec. This value is in the range of that for normal corticorubral fibers, or slow conducting pyramidal tract fibers. The frequency distribution of conduction velocities of the neurons responsible for the c-CP-EPSPs is illustrated in Fig.5C.

In normal adults, the fast-conducting pyramidal tract projects to inhibitory interneurons in the RN region and inhibits the rubrospinal (RN) neurons, whereas slow conducting pyramidal and corticorubral fibers terminate on RN neurons and excite them. Therefore, the question arises as to how this organization

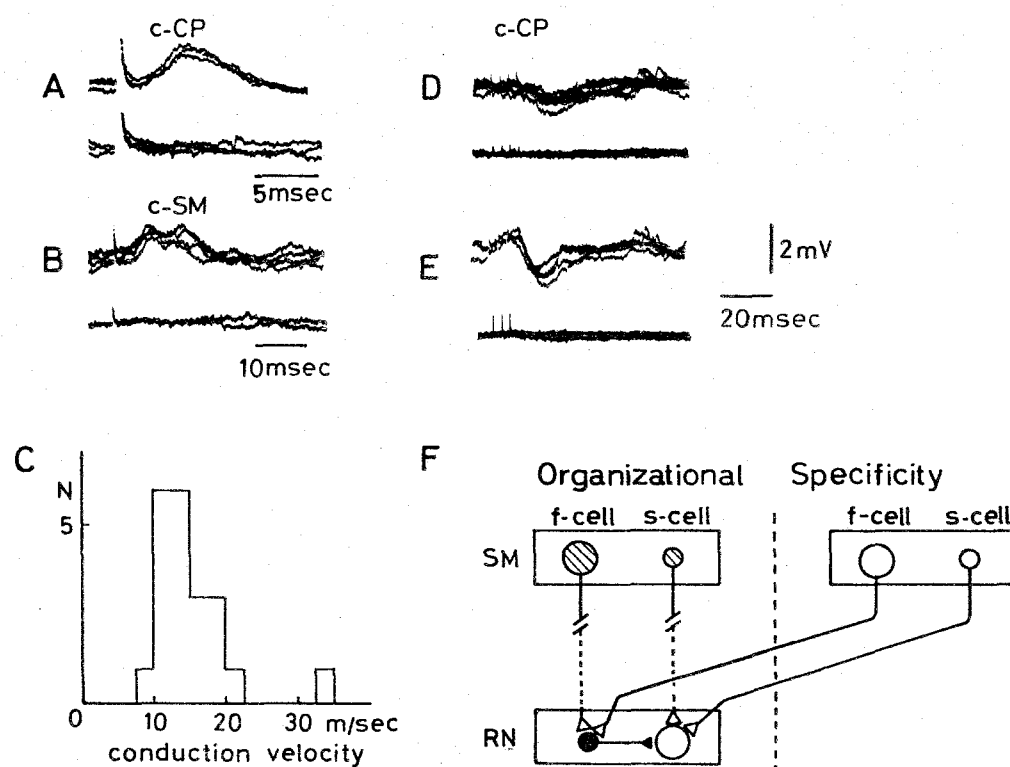


Fig.5 Specificity of organization of excitatory and inhibitory pathways in newly-formed cerebrotubal projections after destruction of ipsilateral cerebrotubal input

A,B: Newly-appeared corticorubral EPSPs evoked in a RN cell by stimulation of the c-CP (in A) or the contralateral sensorimotor

cortex (c-SM, in B). C: Frequency distribution of conduction velocities of fibers mediating newly-appeared contralateral cerebrotubal EPSPs. Ordinate, number of cells. Abscissa, conduction velocities. D and E show train stimulation of the c-CP. Intensities of stimulation were increased from D to E. IPSPs were produced in D, although they were preceded by EPSPs. Lower traces in A-E show extracellular recordings. F: Diagram of the organizational specificity of the newly-formed cerebrotubal projection. Dashed vertical line shows the midline. f-cell, fast conducting pyramidal tract cell; s-cell, slow conducting pyramidal tract or corticotubal cell. Shaded cells were destroyed by lesioning. Filled circles represent inhibitory interneurons.

specificity is preserved in experimentally induced crossed corticorubral projections. As in the normal ipsilateral projection, the threshold during a train of CP stimuli is lower for an IPSP than an EPSP in operated cats, as shown in Fig.5D E. This result suggests that, as in normal animals, fast-conducting corticofugal fibers innervate inhibitory interneurons, whereas slow conducting corticofugal fibers excite the RN neurons directly (see Fig.5F). This is consistent with the observation that the conduction velocities of fibers mediating the slow-rising EPSPs is in the range of 10-20 m/sec which is, in turn, in the range of slow conducting pyramidal tract fibers.

The area producing the slow-rising EPSPs in the contralateral cerebrum is somatotopically organized as in the case of the normal ipsilateral corticorubral projection. RN cells innervating the upper spinal segment (C-cells) receive EPSPs from the lateral part of the sensorimotor cortex, while RN cells innervating the lower spinal segment (L-cells) receive EPSPs predominantly from the medial part of the sensorimotor cortex (see Fig.6). However, this topographical specificity appears to be somewhat plastic. Fig.7 illustrates an experiment in which additional lesions were made in the forelimb region of the contralateral sensorimotor cortex in addition to the ipsilateral cortical lesion. In this case, the remaining medial hindlimb region of the sensorimotor cortex projects onto both C-cells and L-cells

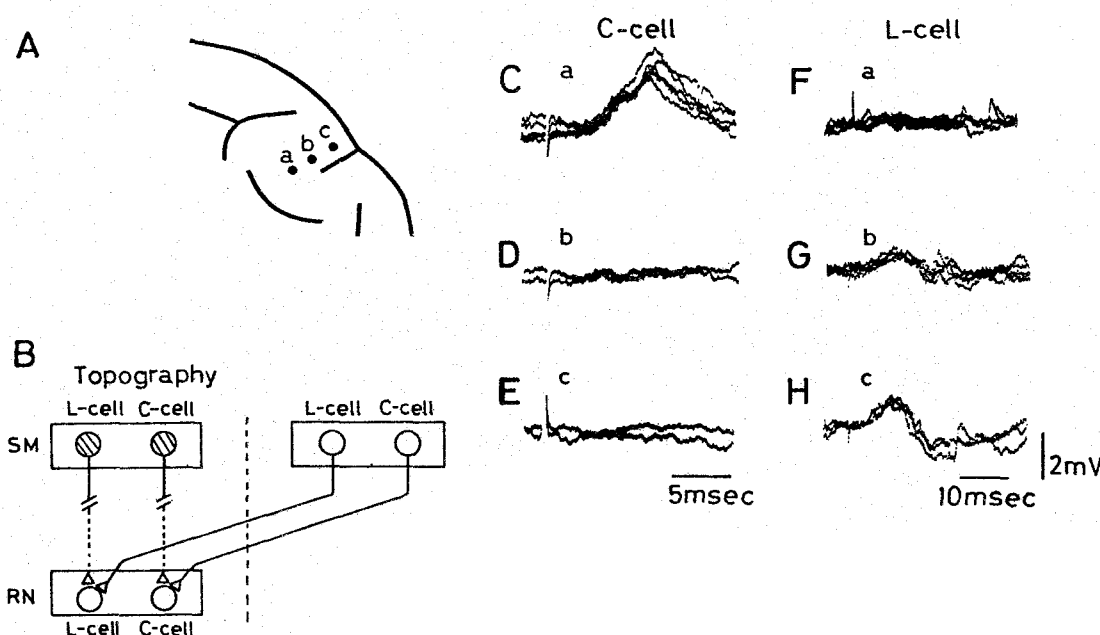


Fig.6 Topographical specificity of the newly-formed corticorubral projections A: Diagram of the sensorimotor cortex (SM) showing points of stimulation a,b,and c. B: Diagram of topographical specificity of newly-appeared corticorubral projection after destruction of the ipsilateral SM. Dashed line indicates the mid-line. L-cell, cell innervating the lumbosacral spinal cord, C-cell, cells innervating cervico-thoracic spinal cord. C,D,E: Newly-appeared EPSPs induced in a C-cell in the RN by stimulating three loci in the contralateral SM. Labels in C-E indicate the stimulating points. Data from a cat with an ipsilateral SM lesion at the 27th day postnatally. F,G,H: Same as C-E but EPSPs in a L-cell in the RN. Data from a cat with an ipsilateral SM lesion at the 35 th day. Time calibration in E also applies to C and D. Time calibration in H also applies to F and G. Voltage calibration in H also applies to C-G.

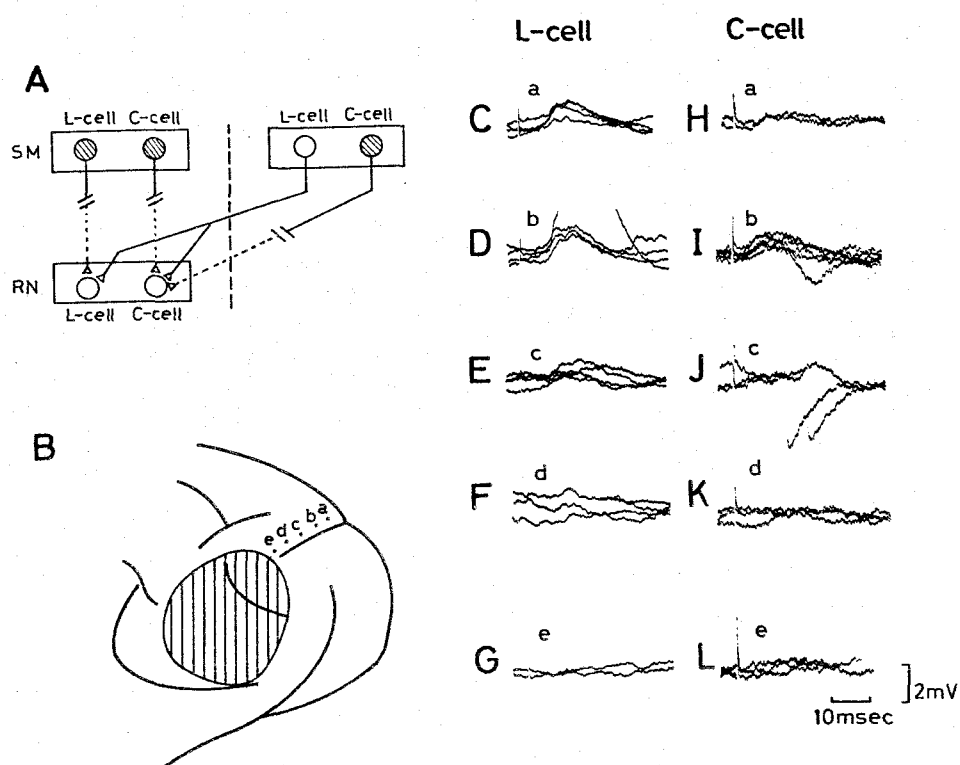


Fig.7 Plasticity of topographical specificity of newly-appeared cerebrocortical projection in kitten with ipsilateral cerebral cortex and contralateral forelimb region destruction.

A: Diagram showing the plasticity of topographical organization of the newly formed corticorubral projection. B: Diagram of stimulating sites and destroyed area in the contralateral cerebral cortex. C-L: EPSPs induced by stimulating the contralateral SM. Labels of a-e indicate the stimulating points as shown in B. C-G: Newly-appeared EPSPs induced in a L-cell by stimulating five sites on the contralateral SM. H-L: Same as C-G but in a C-cell from the same cat. Voltage and time calibrations in L also apply to C-K. Data from a cat with SM lesions performed at 30th day postnatally.

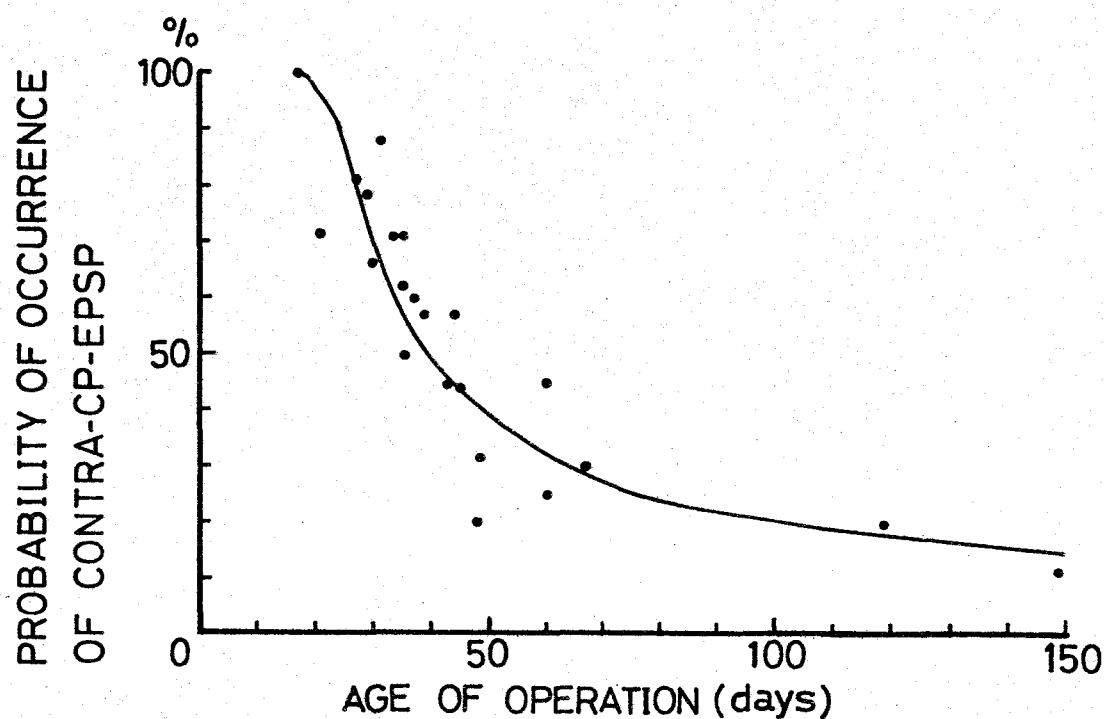


Fig.8 Time course of the probability of occurrence of newly-appeared CP-EPSPs with stimulation of the contralateral CP.

Ordinate: Ratio of the number of RN cells in which c-CP-EPSPs were recorded to the total number of sampled RN cells in each animal. Abscissa: Age of cat when normal ipsilateral cerebrotubal input was destroyed.

3. Time course of the appearance of the newly-formed crossed corticorubral projection

To establish the time of appearance of slow-rising c-CP-EPSPs, recording were made from kittens operated upon at different times after birth. The probability of appearance of detectable slow-rising c-CP-EPSPs recorded as a percentage of all impaled RN neurons is plotted against the time of ipsilateral cerebral ablation (Fig.8).

These data show that the probability of development of c-CP-EPSPs is highest in kittens operated upon at 20 days after birth and gradually decreases.

4. Lesions of the contralateral nucleus interpositus

After lesion of the contralateral IP by hemicerebellectomy at an early developmental stage (within several weeks after birth), new functional connections appears from the ipsilateral nucleus interpositus in a few RN cells (data from 7 cats). Stimulation of the ipsilateral IP produced monosynaptic EPSPs (see Fig.9) in 18 cells out of the 48 RN cells examined. Such i-IP-EPSPs have not been found after adult lesions and are never observed in normal kittens. However, the frequency of the newly-appeared ipsilateral connections is very low and the amplitude of the EPSPs is also very small. As in adult cats, lesions of the contralateral IP produced a fast-rising component in the i-CP-EPSPs as has been reported in adult (Tsukahara et al., 1975), suggesting that sprouting occurs from the ipsilateral corticorubral fibers on the proximal portion of the soma-dendritic membrane of RN cells.

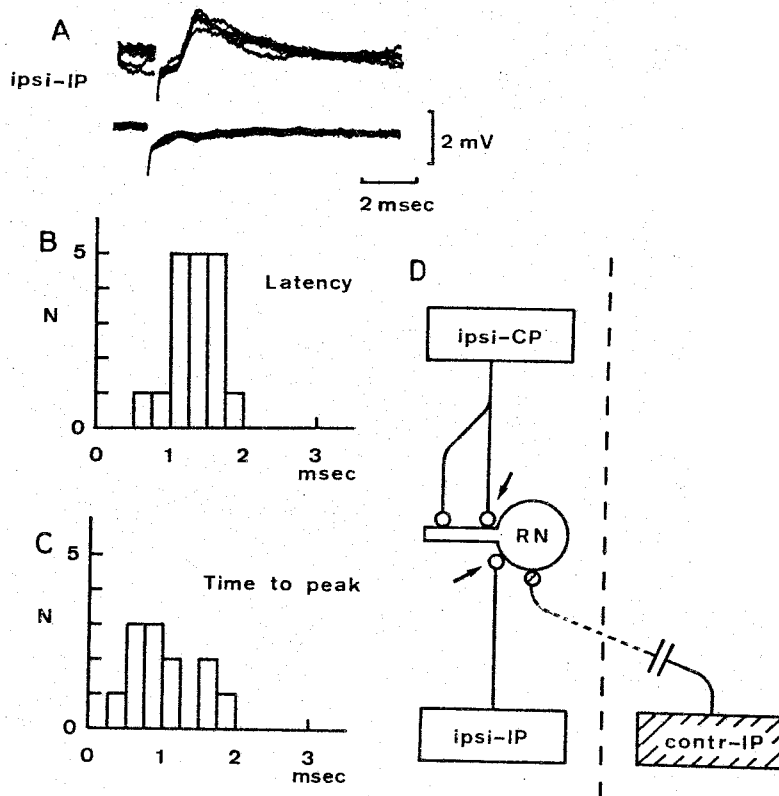


Fig.9 Sprouting in kitten red nucleus after hemicerebellectomy.

A: Newly-appeared EPSPs in a RN cell induced by stimulation of the ipsilateral IP. Upper trace, intracellular record, lower trace, corresponding extracellular record. B,C: Frequency distribution of latency (B) and time-to-peak (C) of the newly-appeared EPSPs. N is the number of EPSPs. D: Diagram of connections after the contralateral hemicerebellectomy. Arrows indicate sprouting of the i-IP-rubral and the i-CP-rubral fibers. Sprouting of ipsilateral corticorubral fibers onto the proximal part of the RN dendrites has also been observed after c-IP lesions in the adult cat (Tsukahara et al., 1974, 1975a).

DISCUSSION

In agreement with the histological studies in rats of Nah and Leong (1976a,b), the present study has shown that crossed corticorubral projections appear after lesions of the ipsilateral cerebral cortex in the kitten. The present study also demonstrates that the newly-formed corticorubral projections are functional.

The degree of plasticity following neonatal lesions of synaptic inputs of RN neurons is more remarkable than that observed after adult lesions (Tsukahara, 1981) in two ways. First, sprouting has not been observed in adult cats after SM lesions (Tsukahara, unpublished), while three sources of sprouting have been observed after similar lesions performed at the neonatal stage. Secondly, newly-formed corticorubral or interpositorubral sprouts seem to elongate a considerable distance, up to several millimeters, after neonatal lesions (Nah and Leong, 1976a,b). This is in sharp contrast to the sprouting after adult IP lesions where remaining corticorubral fibers terminating of the distal dendrites give sprouts only a few hundred microns proximally of in length (Tsukahara et al., 1974, 1975a, Murakami et al., 1977a,b).

How specifically are newly-formed cerebro-rubral projections organized in the kitten? Three kinds of specificity have been investigated in this study, as diagrammatically illustrated in Fig.10. First, "topographical specificity" was found to be preserved since the newly-formed corticorubral projections

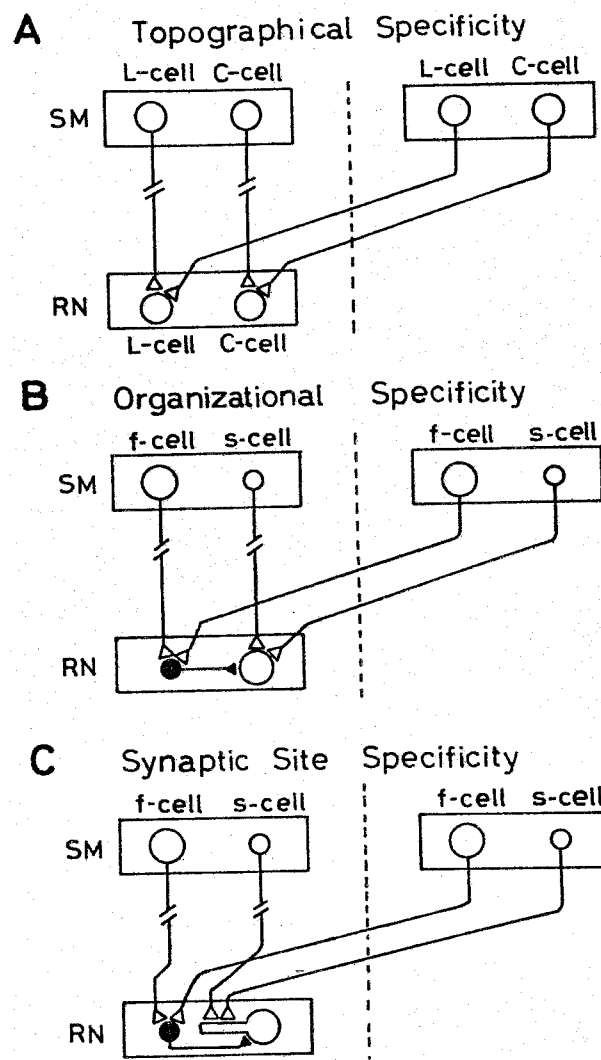


Fig.10 Specificity in newly-formed cerebro-rubral projections

A: SM, sensorimotor cortex, RN, red nucleus, L-cell, cells innervating lumbosacral spinal cord, C-cell, cells innervating cervicothoracic spinal cord. Dashed vertical line, midline.

B and C: f-cell, fast conducting pyramidal tract cell, s-cell, slow conducting pyramidal tract or corticorubral cell. Open circles, excitatory neurons, Filled circles, inhibitory neurons.

from the contralateral cerebrum were somatotopically organized as in normal ipsilateral corticorubral projections (Fig.10a). Secondly, the "specificity of synaptic connections" seemed to be preserved, at least in part. As shown in Fig.10b, ipsilateral fast pyramidal tract neurons project onto inhibitory interneurons while slow conducting pyramidal or corticorubral fibers terminate on rubrospinal (RN) neurons directly (Allen and Tsukahara, 1974). In the newly-formed corticorubral system slow conducting pyramidal tract and corticorubral fibers project onto the rubrospinal cells directly, as in the normal animal, while fast conducting pyramidal tract cells do not. Whether the latter cells project onto inhibitory interneurons is shown by the fact that threshold of IPSPs are lower for the train of CP stimuli than that for the EPSPs. Thirdly, the "specificity of synaptic location" seems to be preserved after neonatal ipsilateral cerebral lesions.

The present results have been interpreted to be due to sprouting of corticorubral fibers from the contralateral cerebral cortex. However, the possibility exists that the observed postsynaptic potentials could be due to retardation of the retraction of crossed corticorubral projections which may exist at an early developmental stage. However, there is no histological data indicating that there are crossed corticorubral projections at an early developmental stage. Furthermore, we have examined normal animals at 37 days after birth and found no crossed projection, while ipsilateral cortical lesions at this period produce the appearance of crossed corticorubral EPSPs in about 60 % of the tested RN cells. Therefore, the possibility

that the appearance of new synaptic potentials is due to the retarded elimination of once established crossed corticorubral projection is remote (cf. Clark and Cowan, 1976; Clark et al., 1976). There appears to be some competitive interaction between the three sources of sprouting (contralateral CP, contralateral and ipsilateral IP) observed after ipsilateral cerebral lesion. In neuromuscular junction Betz et al. (1980) has shown that competitive interaction is the only factor involved in the synaptic withdrawal. Whether the same sort of competition occurs in the CNS remains unknown.

SUMMARY

We have examined the extent of neuronal sprouting that occurs in the kitten red nucleus (RN) following lesions of the cerebral cortex or cerebellum. In normal 2-3 month old kittens, stimulation of the ipsilateral cerebral cortex or cerebral peduncle (CP) produces slow-rising monosynaptic EPSPs in RN cells; while fast-rising EPSPs are produced by stimulating the contralateral nucleus interpositus (IP) of the cerebellum. In these normal animals stimulation of the contralateral cerebral cortex or CP, or the ipsilateral IP never produces detectable postsynaptic potentials.

In contrast, in kittens with chronic lesions of the ipsilateral sensorimotor cortex performed at less than 2 months after birth, it was found that 1) stimulation of the contralateral sensorimotor cortex or CP produced slow-rising EPSPs. 2) Upon stimulation of the contralateral IP a slow-rising component appeared superimposed on the fast-rising IP-EPSPs. 3) In some cells, stimulation of the ipsilateral IP produced slow-rising EPSPs. These results indicate that new synapses were formed on the dendrites of RN cells by neurons from the contralateral CP, contralateral IP and ipsilateral IP. The majority of denervated RN dendrites were found to receive new synapses from only one of these three inputs, those from the contralateral cerebral cortex being most prominent.

The conduction velocities of fibers responsible for the EPSPs recorded in these lesioned animals are similar

to those of slow conducting pyramidal tract fibers. Sometimes IPSPs were also produced by a train of CP stimuli. The IPSPs are probably mediated by fast conducting pyramidal tract fibers because their threshold is lower than that of the EPSPs. These findings suggest that newly formed cortico-rubral projections have organizational specificity with respect to excitatory vs. inhibitory connections which is similar to that of normal ipsilateral corticorubral projections. Also, since all the newly-formed excitatory connections are formed on the distal dendrites, newly-formed cortico-rubral projections apparently have synaptic site specificity (somatic vs. dendritic synaptic sites).

Somatotopical organization was found in the newly-formed corticorubral excitatory projections. The forelimb cortical area was found to project to contralateral RN neurons innervating the forelimb spinal segments, while the hindlimb cortical area was found to project to RN neurons innervating the lumbar segments. However, after chronic ablation of the forelimb area of the contralateral sensorimotor cortex, in addition to the ipsilateral cerebral cortex, a new connection was formed from the hindlimb area of the contralateral cerebral cortex to the RN neurons innervating the spinal forelimb segments. This indicates that the specificity of the topographical organization is somewhat plastic.

In chronically hemicerebellectomized kittens, ipsilateral IP stimulation produced fast-rising monosynaptic EPSPs in some

cases. Thus, it was concluded that new synapses were formed on the somatic or proximal dendritic portion of RN cells from the ipsilateral IP after ablation of the contralateral IP.

REFERENCES

- Allen GI, Tsukahara N (1974) Cerebrocerebellar communication systems. *Physiol Rev* 54: 957-1006
- Betz WJ, Caldwell JH, Ribchester RR (1980) The effects of partial denervation at birth on the development of muscle fibers and motor units in rat lumbrical muscle. *J Physiol (Lond)* 303: 265-279
- Bruce IC, Tatton WG (1980) Sequential output-input maturation of kitten motor cortex. *Exp Brain Res* 39: 411-419
- Castro A (1978) Projections of superior cerebellar peduncle in rats and the development of new connections in response to neonatal hemicerebellectomy. *J Comp Neurol* 178: 611-628
- Clarke PGH, Cowan WM (1976) The development of the isthmo-optic tract in the chick with special reference to the occurrence and correction of developmental errors in the location and connections of isthmo-optic neurons. *J Comp Neurol* 167: 143-164
- Clarke PGH, Rogers LA, Cowan WM (1976) The time of origin and the pattern of survival of neurons in the isthmo-optic nucleus of the chick. *J Comp Neurol* 167: 125-142
- Cotman CW, Lynch GS (1976) Reactive synaptogenesis in the adult nervous system: the effect of partial deafferentation on new synapses formation. In: Barondes^S (ed) *Neuronal recognition*. Plenum, New York, pp 69-108
- Cotman CW, Nadler JY (1978) Reactive synaptogenesis in the hippocampus In: Cotman CW (ed) *Neuronal plasticity*. Raven, New York, pp 227-271
- Edds MV Jr (1953) Collateral nerve regeneration. *Q Rev Biol* 28: 260-276

- Fujito Y, Oda Y, Maeda J, Tsukahara N (1978) Synaptic inputs of the red nucleus neurons in the cat--- A further study --- Proc Jap Acad Ser B 54: 65-68
- Fujito Y, Tsukahara N, Yoshida M (1980) Synaptic plasticity of the red nucleus in chronically hemicerebellectomized or hemispherectomized kittens. Neurosci Lett [Suppl] 4: S42
- Fujito Y, Tsukahara N, Oda Y, Yoshida M (1982) Formation of functional synapses in the adult cat red nucleus from the cerebrum following cross-innervation of forelimb flexor and extensor nerves. II. Analysis of newly-appeared synaptic potentials. Exp Brain Res (in press)
- Kawaguchi S, Yamamoto T, Samejima A (1979) Electrophysiological evidence for axonal sprouting of cerebellothalamic neurons in kittens after neonatal hemicerebellectomy. Exp Brain Res 36: 21-39
- Leong SK (1977) Plasticity of cerebellar efferents after neonatal lesions in albino rats. Neurosci Lett 7: 281-289
- Lim KH, Leong SK (1975) Aberrant bilateral projections from the dentate and interposed nuclei in albino rats after neonatal lesions. Brain Research 96: 306-309
- Lund RD (1978) Development and plasticity of the brain: An introduction. Oxford University Press, New York
- Mabuchi M, Kusama T (1966) The cortico-rubral projection in the cat. Brain Research 2: 254-273

- Moore RY, Björklund A, Stenevi U (1971) Plastic changes in the adrenergic innervation of the rat septal area in response to denervation. Brain Research 33: 13-35
- Murakami F, Tsukahara N, Fujito Y (1977) Properties of the synaptic transmission of the newly formed cortico-rubral synapses after lesion of the nucleus interpositus of the cerebellum. Exp Brain Res 30: 245-258
- Nah SH, Leong SK (1976)^a Bilateral corticofugal projection to the red nucleus after neonatal lesions in the albino rat. Brain Research 107: 433-436
- Nah SH, Leong SK (1976)^b An ultrastructural study of the anomalous corticorubral projection following neonatal lesions in the albino rat. Brain Research 111: 162-166
- Raisman G (1969) Neuronal plasticity in the septal nuclei of the adult rat. Brain Research 14: 25-48
- Steward O, Cotman CW, Lynch GS (1973) Re-establishment of electrophysiologically functional entorhinal cortical input to the dentate gyrus deafferented by ipsilateral entorhinal lesions: innervation by the contralateral entorhinal cortex. Exp Brain Res 18:396-414
- Tsukahara N (1980) Synaptic plasticity in the red nucleus. Proc Int Congr Physiol Sci 14: 43
- Tsukahara N (1981) Synaptic plasticity in the mammalian central nervous system. Ann Rev Neurosci 4: 351-379

- Tsukahara N, Fujito Y (1976) Physiological evidence of formation of new synapses from cerebrum in the red nucleus neurons following cross union of forelimb nerves. *Brain Research* 106: 184-188
- Tsukahara N, Fujito Y (1981) Neuronal plasticity in the newborn and adult feline red nucleus. In: Flohr H, Precht W (ed) *Lesion-Induced Neuronal Plasticity in Sensorimotor systems*. Springer-Verlag, Heidelberg, pp 64-74
- Tsukahara N, Fujito Y, Oda Y, Maeda J (1982) Formation of functional synapses in adult cat red nucleus from the cerebrum following cross-innervation of flexor and extensor nerves. I. Appearance of new synaptic potentials. *Exp Brain Res* (in press)
- Tsukahara N, Hultborn H, Murakami F (1974) Sprouting of cortico-rubral synapses in red nucleus neurones after destruction of the nucleus interpositus of the cerebellum. *Experientia* (Basel) 30: 57-58
- Tsukahara N, Hultborn H, Murakami F, Fujito Y (1975a) Electrophysiological study of formation of new synapses and collateral sprouting in red nucleus neurons after partial denervation. *J Neurophysiol* 38: 1369-1372
- Tsukahara N, Kosaka K (1968) The mode of cerebral excitation of red nucleus neurons. *Exp Brain Res* 5: 102-117
- Tsukahara N, Murakami F, Hultborn H (1975b) Electrical constants of neurons of the red nucleus. *Exp Brain Res* 23: 49-64

VI LIST OF PUBLICATIONS

1. Tsukahara N, Hultborn H, Murakami F, Fujito Y (1975)
Physiological evidence of collateral sprouting and formation of new synapses in the red nucleus following partial denervation. In: Santini M (ed) Golgi Centennial Symposium Proceedings. Raven Press, New York, 299-303
2. Tsukahara N, Hultborn H, Murakami F, Fujito Y (1975)
Electrophysiological study of formation of new synapses and collateral sprouting in red nucleus neurons after partial denervation. J Neuophysiol 38: 1359-1372
3. Murakami F, Fujito Y, Tsukahara N (1976) Physiological properties of newly formed corticorubral synapses of red nucleus neurons due to collateral sprouting. Brain Res 103: 147-152
4. Tsukahara N, Fujito Y (1976) Physiological evidence of new synapses from cerebrum in the red nucleus neurons following cross-union of forelimb nerves. Brain Res 106: 184-188
5. Murakami F, Tsukahara N, Fujito Y (1977) Analysis of unitary EPSPs mediated by the newly-formed cortico-rubral synapses after lesion of the nucleus interpositus of the cerebellum. Exp Brain Res 30: 233-243
6. Murakami F, Tsukahara N, Fujito Y (1977) Properties of the synaptic transmission of the newly-formed cortico-rubral synapses after lesion of the nucleus interpositus of the cerebellum. Exp Brain Res 30: 245-258

7. Fujito Y, Oda Y, Maeda J, Tsukahara N (1978) Synaptic inputs of the red nucleus neurons in the cat. A further study. Proc Jap Acad 54B: 65-68
8. Fujito Y, Tsukahara N, Yoshida M (1980) Synaptic plasticity of the red nucleus in chronically hemispherectomized or hemispherectomized kittens. Neurosc Lett Suppl 4: S42
9. Tsukahara N, Fujito Y (1981) Neuronal plasticity in the newborn and adult feline red nucleus. In: Flohr H, Precht W (ed) Lesion-Induced Neuronal Plasticity in Sensorimotor Systems, Springer-Verlag, Berlin Heidelberg pp 64-74
10. Fujito Y, Tsukahara N, Kubota M (1981) Specificity and plasticity of the newly-formed corticorubral projection in chronically hemispherectomized kittens. Neurosc Lett Suppl 6: S81
11. Tsukahara N, Fujito Y, Oda Y, Maeda J (1982) Formation of functional synapses in the adult cat red nucleus from the cerebrum following cross-innervation of flexor and extensor nerves. I. Appearance of new synaptic potentials. Exp Brain Res (in press)
12. Fujito Y, Tsukahara N, Oda Y, Yoshida M (1982) Formation of functional synapses in the adult cat red nucleus from the cerebrum following cross-innervation of forelimb flexor and extensor nerves. II. Analysis of newly appeared synaptic potentials. Exp Brain Res (in press)

ACKNOWLEDGEMENTS

I wish to acknowledge my debt to professor Nakaakira Tsukahara for his continuous encouragement and helpful advices throughout this study.

I also wish to thank staffs of the laboratory of neurosciences, and Yoichi Oda, Jun Maeda, Makoto Yoshida, Michinori Kubota and Dr. Fujio Murakami for good collaborations.